



2008 Activity Report

SUMMARY

1. **INTRODUCTION AND KEY RESULTS**
2. **RFP PHYSICS**
3. **ITER NEUTRAL BEAM INJECTOR**
4. **DIAGNOSTICS**
5. **THEORY AND MODELLING**
6. **TOKAMAK PHYSICS**
7. **INTEGRATED TOKAMAK MODELING**
8. **ENGINEERING**
9. **BROADER APPROACH**
10. **NON FUSION APPLICATIONS**
11. **EDUCATION AND INFORMATION TO THE PUBLIC**
12. **LIST OF PUBLICATIONS 2008**

1 INTRODUCTION AND KEY RESULTS

The programme of Consorzio RFX for the year 2008 has been presented and discussed at the 19th meeting of the RFX Scientific-Technical Committee on 16 November 2007. The programme has then been endorsed by the Board of Directors of Consorzio RFX on 4 December 2007 and by the Steering Committee of the Euratom-ENEA Association on 6 December 2007.

The final approval of the 2008 programme and of the relevant budget was given by the Consorzio RFX Partners on 28 February 2008.

The 2008 programme of Consorzio RFX was strongly focused towards two main objectives.

“The key objective of the RFX physics program in 2008 will be the development of extensive campaigns at plasma currents ranging between 1 and 1.5 MA, in parallel to the technical preparation for bringing the performance towards the rated current level of 2 MA”.

“The key objective of the technology program is to start, in the frame of the new Fusion for Energy (F4E) organization, the realization of the EU share of the ITER Neutral Beam Injectors”.

As far as the experimental campaigns on RFX are concerned, the plan foresaw 37 weeks of operation (including commissioning after shutdown) and 15 weeks of shutdown for maintenance and improvements to diagnostics and power supplies. RFX operation has been very smooth throughout the year, owing to the excellent reliability of the whole plant. As planned, a substantial effort has been dedicated to the upgrade of the energy transfer system in preparation of the 2 MA operation. A total of 160 runs (experimental days) were performed and more than 2200 pulses executed, about 1000 of them being plasma pulses useful for physics studies. It's worth underlining that, at high plasma current, the time interval between pulses is rather long (more than half an hour), so the number of high current pulses per day is necessarily rather low.

At the end of the year, it is possible to conclude (Chapter 2) that all the main scientific objectives defined by the Activity Plan have been met. Owing to further improvements of magnetic boundary and of density control, extensive operation at high plasma current (between 1.0 and 1.5 MA) has been possible, resulting in strong improvement of plasma performance with electron temperatures in the 1 keV range. By pellet injection, we also started addressing the key issue of high density operation. Extensive work has been done on active MHD mode control, including both the highly Tokamak-relevant RWM stabilization and tearing mode control, where a new helical state, predicted by theory and called “Single Helical Axis” was obtained, characterized by strong chaos reduction and being the closest ever achieved to the theoretical Single Helicity regime.

Chapter 3 of this report is dedicated to the second pillar of the programme: the design of the ITER Neutral Beam Injector and of its Test Facility. In the first months of the year, the relevant activities, in collaboration with CEA Cadarache, IPP Garching, UKAEA Culham and FZK Karlsruhe, were performed under EFDA tasks. After conclusion of them, the plan was that the coordination of all the European effort on ITER NBI should be taken over by Fusion

for Energy. Unfortunately, due to various delays mainly related to the establishment of the new F4E team in Barcelona and to the definition of administrative rules, the invitation to submit a proposal for a Grant regarding the design of components for the NBTF system and the design and follow-up of infrastructures for NBTF was issued only on 11 August 2008 and the contract has been signed on 19 December 2008. Nevertheless, RFX continued to provide the foreseen human resources without any interruption, so that the objectives of the agreed technical tasks were fully accomplished. In particular, the design activities have been mainly focused on the full-size Ion Source test bed; as an outcome of this effort, the technical specifications for the calls for tender to be issued in 2009 are now almost ready. As far as the buildings and relevant plants are concerned, the Italian Government confirmed full financial support and the “build-to-print” design is now ready; the process to obtain the permit to build has been started, so that we are ready to begin construction at the middle of 2009. Besides this, an accompanying activity aimed to acquire numerical tools to optimize injector design and to train personnel on negative ion source and high voltage issues has been developed.

Chapter 4 reports about diagnostic developments, where significant progress has been achieved; in particular the RFX FIR polarimeter is now operational and a new diagnostic system has been set up to aid density control. We continued working on ITER Magnetics and core LIDAR, whereas the RFX commitments on JET Magnetics and High Resolution Thomson Scattering have been successfully concluded.

Chapter 5 reviews the most significant results from the theory and modeling activities, where a new version of a 3D code allowing extended MHD modeling has been implemented and Tokamak microturbulence codes were adapted to RFP regimes where magnetic chaos no longer rules anomalous transport.

A very important objective of our programme was to further improve integration with the Tokamak community: Chapter 6 shows that, despite the very strong effort on RFX-mod, the contribution of RFX physicists to Tokamak issues, in particular in the fields of MHD and transport, has been significant, mainly through collaborations to JET and ASDEX Upgrade. Chapter 7 reports on the Padova contribution to the EFDA Task Force Integrated Tokamak Modeling.

The following two chapters are dedicated to technological issues: Chapter 8 reports on the engineering developments for RFX-mod and on the RFX contribution to JET EP2 and to ASDEX Upgrade preferential support action on MHD control, whereas Chapter 9 describes the Padova contributions to Broader Approach regarding JT-60 SA power supplies.

Finally, Chapter 10 gives the results of the limited effort dedicated to non-fusion applications of plasmas and Chapter 11 reports on education and public information, where an important milestone has been met with the first year of the joint European Research Doctorate in Fusion Science and Engineering.

2 RFP PHYSICS

2.1 Background and framework

In 2008 the development of the RFX-mod scientific program has been accomplished on the basis of a public call for proposals open to scientists from RFX and external laboratories. The related experimental and interpretative activities have been assigned to 6 Task Forces, each covering a well defined topical area. Such organization, experienced for the first time at RFX, allowed an efficient and well shared exploitation of the experiment, with a wide participation to the elaboration of the program, discussed during a general workshop held before the beginning of the 2008 experimental campaigns. In this context, a high level of collaboration with other laboratories has been reached, in particular with the MST and EXTRAP T2R groups and with IPP-Garching.

During the whole 2008 campaigns, RFX-mod has been operated with high reliability and efficiency and no major fault occurred. About 1000 plasma discharges have been performed, about 500 of them with a flat-top current level higher than 1 MA. The device has also been commissioned in order to allow the current increase up to 2 MA, the target value for RFX-mod. Due to the high availability of the machine, all the main scientific objectives placed for the 2008 scientific activity have been attained (quoting the 2008 Activity Program):

- Exploration of RFP physics and confinement optimization in high plasma current regimes
- Contribution to the fusion community effort on MHD mode control studies in high temperature high density plasmas
- Fundamental research to contribute to the understanding of physics problems relevant for the advancement of fusion science

More specifically, extensive work has been done in the field of the MHD mode control, both RWM and core resonant. The optimization of the Clean Mode Control (CMC) algorithm led to a significant improvement of the magnetic boundary. Progress has been made in the density and plasma-wall interaction control too. In this framework, a safe and extensive operation at high plasma current has been pursued, with strong improvement of the plasma performance at 1.5 MA, with electron temperatures in the 1 keV range. In particular, the problem of sustaining high currents at high densities has been put in evidence; first promising results have been obtained on this topic by pellet injection and these experiments will continue in the next campaign. The obtained results open good perspectives for a further optimization of the 1.5 MA plasmas and for a gradual increase of the current up to 2 MA with improving performance.

A significant part of the scientific activity has been devoted to particle, energy and momentum transport studies, characterizing in particular the hot helical structures spontaneously developing in the core at high current and the plasma edge turbulence. Experiments with plasmas approaching the Greenwald density limit have been also performed, with the aim of contributing to the understanding of the physics behind this limit, common to RFPs and Tokamaks.

2.2 RFP performance: high current operation and advanced scenarios

With the ameliorated plasma boundary control obtained with the CMC algorithm, a large part of the RFX- mod 2008 experimental time has been dedicated to high current and advanced scenarios operations: about 500 discharges have been operated at high current, $I_p > 1$ MA, of which 118 with OPCD (Oscillating Pulse Current Drive). It has been demonstrated that at high current the magnetic topology spontaneously self-organizes in an ohmic helical symmetry, quasi single helicity state (QSH), in which the magnetic dynamics is dominated by the innermost resonant mode, with the new magnetic axis helically twisting around the geometrical axis of the torus. The QSH state approximates the theoretically predicted Single Helicity state (SH) found by Visco resistive MHD simulations [Cappello92,Cappello04]: in the SH the dynamo mechanism required to sustain the equilibrium fields in a RFP is provided by a

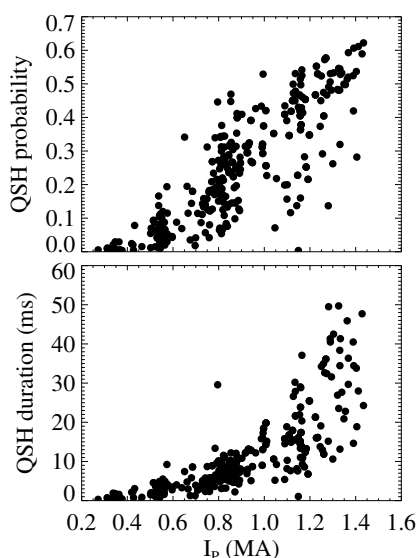


Fig.2.2.1: QSH probability and duration as a function of plasma current. For each pulse the QSH probability is computed as the ratio between the total time ,when QSH is present divided by the current flat-top period; QSH duration is defined as the longest QSH time interval

($I_p > 500$ kA). During the OPCD the edge toroidal field is modulated in order to transiently induce a current profile modification in the plasma, concentrating the toroidal flux in the core. As an effect, secondary modes decrease while the resonant one increases and the electron temperature and energy confinement increase. During the QSH regimes, both spontaneous or induced by OPCD, the formation of a clear structure in the soft-X ray emissivity distribution is observed by the tomographic reconstruction [Martin07], well correlated with the observed magnetic topology. Inside the helical structure, energy confinement is enhanced and at higher plasma currents electron temperatures of the order of 1 keV are measured (Fig.2.2.2). In these cases the QSH effect on the electron temperature is very strong with steep gradients which identify an internal transport barrier ($1/L_{Te}$ of the order of 20 m^{-1} is measured).

kink-like deformation of the plasma that attributes to the configuration a chaos free helical symmetry. The theoretical SH state is not affected by the high level of magnetic turbulence, typical of an RFP in standard conditions (Multiple Helicity (MH) scenario) where many modes of comparable amplitude are simultaneously present.

The probability to develop QSH and its persistency (defined as the ratio between the total time in which the plasma stays in QSH and the flattop duration) is found to increase with plasma current and above 1 MA QSH occupies a significant fraction of the current flat top, up to about 65%, as shown in Fig. 2.2.1.

Transient strong QSH states are reproducibly induced by oscillating poloidal current driven operation (OPCD), also at lower currents

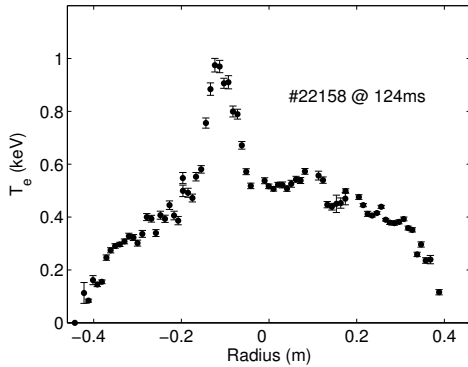


Fig.2.2.2: Electron temperature profile measured by Thomson Scattering in a QSH regime

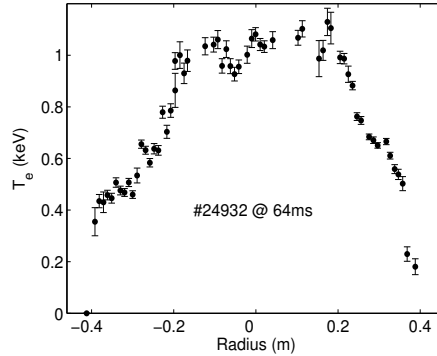


Fig.2.2.3: Electron temperature profile measured by Thomson Scattering in a SHAx regime

The best results in terms of plasma energy content are obtained when the chaos reduction involves also the plasma outside the island; in these cases the X-point of the QSH thermal island and the unperturbed magnetic axis merge leading to the expulsion of the island separatrix and to a hot, self-organized helical structure without island with a Single Helical Axis (SHAx) [Lorenzini08a], as predicted by the theory [Escande00].

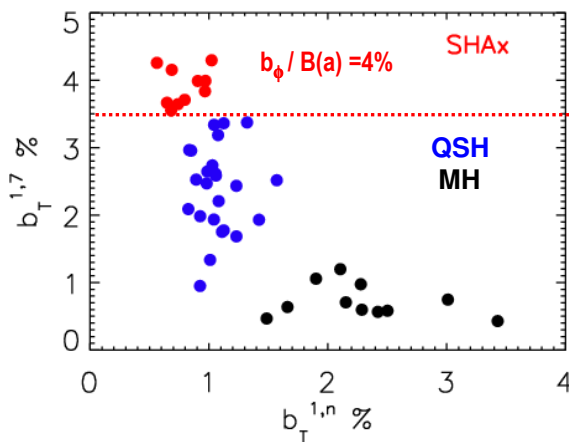


Fig.2.2.4: SHAx states appear when the amplitude of the mode $n=-7$ exceeds a threshold of 4% of the total magnetic field at the edge

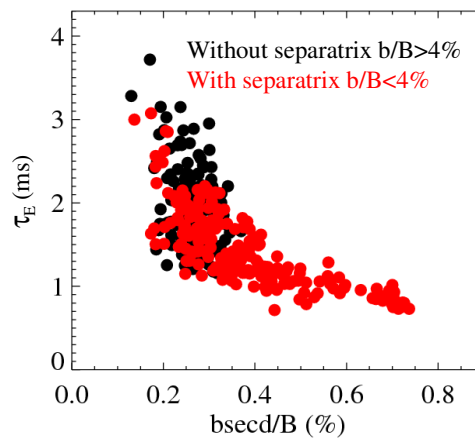


Fig. 2.2.5: Energy confinement time (assuming equal ion and electron temperatures) towards the secondary modes total amplitude

The SHAx regime is the closest ever achieved to the predicted Single Helicity regime and the volume affected by the ameliorated condition represented by QSH is large enough to have an impact on global confinement (see Fig.2.2.3). The SHAx states are obtained when the ratio between dominant mode and total B at the edge is larger than 4%, as can be seen in Fig 2.2.4. It is worth of notice that, when this ratio is larger than 4.5%, every QSH corresponds to a SHAx. Electron density profiles are essentially flat in RFX-mod [Lorenzini07], except at the edge of the plasma, in either standard or QSH regimes and SHAx; in virtue of their broader temperature profiles, SHAx regimes have confinement times that can be a factor of 2 higher than those of a QSH that has developed an island [Piovesan08], as shown in Fig 2.2.5. The

radial profile of electron heat diffusivity χ_e in stationary conditions has been determined by adopting a 1D single fluid approach and solving the power balance equation: during QSH states χ_e strongly decreases in correspondence of the transport barrier of the thermal structure. The χ_e improvement during a SHAx state in the best cases can be more than one order of magnitude and involves about one half of minor radius (as an example, Fig.2.2.6 shows χ_e profiles calculated during MH and SHAx states in the same discharge).

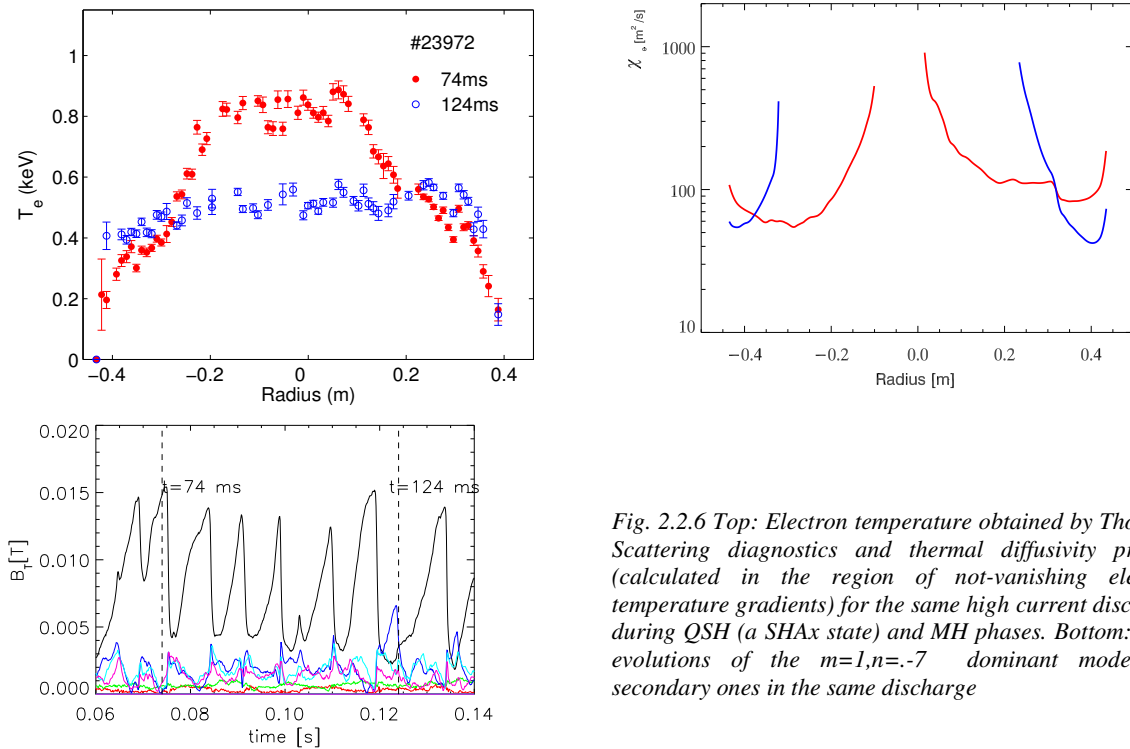


Fig. 2.2.6 Top: Electron temperature obtained by Thomson Scattering diagnostics and thermal diffusivity profiles (calculated in the region of not-vanishing electron temperature gradients) for the same high current discharge during QSH (a SHAx state) and MH phases. Bottom: Time evolutions of the $m=1, n=-7$ dominant mode and secondary ones in the same discharge

The spontaneous transitions to a QSH regime are observed in RFX-mod only for electron densities normalized to the Greenwald density $n/n_G \leq 0.3 \div 0.4$ [Puiatti09].

This corresponds to the observed increasing QSH persistency vs Lundquist number (ratio of resistive to Alfvén times)

$$S = 30 I_\phi T_e(0)^{3/2} / \left[(0.4 + 0.6 Z_{eff}) \ln \Lambda \sqrt{m_i n_e} \right]$$

since high current plasmas at relatively high density ($n/n_G > 0.4$) display a lower Lundquist number and consistently a lower dominant to residual mode ratio. When a transition to a multiple dynamo mode occurs, confinement degrades by approximately a factor of two and for this reason RFX-mod high current discharges have been run mainly at low densities, typically below $n/n_G=0.3$. Moreover, at high current the input power increases and therefore the requirements for a low recycling wall become more stringent. A still open question is if the QSH low persistency at higher densities reflects a fuelling problem which could be overcome by depositing particles in the plasma centre with pellets injection. In this respect, promising

experimental evidences of dominant mode sustainment by pellet in a phase in which the QSH was disappearing have been found (see Fig.2.2.7).

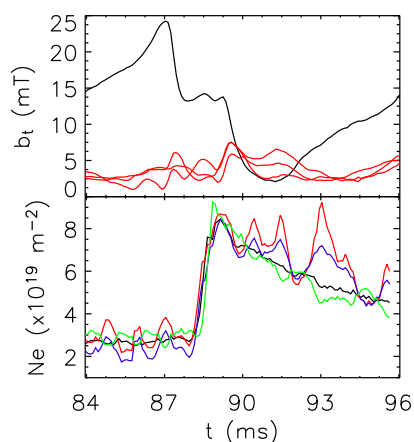


Fig. 2.2.7 Example of sustainment of the dominant mode by pellet. Top: time behavior of the toroidal component of dominant (black) and secondary modes (red) and interferometer central chords measurements (bottom).

Finding suitable conditions for high current high density discharges will be matter of investigation in the next experimental campaign.

As already mentioned, OPCD is an effective technique to systematically induce strong QSH at medium-high plasma current ($I_p=0.6-1.2$ MA). At higher currents QSH properties are essentially the same when comparing standard discharges at shallow reversal with OPCD discharges (the reversal parameter averaged over an OCPD cycle results deeper). High current standard discharges do not show spontaneous QSH states for $n/n_G > 0.3$; it still remains to be investigated if OPCD operation could stimulate QSH at high current and high density.

2.3 MHD and active control of instabilities

2.3.1 Tearing mode Control improvement

The Clean-Mode-Control (CMC), implemented in RFX-mod during 2007 [Zanca07], has been further improved at the beginning of 2008. The transfer function between the reference currents and the currents generated by the coils power supplies can be modeled by the one-pole law $F(s)=G/(1+\tau s)$. The optimization of the internal controller of the saddle coils power supply

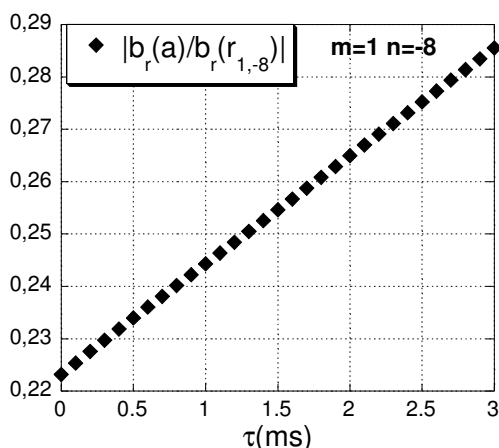


Fig. 2.3.1: Edge radial field normalized to the amplitude at the resonant surface for the $m=1$ $n=-8$ tearing mode. The computation is made with the model developed in [Zanca07].

has increased their dynamic response, reducing the pole from $\tau \approx 2$ ms to $\tau \approx 0.5$ ms [Marrelli08]. This was expected to improve the edge radial field control, according to the model for the feedback control of tearing modes described in [Zanca07]. The prediction of the model is shown in figure 2.3.1. The experimental data, plotted in figure 2.3.2, show that the new CMC (2008) allows operations at higher current with respect to the old CMC (2007): for the same current level the dominant $m=1$ $n=-7$ mode has similar amplitudes with the two control schemes, while the secondary mode ($n \leq -8$) amplitudes

are smaller with the new CMC. These are clear indications of a better control of the edge radial field.

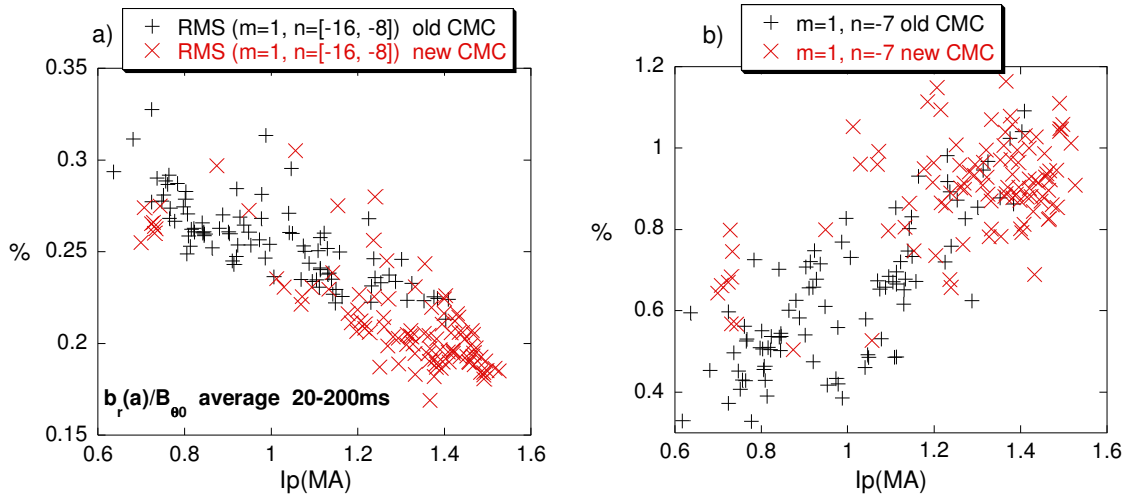


Fig. 2.3.2: Edge radial field normalized to the poloidal equilibrium field for the $m=1$ modes; a) RMS of the secondary modes; b) dominant mode. The data are averaged between 20-200ms

2.3.2 QSH dynamics

The QSH persistency (total QSH time/flattop duration) is observed to increase with plasma current (see paragraph 2.2). Nevertheless, the QSH shows a non-stationary behaviour characterized by back-transitions to multi-helical states (figure 2.3.3a) top), which still waits for a full explanation. The CMC induced rotation for the $m=1$ $n=-7$ is non-uniform, with sudden accelerations when the amplitude drops (figure 2.3.3b) bottom). This phenomenology is discussed in detail in [Grando08]. It is reproduced by simulations performed with the code described in [Zanca08], which simultaneously evolves the phases for all the $m=0$, $m=1$ tearing modes, taking for the amplitudes at the resonant surfaces the experimental values. In the simulation shown in figure 2.3.3b) the code has been adapted to the RFX-mod front-end system, which is composed by the vessel, the shell, the mechanical structures and the active

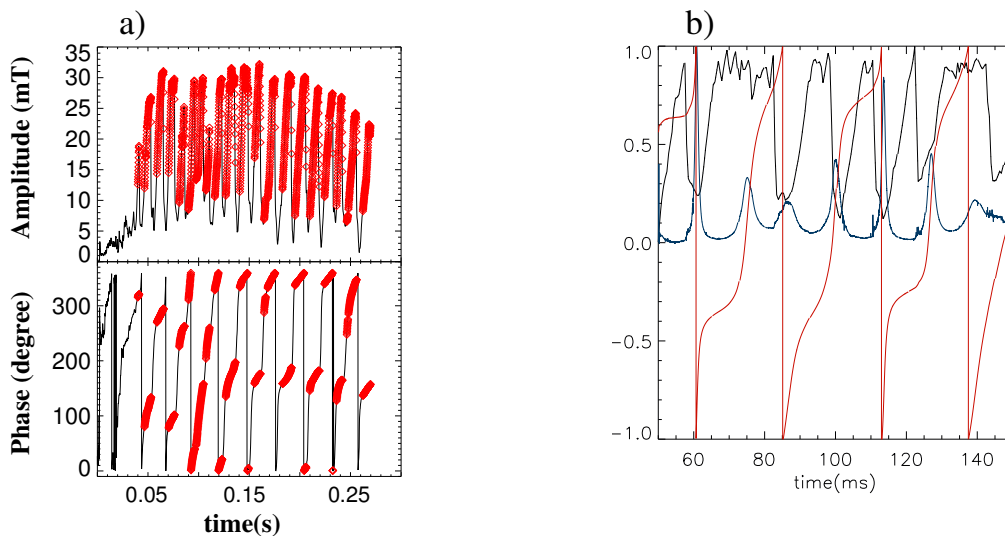


Fig. 2.3.3: a) Edge toroidal field amplitude and phase for the $m=1$ $n=-7$ mode on the shot 23841. b) Data for the $m=1$, $n=-7$ mode from a simulation with the code described in [Zanca08]; black: normalized imposed mode amplitude at the resonant surface; red: mode phase normalized to π computed by the code; blue: normalized mode angular velocity computed by the code. Both in the experiment and in the simulation the mode accelerates at the amplitude drops

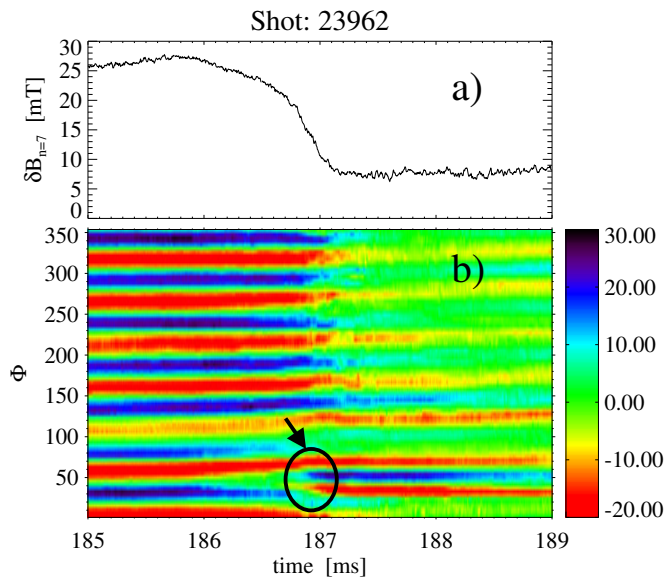


Fig.2.3.4: a) Time evolution of the $m=1$ $n=-7$ mode. b) Contour plot of the time evolution of the b_ϕ ISIS signals (48 toroidal positions); the arrows indicate the formation of the poloidal current sheet.

coil grid. There is not a clear indication that the QSH duration can be increased by a fine tuning of the feedback gains. There are instead evidences (see paragraph 2.2) that pellet injection with particle deposition inside the island can sustain the QSH during the decreasing phase.

The back-transition to the multi-helical states has been analyzed with ISIS, a system of magnetic and electrostatic probes located inside the vacuum chamber [Piovesan08]. The transition is characterized by a fast growth of a

toroidally localized perturbation as shown in figure 2.3.4b): this growth, which triggers the dominant mode crash, is followed by reconnection of magnetic field lines identified by the formation of a poloidal current sheet at the same toroidal location.

2.3.3 Single Helical Axis states (SHAx)

As discussed in sec. 2.2, experimental evidences of a new QSH state where the helical axis becomes the main magnetic axis and the original symmetry axis ceases to exist are found in high current operations (SHAx) [Lorenzini08a]. Figure 2.3.5 compares a QSH with separatrix (22158) with a SHAx (24932), showing

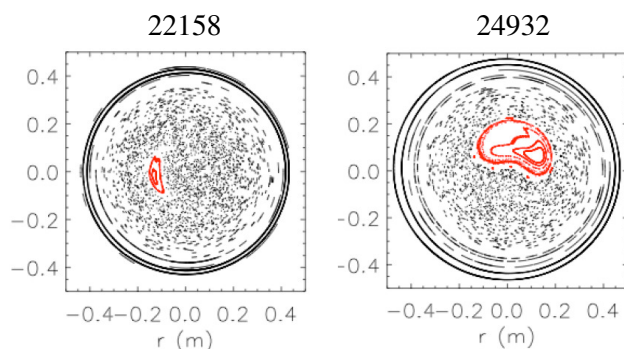


Fig.2.3.5: Poincaré plots computed with the FLiT code for a QSH state with separatrix (22158) and for a SHAx (24932).

that the latter is more resilient to the magnetic chaos produced by the secondary modes. The two Poincaré plots are computed with FLiT, a field line tracing code based on the reconstruction of the magnetic perturbation inside the plasma starting from the edge measurements [Lorenzini08a]. In the SHAx case a

relatively large structure of nested helical magnetic surfaces is present.

2.3.4 RWM studies

Experiments have shown that the controlled growth of selected RWM ($m=1, n=5,-6$) is fully compatible with 1.5MA current operation. Previous observations of negligible mode-mode interactions seem to be confirmed.

	ETAW	MARSF	CarMa	Exp.
$n=4$	5.27	5.07	7.30 7.48	≈ 6
$n=5$	8.63	8.55	12.8 13.1	≈ 12
$n=6$	14.5	14.4	22.6 23.4	≈ 22

TABLE I. Comparison between numerical and experimental RWM growth rates. Data in s^{-1} .

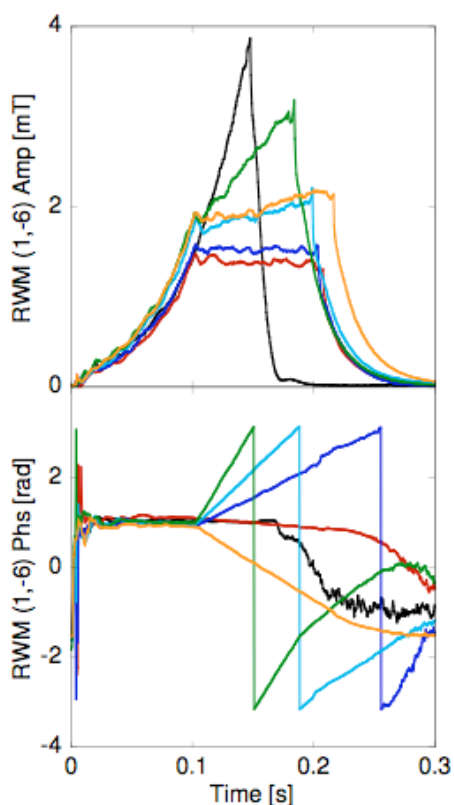


Fig.2.3.8: Imaginary gain scan on the (1,-6) RWM. (top) mode amplitudes, (bottom) mode phases. Black full traces represent a reference shot where (1,-6) RWM is initially free to grow and later in the discharge fully controlled. Other colors correspond to the application of different finite imaginary gains (active from 0.1s).

2.3.5 $m=0$ studies

A stability analysis of $m=0$ modes at shallow F with applied external perturbations has been done [Pizzimenti08]. The plasma response has been computed using a linear model. The results indicates the stability of the 0,1 mode shallow F and its poor contribution to the dynamo.

The RFX-mod experimental growth rates have been compared with the predictions of different numerical codes: the cylindrical code ETAW, the toroidal MHD code MARS-F, and the code CarMa, which takes into account 3D effects in the passive structures [Villone08]. It is

important to note that benchmarking CarMa prediction against RFX-mod experimental data is very useful for its application to ITER. Some of the results are presented in Table I. There is in general good agreement between experiment and numerical models, with a clear improvement when 3D effects are taken into account. For the first time in a RFP, it was also demonstrated that the RWM can be detached from the wall using a feedback control with complex proportional gains [Bolzonella08a, Igochine08]. The experimental results are shown in figure 2.3.8. It is found that plasma rotation, plasma current and coupling with other modes have no impact on the rotation frequency of the RWMs, which instead depends on the imaginary part of the complex gain. A computation, based on the Newcomb's equation to describe the RWM eigenfunction and the thin-shell dispersion relation to model the shell physics, is able to reproduce the experimental RWM frequency dependence on the complex gain.

The relationship of the $m=0$ island with the edge temperature, density, flow shear profiles has been established [Vianello08].

The outer region of RFP plasmas is dominated by the presence of a chain of almost poloidally symmetric $m=0$ magnetic islands around the reversal surface. These islands arise because of the resonance of $m=0$ modes and the beating of $m=1$ modes [Spizzo06] and, according to numerical models, they are believed to significantly influence transport properties at the edge, as discussed in sec. 2.4.5.1. According to the reversal parameter values F , these structures can directly intercept the first wall (for shallow reversal condition, F around -0.05) or not (for deep reversal condition, $F = -0.2$).

2.4 Particle, momentum and energy transport

2.4.1 Transport in helical states

2.4.1.1 Energy confinement and transport in helical states

Experimentally, the electron energy confinement time increases by a factor of ≈ 2 in QSH states with separatrix with respect to MH states. In SHAx states an additional factor of ≈ 2 is gained, which leads to an overall gain by a factor of ≈ 4 with respect to standard MH RFP plasmas. Best electron energy confinement values τ_{Ee} obtained in stationary conditions at $n/n_G < 0.3$ are around 2 ms [Martin08]. In SHAx regimes, an analysis of electron temperature profiles has

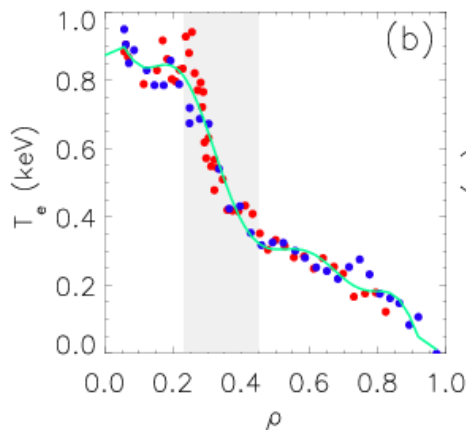


Fig.2.4.1: Electron temperature data as function of the helical-flux radial co-ordinate

been performed in terms of helical coordinates (fig. 2.4.1). The inner and outer branches of the electron temperature profile, detected by the Thomson scattering, asymmetric with respect to the geometrical axis of the vacuum vessel, becomes symmetric using as radial co-ordinate ρ , the square root of the helical flux.

In SHAx the magnetic driven transport could be so small that drift modes, of electrostatic nature, may become important, in particular where the thermal transport barriers develop.

Both gyrokinetic and fluid approaches have been adopted to study Ion Temperature Gradient (ITG) modes in RFP plasmas. The result is that these modes are in general more stable in a RFP than in a tokamak, due to the shorter connection length in RFP, but can be excited in the regions where very high T_e gradients are present, namely at the edge of the islands associated to a QSH and in the plasma edge [Guo08].

2.4.1.2 Particle transport in helical states: main gas and impurities

Plasmas in SHAx states provide an interesting environment to study central fuelling of the thermal island and particle transport using pellet injection [Carraro08].

Figure 2.4.2 shows the effect of a thermal island on the ablation rate of a pellet: as soon as the pellet enters the hot structure (bottom red trace), its ablation rate increases as shown by the

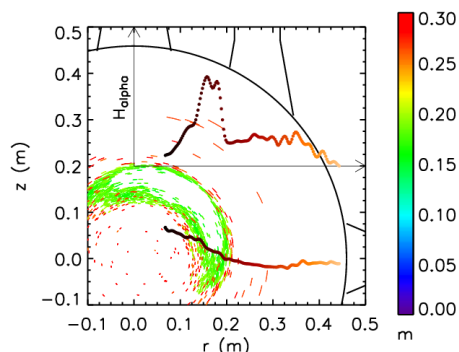


Fig. 2.4.2: pellet ablation rate correlated to the presence of an internal hot magnetic island.

H_α peak (top red trace) correlated to the internal island as reconstructed by the FLiT code (green area).

Given this result, pellet injection into hot thermal structures was attempted successfully showing that density refueling inside the hot structure is possible.

The interpretation of the interferometric data required the development of a new inversion algorithm based on the use of helical flux coordinates in order to correctly interpret asymmetries between homologous chords. In figure 2.4.3, the result of a pellet injected into a SHAx state is shown [Terranova08, Lorenzini08b]. Panel (a) shows that experimental and inverted data match very well, so that the two-dimensional reconstruction of the density has been allowed, as shown in panel (c).

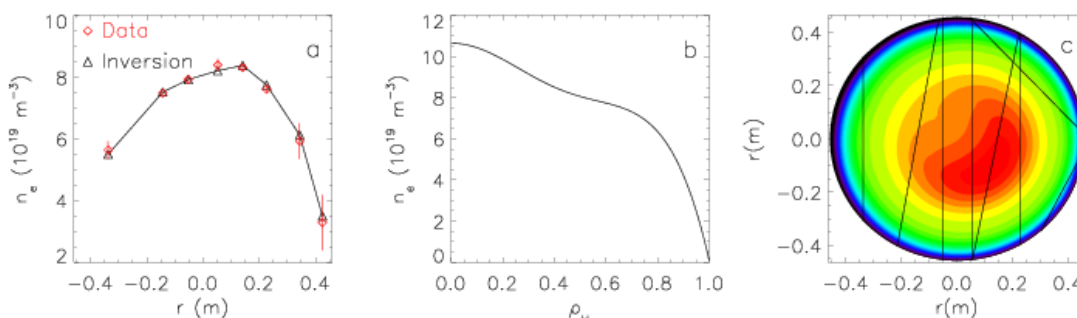


Fig. 2.4.3: pellet injection into a SHAx state: (a) experimental data and inverted data for the interferometric chords. (b) inverted density profile as a function of the helical radial coordinate. (c) two-dimensional reconstruction of the density.

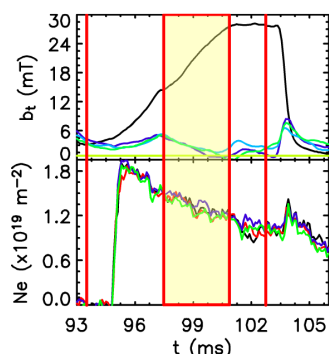


Fig. 2.4.4: time evolution of magnetic field fluctuations and electron density after pellet injection.

The possibility to reconstruct density profiles also in these extremely asymmetrical states allowed the estimate of the particle confinement time, providing indications on the particle transport.

In particular, interesting results were obtained injecting a pellet into a MH state while evolving towards a QSH state [Terranova08], as shown in figure 2.4.4. The ablation ends at about 95 ms, before a QSH state is developed. As density diffusion takes place, the evolution of the internal magnetic structure occurs in a higher density regime; as soon as the

system reaches a SHAx state, the density diffusion stops, indicating a better particle confinement. Considering the time intervals indicated by the two red lines and the shaded region, the particle confinement time has a 50% increase going from MH to QSH state and a bit less than 50% going from QSH to SHAx state.

Even when pellets do not actually enter the internal structure, the particle confinement time increases with respect to a standard MH state, indicating that the SHAx state is actually characterized by a reduced level of chaos also outside the thermal structure.

In addition to pellet injection, Ni Laser Blow Off was also performed for the first time in RFX-mod as a way to provide a traceable source inside the island present in QSH, thus allowing the study of impurity transport [Carraro08]. The injection into the hot structure was successful since the emission lines Ni XVII 249 Å and Ni XVIII 292 Å have been observed together with a significant increase of SXR emissivity, indicating that the impurity reached the high temperature region inside the helical structure.

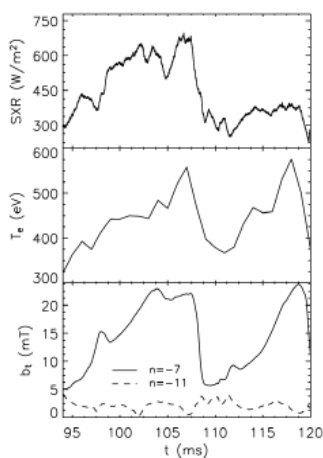


Fig. 2.4.5 Shot #24073 at 1.2 MA. Top: line integrated SXR brightness. Centre: T_e measured with a double filter diagnostic. Bottom: b_t of dominant mode $m=1, n=-7$ and $m=1, n=-11$ (representative of the secondary modes).

Fig.2.4.5 shows an example of the SXR signals following Ni injection when a QSH is developing: the SXR signal lasts for the whole QSH phase (taking as indicator the amplitude of the $n=7$ dominant mode, bottom panel of the figure), following the time evolution of the electron temperature measured with a double filter diagnostic. Due to the strongly varying plasma conditions (including poloidal and toroidal asymmetries in the T_e profile due to the helical geometry) and to the small number of LBO pulses performed, only preliminary indications on the Ni transport parameters have been obtained by reproducing the emission pattern with a 1D collisional-radiative impurity transport code [Mattoli02]. Such simulations indicate that the observed time evolution depends on the electron temperature evolution (i.e. on the energy content of the island) rather

than on strong differences in the Ni transport properties inside the thermal island. Ni emission data have been reasonably reproduced using for both the MH and QSH phases the same transport parameters ($D \sim 10\text{--}20 \text{ m}^2/\text{s}$ in the plasma centre) [Carraro06].

2.4.2 High density limit in RFX-mod

In RFX-mod plasmas the maximum density is limited to the Greenwald value ($n_G = I_p / \pi a^2$), despite the careful control of the magnetic boundary. When the density approaches the Greenwald value, plasma cools down, resistivity increases and plasma current decreases, bringing to a soft landing of the plasma discharge (and not to a disruption, as is customary in the Tokamak case). During this year, a rather comprehensive (experimental and theoretical) study of the density limit has been undertaken, showing that its phenomenology can be related to the deformation of the Last Closed Flux Surface (LCFS) due to the coherent superposition of MHD $m=0$ and $m=1$ modes (higher m 's are likely to contribute, too). The LCFS is not toroidally symmetric, but it is a coherent sum of $m=1$ and $m=0$ MHD instabilities, which is globally referred to as Locked Mode (LM). In RFX-mod is it possible to put the LM into rotation through

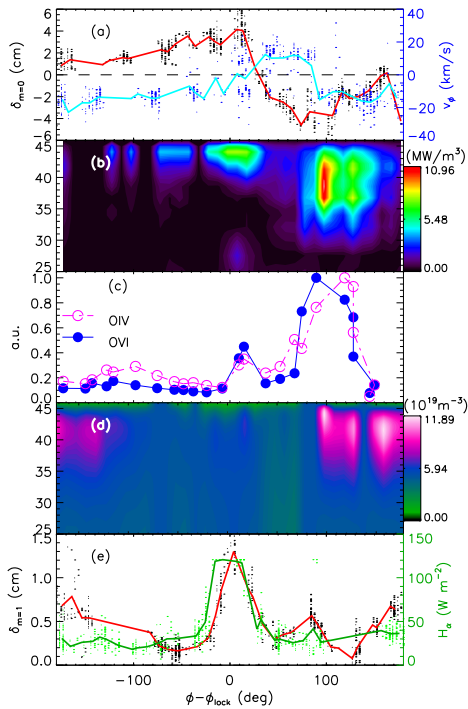


Fig. 2.4.6: As a function of the toroidal angle: (a) local displacement ψ^0 (red) and plasma flow (blue); (b) total radiation (in y axis the radial coordinate is shown in cm); (c) OIV and OVI emissivities; (d) electron density radial profiles; (e) $H\alpha$ emissivity (green) and $m=1$ perturbation ψ^1 (red).

obtained by the tomographic bolometry system, compared with the LCFS displacement due to $m=0$ modes only, ψ^0 (frame (a), red curve). Most of the radiation is toroidally localized in a belt 30° - 90° wide, corresponding to the region where the LCFS is shrunk due to the action of the $m=0$ modes, approximately at $\phi - \phi_{\text{lock}} \sim 100^\circ$. This behavior cannot be simply described in terms of localized plasma-wall interaction, since in this latter case radiation should be larger where the plasma column bulges out, at $\phi - \phi_{\text{lock}} \sim 0$. This toroidal asymmetry is not observed at lower densities, namely when $n/n_G < 0.4$.

The toroidal asymmetry is seen also in the ratio of oxygen line intensities, as shown in Fig. 2.4.6(c). As in the case of total radiation, the OVI line (Li-like) and OIV (B-like) line intensities increase at $\phi - \phi_{\text{lock}} \sim 100^\circ$. This implies, rather than a strongly recombining plasma, a widening of the radial region at low temperature (namely, between 20 and 40 eV) where these ions mainly emit. Measurements from Thomson Scattering confirm this indication.

The toroidal asymmetry at $\phi - \phi_{\text{lock}} \sim 100^\circ$ characterizes electron density as well: in Fig. 2.4.6(d) inverted density profiles obtained from the multichord interferometer are plotted as a function of the toroidal angle, showing a strong increase at the edge at $\phi - \phi_{\text{lock}} \sim 100^\circ$. The increased density is not a simple consequence of a local enhancement of the source, since the $H\alpha$ intensity, proportional to the neutrals entering the plasma, peaks in correspondence of the locking angle, at $\phi - \phi_{\text{lock}} \sim 0$ [Fig. 2.4.6(e)].

the saddle coil system: the scheme is called Virtual Shell+ Rotation perturbation, or VS + rot.pert. [Martini07]. This offers the advantage of dragging the LM around the torus, and to exploit different diagnostics to study the plasma in different toroidal positions. If the coherence of the LM is maintained in time (usually, during the whole plasma discharge in VS + rot.pert. experiments), then the time evolution of the signals is equivalent to a toroidal scan of the plasma and all signals can be plotted as a function of the toroidal distance between the diagnostic and the locking angle, $\phi - \phi_{\text{lock}}(t)$.

We analyzed a set of discharges with VS + rot.pert. and different densities. An example of this type of study [Puiatti08a, Puiatti09] is shown in Fig. 2.4.6, for a plasma discharge at $n/n_G = 0.8$. Fig. 2.4.6 (b) shows a toroidal section of the whole 3D total emissivity map $\epsilon(r, \theta, \phi)$, as

A possible explanation for the toroidal accumulation of density, which in turn causes edge cooling, radiation impurity emission and enhanced radiation [as shown in Fig.2.4.6(b)-(c)-(d)] comes from the Gas Puffing Imaging (GPI) measurements of the toroidal velocity of density blobs, which is a good approximation of the plasma flow itself. This toroidal velocity is (under reasonable assumptions) $v_\phi \approx E_r B_\theta$, where a negative sign of v_ϕ corresponds to an inward-pointing E_r . Fig. 2.4.6(a) shows that when

$$\frac{\partial \psi^0}{\partial \phi} = -B_r < 0$$

then $v_\phi > 0$, i.e. v_ϕ reverts direction with respect to the average negative value. This plasma flow reversal brings about the formation of two stagnation points: one at $\phi - \phi_{\text{lock}} \sim 0$ and the other at $\phi - \phi_{\text{lock}} \sim 100^\circ$. A simple estimate of this convective flow gives $n_{\text{edge}} v_\phi \approx 10^{23} \text{ m}^{-2} \text{ s}^{-1}$, well over the diffusive flux which, taking the coefficients calculated for RFX-mod [Innocente07], gives $D \partial n_{\text{edge}} / \partial r \approx 10^{22} \text{ m}^{-2} \text{ s}^{-1}$. This justifies the toroidal density accumulation at $\phi - \phi_{\text{lock}} \sim 100^\circ$, also favored by the behavior of the turbulent diffusion due to blobs [Scarin08a] which decreases with n/n_G , with a threshold at $n/n_G \sim 0.4$, i.e. the same threshold for the appearance of radiation belts.

2.4.3 Flow measurements and Momentum transport studies

The plasma flow profiles have been investigated in RFX-mod low-current discharges using two different types of insertable probes. One of them, a Gundestrup probe [MacLatcy92], simultaneously measures the plasma flow velocity components in directions parallel and perpendicular to the magnetic field (poloidal and toroidal in the RFP edge). The probe has been

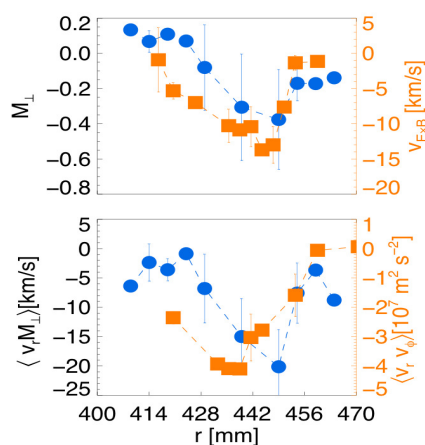


Fig. 2.4.7: Top: Profiles of the perpendicular Mach number measured by the Gundestrup (blue) and of the ExB velocity measured by the U-probe (orange); Bottom: Profiles of Reynolds stress measured by the Gundestrup (blue) and by the U-probe (orange).

used with all the pins collecting floating potential signals, and the flow has been reconstructed according to a suitable model [Jachmich00]. The other, dubbed U-probe, allows to evaluate the toroidal $E \times B$ flow profile and to estimate the Reynolds and Maxwell stresses and their radial profiles. The typical perpendicular (toroidal) plasma flow profiles measured by the Gundestrup probe are shown in the top panel of Fig. 2.4.7. The graph displays the Mach number, which is the plasma velocity normalized to the ion sound speed. As in the old RFX [Antoni97], the perpendicular velocity displays a double shear: a first shear region is located more or less across the $r = a$ surface, whereas a second shear is found deeper into the plasma. For comparison, in the same figure the radial $E \times B$ velocity

profile obtained in another set of discharges is shown. The two profiles are in quite good agreement, taking into account possible toroidal asymmetries and slightly different discharge conditions.

The generation of a sheared perpendicular flow profile has been explained in RFPs through the turbulent Reynolds stress [Vianello05]. Despite the high level of magnetic turbulence, electrostatic fluctuations seem to play a fundamental role in driving the flow at the edge, being the Reynolds stress gradient larger than the Maxwell stress one. As a further confirmation, the contribution $\langle v_r M_L \rangle$, reconstructed using the Gundestrup probe, is shown in the bottom panel of Fig. 2.4.7. As a comparison, the radial profile of $\langle v_r v_\phi \rangle$ calculated from the U-Probe in a different set of discharges is also shown. The strong gradient in the innermost shear region and consequently the role of Reynolds stress in driving the plasma flow at the edge is confirmed.

2.4.4 Edge profiles monitoring and scalings

A Thermal Helium Beam (THB) diagnostic [Scarino08b] aimed at studying the edge profiles of electron temperature (T_e) and density (n_e) has been installed in RFX-mod during 2008. A summary of the plasma parameters explored during this year by this edge diagnostic (from 0 to 50 mm inside the plasma) is shown in figure 2.4.8.

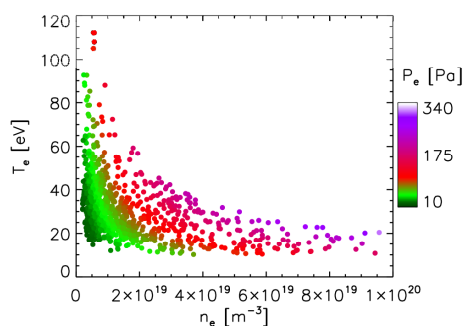


Fig.2.4.8: Edge electron pressure as a function of edge electron density and temperature measured by THB in RFX-mod. Every point is an average over 100 ms

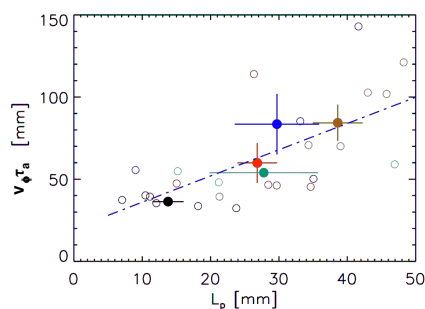


Fig.2.4.9: Characteristic perpendicular length of edge structures as a function of the characteristic radial length of the edge electron pressure L_p .

A detailed comparison with different edge diagnostics (electrostatic triple probes and edge Thomson scattering) is in progress. The THB diagnostic has been used in combination with the GPI diagnostic [Agostini06] for edge turbulence studies. In particular the link between the electron pressure gradient and the spatial dimensions of edge structures is pointed out, as shown in figure 2.4.9. The perpendicular characteristic width of the edge structures has been evaluated by the GPI as $v_\phi \tau_a$, where v_ϕ is the toroidal velocity of the edge fluctuations and τ_a is the autocorrelation time. The characteristic pressure gradient scale $L_p = -\min(P_e / \nabla P_e)$ is evaluated with the THB. In figure 2.4.9 every empty point is referred to a single discharge; the full points are averages over similar plasma discharges. A quasi-linear relation exists between $v_\phi \tau_a$ and L_p , suggesting the pressure gradient as a possible source of free energy for the development of the edge structures [Myra06].

2.4.5 Turbulence studies

2.4.5.1 Turbulence, transport and their relation with the magnetic boundary

The role of the $m=0$ magnetic islands developing around the field reversal surface (see sec. 2.3.5) and their influence on plasma transport properties have been studied. A detailed analysis has been performed in low current discharges ($I_p=300-400$ kA), where the most external part of the plasma can be diagnosed also using insertable probes. Figure 2.4.10 shows a temperature profile as a function of minor radius, as reconstructed combining Edge Langmuir probe (orange dots) and Thomson scattering diagnostic (blue diamonds) measurements. The Thomson scattering data refer to outboard and inboard side of the torus, the latter traced to outboard midplane using the Field Line Tracing code FLiT [Innocente07]. The resulting temperature profile exhibits a double gradient with a plateau located in the region $360 < r < 410$ mm.

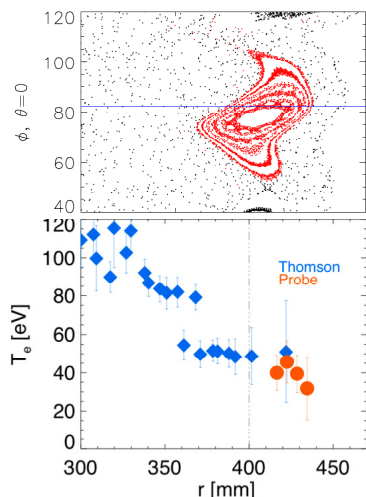


Fig.2.4.10: Poincaré plot in the $r-\phi$ plane, with a blue line marking the line of sight of the Thomson scattering (top), and temperature profile given by Thomson scattering (blue) and probe (orange) data.

The origin of this plateau can be understood by looking at the Poincaré plot computed by the FLiT code on the radial toroidal outboard plane, also shown in figure 2.4.10: in the same plot the toroidal angle of the Thomson scattering diagnostic is marked with a blue horizontal line. It

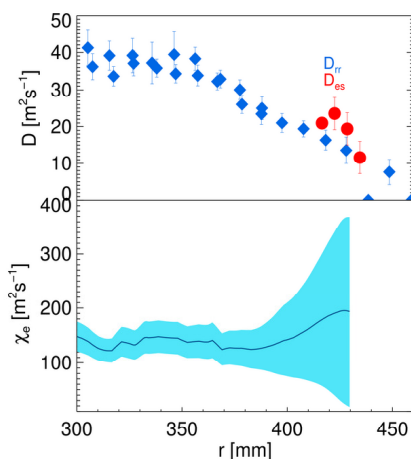


Fig.2.4.11: diffusion coefficient measured by probes (red) and estimated according to theory of transport in stochastic magnetic field (blue). Bottom: computed thermal diffusivity with a shaded region marking the uncertainty.

can be seen that the temperature plateau is due to the presence of an $m=0$ island, which, in analogy to what happens on NTM's in tokamaks, short-circuits different radial positions, smoothing the temperature (as no significant energy source is present in this region). The measured temperature and density profiles have been used to compute the diffusion coefficient and the electron thermal diffusivity shown in figure 2.4.11. In the upper panel, the diffusion coefficient as obtained from electrostatic particle flux measured from probes is compared with the diffusion coefficient calculated according to [Harvey81], that is believed to describe particle diffusivity in the presence of a stochastic magnetic field.

In the most external region, the experimental points due to the electrostatic turbulence are found larger than the stochastic ones, thus re-enforcing the analogy with tokamak. The

presence of $m=0$ islands and more generally the magnetic topology influences also the $\mathbf{E} \times \mathbf{B}$ velocity and relative shear at the edge. An example is shown in figure 2.4.12 where the time

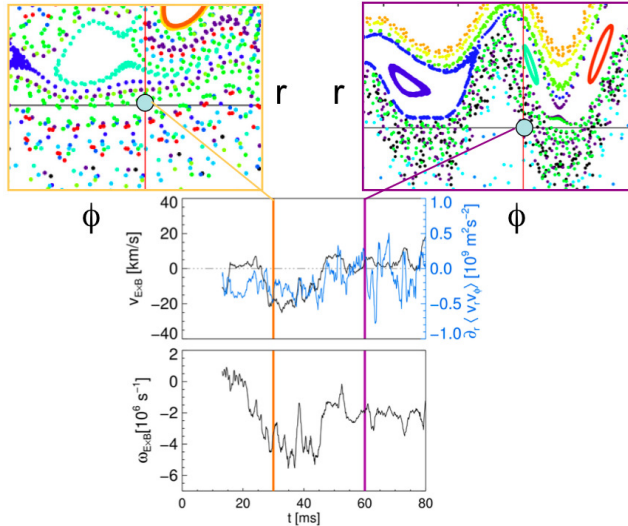


Fig 2.4.12: $\mathbf{E} \times \mathbf{B}$ and $\partial_r \langle \bar{v}_r \bar{v}_\phi \rangle$ (top) and $\omega_{\mathbf{E} \times \mathbf{B}}$ as a function of time. The two upper box shows the Poincaré plots as computed in the time instant indicated with vertical color lines.

evolutions of drift velocity and relative shear are shown as a function of time. The two colored regions indicate different values of $\mathbf{E} \times \mathbf{B}$ velocity and shear. The different behavior can be related to a change of the magnetic topology where the probe is embedded as shown in the two Poincaré plots. The higher values of flow and shear are measured on conserved surfaces around the $m=0$ island (left Poincaré plot), whereas lower values of velocity and relative gradients are observed on X-point in between the island [Vianello08].

2.4.5.2 Turbulence properties and coherent structures

Understanding and controlling the mechanism driving anomalous transport is a key issue for fusion experiments.

The observation in different devices of improved confinement regimes associated to a reduction of plasma fluctuations has fostered the research on plasma turbulence with strong emphasis on

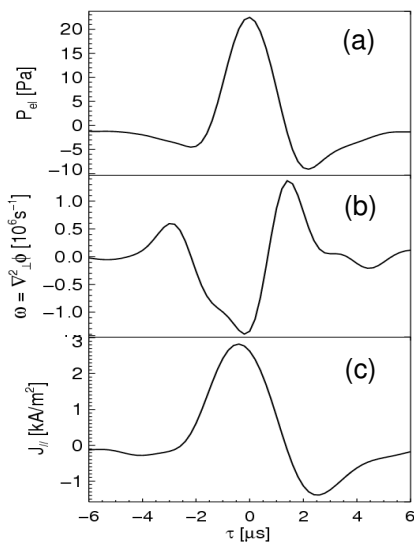


Fig 2.4.13 Typical coherent structure as seen on pressure, parallel vorticity and parallel current density at the scale $\tau = 3.3 \mu\text{s}$.

the underlying mechanisms. Experimental observations performed in tokamaks, stellarators, reversed field pinches and linear devices (see ref. [Serianni07] for a review) have revealed the intermittent nature common to plasma turbulence in all the different devices, and the fact that intermittency is generally associated to the presence of “blobs”, that is coherent structures. These structures are the results of strong non-linearities, and although originally believed to be 2D lying in the perpendicular plane, they are now generally described as 3D structures elongated in the parallel direction.

Measurements of different electrostatic quantities, obtained with a composite insertable probe named U-probe, have been analyzed using the statistical techniques described in [Farge92, Antoni01], with the aim of identifying coherent structures associated to

bursts in the fluctuation time series. Peaks on the electron pressure signal have been used as trigger. The average features of these events have then been extracted by applying the conditional average method on time window widths adequate to their time scale. The typical coherent structure detected by this method at the scale $\tau = 3.3 \mu\text{s}$ is shown in Fig. 2.4.13. The pressure peak is accompanied by a parallel vorticity peak, so that it can be deduced that the pressure structure is associated to a local velocity eddy [Spolaore08a]. It has to be mentioned that the electromagnetic nature of the coherent structures emerging from the turbulent background has been experimentally confirmed also at higher current regimes (1.5 MA) by the GPI [Spolaore08b]. The measured local structure of magnetic fluctuations results to be consistent with the one expected for a poloidally elongated 1D current filament structure moving with the local plasma $E \times B$ velocity.

2.5 Optimization of RFX-mod discharges

2.5.1 *Error field and Start-up optimization*

The fast evolution of the plasma in the very first part of the discharge, when the RFP configuration is forming, is well beyond what the feed-back (FB) system can deal with. To this end the control scheme was modified in order to allow a feed-forward (FF) control adding on top of the FB system a set of 192 current references for the power supplies of the saddle coils system. The control software is now operational and the FF scheme was tested in vacuum discharges.

The first tests of the FF control scheme were based on two approaches: first determine the error fields (or more precisely the non-uniformities) produced by each axisymmetric winding along with the passive structures; second consider only the main non-uniformities (i.e. the two poloidal gaps) with a reference winding programming. The first approach allowed a more general evaluation of the error fields to be corrected along with a scaling of the fields with the current in each winding, putting into evidence the main non-uniformities: the two poloidal gaps, the toroidal gap, the five oblong windows, and the layout of the magnetizing winding busbars placed in high field regions of the torus. However, given the complex results obtained and the need to calculate from those error fields the currents required to control them by means of a dynamic decoupler (not yet completely reliable), the second approach was considered simpler for determining the effectiveness of the FF scheme. In this latter scheme the required references were calculated using the static decoupling matrix and applied in FF to a reference discharge. The first results show that the FF system should be able to partially correct the field non-uniformities in the start-up phase. However, the use a dynamic decoupler is necessary in order to avoid a manual optimization of the references. Optimization of the scheme is still ongoing both on experimental and numerical basis.

2.5.2 *Horizontal Equilibrium Control*

The horizontal equilibrium real time control system was formerly implemented and optimized to properly work in the current range 0.6÷1.2 MA. The need to improve equilibrium control for

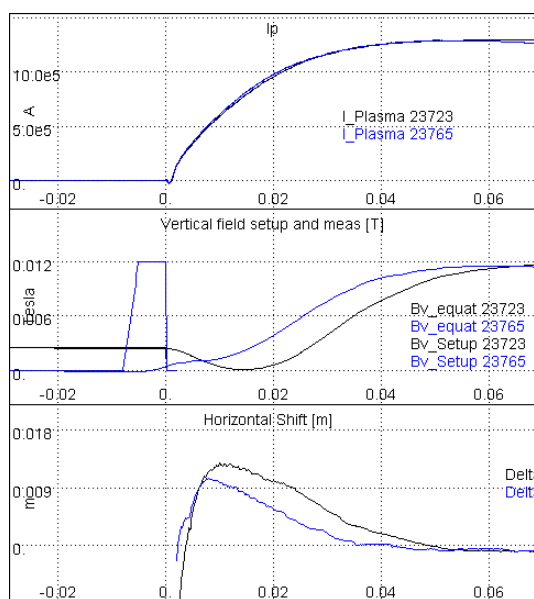


Fig. 2.5.1: comparison of the behavior of the horizontal shift with fixed (#23723 in black) and pulsed bias (#23765 in blue).

reliable operation in all current ranges came either for very low and high current experiments (tokamak with $I_p < 100$ kA and RFP with $I_p \geq 1.5$ MA). To this purpose, a smart PI controller which scales the output proportionally to the plasma current has been successfully implemented, tested and is now routinely used.

The conducting shell on RFX has a characteristic time constant for the vertical field penetration of about 70 ms. This makes the horizontal control during the early part of the discharge (which includes the critical phases of breakdown, field-reversal and current ramping) quite challenging. The traditional

method of applying a bias vertical field requires the use of a relatively high toroidal bias field in order to allow breakdown; this in turn implies a reduction of the breakdown window, forcing the use of a significant filling pressure, a slowdown of the breakdown process, which wastes flux swing, and a relatively frequent failure of the reversal phase. To solve this problem, a pulsed bias scheme has been developed, exploiting the fact that the current rise time is comparable to the vertical field penetration time (Fig. 2.5.1). A more reliable start-up scheme has been established, with a considerable reduction of the gas filling required to get breakdown and field reversal. However, it produces higher field errors at the gaps which have to be corrected with the saddle coil system (see sec. 2.5.1).

2.5.3 Similarity studies between MST and RFX-mod

This activity is included in the framework of the IEA implementing agreement on reversed field pinches, and is part of the long standing collaboration project between the RFX and MST groups. RFX-mod and MST experiments share a similar geometry but use different technological solutions for plasma formation and confinement, e.g. magnetic boundary, plasma-shell proximity, error field control, first wall. In the recent past, they used to operate in a different parameter space and produce optimized plasmas in different conditions. Being the only possible choice for RFX-mod, the filling gas was hydrogen for both machines.

2.5.3.1 On standard pulses

To address the relevance of these machine features on plasma behavior, we carried out a first set of similarity experiments on both RFX-mod and MST by producing standard discharges under controlled conditions, with plasma normalized parameters as comparable as possible. The parameters chosen for this first comparison were: plasma current of 400 kA, electron density of $1 \cdot 10^{19} \text{ m}^{-3}$, and reversal parameter F of -0.05 and -0.2. Preliminary observations can be divided into magnetic [Zanotto08] and kinetic [Reusch08] analysis. By looking at magnetic

data, it is easily confirmed that for a given reversal parameter F (used as control parameter in the discharge setup), the two machines exhibit different magnetic equilibrium profiles with higher Θ values in MST. As for the magnetic fluctuations, the dynamo mechanism in MST shows a more discrete activity while in RFX-mod the fluctuation spectrum is more often in a stable Multiple Helicity state with mode and wall locking. Kinetic measurements include central averaged data and radial profiles: it is interesting to note that, in spite of the different boundary conditions, density and temperature profiles are very similar both on average and also when compared at the time of a reconnection event. The first important result of this similarity exercise between RFX-mod and MST plasmas is that similar plasmas can be obtained and analyzed under similar normalized parameters. We plan to extend in 2009 the database and to deepen the data interpretation, including stability of magnetic equilibria and transport analysis.

2.5.3.2 On PPCD pulses

A similarity study between RFX-mod and MST has also been done taking into account the different response of the two plasmas to the application of the Pulsed Poloidal Current Drive (PPCD) under controlled conditions. The aim was to address modifications or upgrades in the operations to improve performance. In RFX-mod the new CMC control of the magnetic

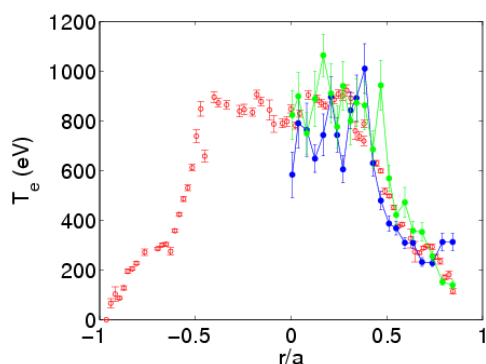


Fig.2.5.5: T_e profiles from Thomson scattering in RFX-mod (red) and MST (blue and green).

boundary and its combination with boronization and glow discharge cleaning (GDC) allowed for a cleaner MHD boundary, making possible the exploration of low density regimes (n_e of about $1 \times 10^{19} \text{ m}^{-3}$). PPCD experiments have been done on these plasmas, keeping the plasma current at about 400kA and setting a reference wave form for the time evolution of F down to deep reversed toroidal magnetic field. Operations have been performed without sustainment of the current

or with limited sustainment during the PPCD: this has allowed a decrease in the loop voltage. In addition, the timing of the PPCD and the minimum value of the reversal parameter F have been changed in the search of the setup which allowed for magnetic mode reduction and increase in electron temperature (the usual outcome of the application of the PPCD).

In MST a similar experimental campaign has been performed. Selecting a few discharges to be used as a reference, namely 400kA PPCD plasma pulses at density between 1 and $2 \times 10^{19} \text{ m}^{-3}$.

The results show that, in both devices, the plasma current and F have the same time evolution (during startup for I_p). In addition, the values of the poloidal electric field E_θ are comparable. Magnetic fluctuations time evolution in RFX-mod is similar to “bad” PPCD pulses of MST. During PPCD experiments on MST, T_e profiles similar to those found on RFX-mod during

SHAx states have been measured (fig.2.5.5), and Poincaré plots from the ORBIT code show similar features in the two experiments [Alfier08b].

In the near future, additional runs will be required in both machines to add data and increase statistics, and to continue the investigation of new types of PPCD in RFX-mod.

2.5.4 Magnetic optimization of the discharge for high current operation

In view of high current operation, the magnetic configuration of the discharge has been optimized both at start-up and during flat-top. At start-up, a different toroidal field setting-up has been assessed that makes use of 12 independent inverters (one for each toroidal winding sector) to produce the bias toroidal field and to perform field reversal. This mode of operation has allowed an improved control over the reversal phase with respect to the standard

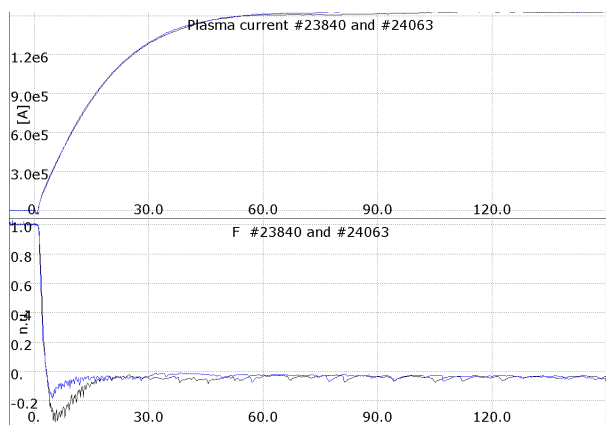


Figure 2.5.6: Reversal parameter undershoot before (black) and after (blue) the optimization.

operation, with series connection of the toroidal winding sectors. In particular, a limitation of the so called undershoot of the reversal parameter has been achieved, as shown in Fig. 2.5.6 where the start-up with standard and improved operation are compared. Further optimization has been performed to improve the symmetry of the current distribution among the toroidal winding sectors.

2.5.5 Tests of Dynamic Pseudo-Decoupler

The term dynamic pseudo-decoupler refers to either an approximation of the inverse of the active system for the control of MHD instabilities and to the algorithm which implements the input-output behavior of such a system. The conceptual design of the pseudo decoupler and the result of simulations with a continuous version of it were made in 2007 [Marchiori07].

The implementation of the pseudo-decoupler algorithm, substantially a discrete state space update, is on-going work. The state space update, which is equivalent to a 576×576 matrix-vector product, has to be performed in 150 microseconds or less. To achieve this performance, an algorithm has been designed to exploit at best the hardware of the computational node (Motorola MV5500) and new kernel options have been set in order to reconfigure its private memory settings. One day of experimental time has been allocated for the early phase of the commissioning of the real-time pseudo-decoupler. Studies on the possibility of applying the pseudo-decoupler paradigm to the radial field error correction have been made.

The purpose of the experimental activity was to test the effect of the above mentioned reconfiguration of the private memory, the overall behavior of the real time control system in the presence of a running instance of the pseudo-decoupler algorithm and also to further check its implementation correctness.

The results were successful from a systemic point of view. The new configuration of the private memory did not alter the operation of the other control system parts and the algorithm run in less than 170 microseconds, which is still compatible with a control sampling frequency of 2.5 kHz.

Careful analysis of the discretised pseudo-decoupler implementation procedure triggered by the error field studies revealed other points to be improved. In particular:

- 1) An integral and consistent model of the geometry and the electromagnetic properties structure is mandatory for any further development of the pseudo-decoupler, and in particular for its applications to the error field correction.
- 2) The design proposed in [Marchiori07] which is based on identifying the pseudo decoupler with 2 poles and 2 zeros transfer functions poses limitations in the discretisation process. A single zero, 2 pole design should be more adequate. This implies that the range of applicability of the dynamic decoupling drops from 0 – 200 Hz to 0 – 50 Hz.

2.6 Density control and plasma-wall interaction

Density control is a primary issue for the operation of the machine. One of the main critical topics concerning density control involves the routine machine operation. In recent years the difficulties found in controlling density during experiments had slowed down the operation and limited the effectiveness of physics experiments, sometimes requiring several pulse repetitions and time consuming Helium glow discharge cleaning in order to obtain the desired density conditions. During this year several efforts have been devoted to address this problem, having in mind the main goal of simplifying the operation of the machine, by keeping the density in a useful range for a significant number of consecutive pulses during experimental sessions. A further more challenging objective was to obtain a predetermined value of electron density in a given experiment.

The main activities carried out during this year to pursue these objectives have been:

- the development and operation of a diagnostic system to measure the effective gas filling and first wall (FW) desorption (see DESO diagnostic in sec. 4.1.7);
- the optimization of start-up scenarios in order to minimize filling requirements (see sec. 2.5.2 and sec. 2.5.5);
- the systematic verification of density behavior after major FW treatments, namely Baking and Boronization, against dedicated benchmark pulses;
- the pre-load of FW by means of short Hydrogen glow discharges.

The use of the DESO diagnostic has allowed a quantitative measurement of the Hydrogen flow to and from the vacuum vessel, prior, during and after the plasma pulse. It is well known that the graphite FW acts as a getter for Hydrogen and the machine is operating always at a recycling factor close to one, since the particle confinement time is of the order of few ms. The

baseline density of each plasma pulse does not depend on the initial filling pressure (Fig. 2.6.1), but on the FW loading condition (Fig. 2.6.2) and on the incident power density (Fig. 2.6.3).

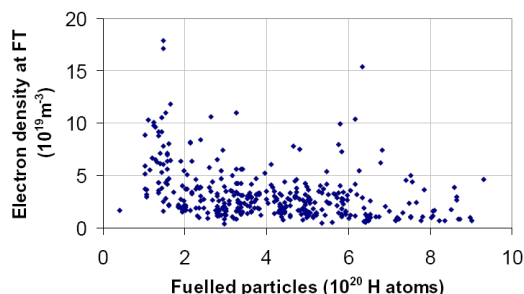


Fig.2.6.1: Flat top electron density as a function of initial filling pressure: the final density does not depend on the filling [Canton08b].

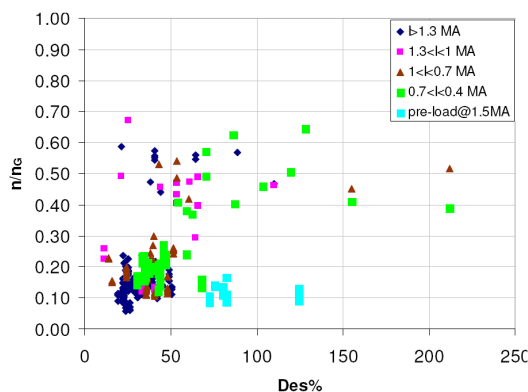


Fig.2.6.2: density normalized to Greenwald limit vs percentage of desorbed particles after the pulse over the total fuelled particles. The Des% factor gives an estimation of the capability of the wall loading factor and its ability to refuel the discharge [Canton08a].

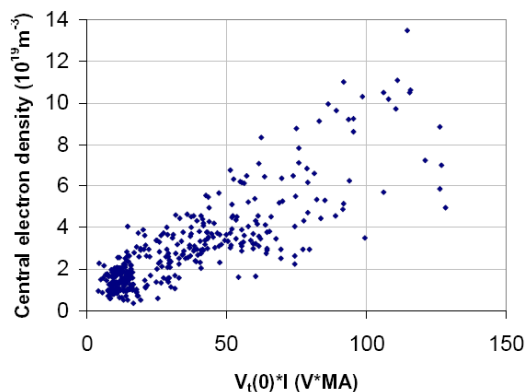


Fig.2.6.3: central electron density at flat top versus ohmic power input [Canton08b]

Pulse after pulse, only a fraction of the Hydrogen fuelled (as the sum of filling, puffing and pellet) is pumped out after the discharge and most of it is adsorbed by the FW. Thus in the absence of FW conditioning an increasing value of the density is observed on a shot by shot basis. Given this constraint the optimizations have been carried out in order to minimize the filling required for a correct plasma startup (sec. 2.5.2 and sec. 2.5.4). In a typical experimental

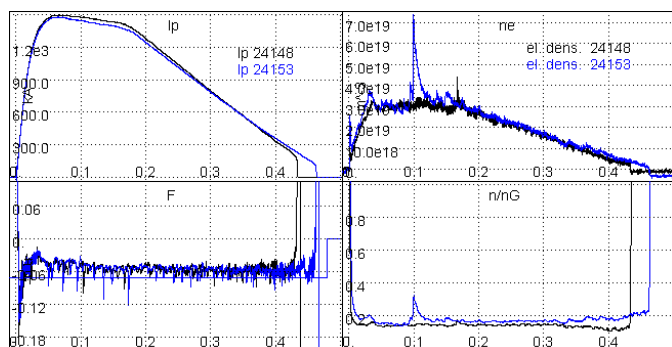


Fig 2.6.4: two highly reproducible discharges obtained after 1 hr Helium GDC and 4 min. of glow in Hydrogen. A pellet injection was added on pulse #24153. It is worth noting that the equilibrium density before the pellet injection is the same.

day, 10 to 15 subsequent high current shots can be obtained before losing the density control because of FW saturation.

In order to achieve a predefined density value, a few minute long glow discharge in Hydrogen has been applied after one hour of standard Helium discharge cleaning. Reproducible

correspondence between the number of implanted particles and plasma density has been obtained (Fig 2.6.4). At the maximum explored plasma currents $I \sim 1.5$ MA, the effect of pre-load lasts for only one shot, while at $I < 1$ MA it lasts for several shots (of the order of 10). However this technique has been

proven useful only for a few weeks after boronization, since later the FW quickly saturates after the first shot.

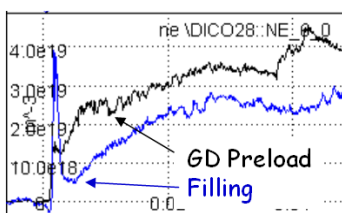


Fig.2.6.5: improvement of density behaviour at startup obtained by FW preload by means of Hydrogen glow discharge.

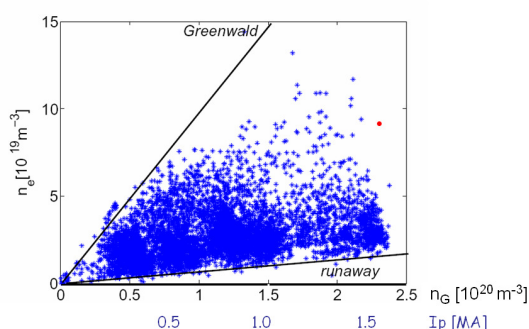


Fig.2.6.6: Achieved density electron versus given nominal Greenwald limit [Puiatti08b]. The red point corresponds to peak density obtained with pellet injection in pulse # 24153 (Fig. 2.6.4).

The wall preload technique has been proven to be very effective also during plasma startup, since it avoids the density loss associated to the reversal phase at RFP formation (Fig. 2.6.5).

Despite the improvements achieved in density control, the density levels obtained at high steady currents around 1.5 MA have been in the range 3 to 5 · 10¹⁹ m⁻³ for the baseline density, with transient values close to 10²⁰ m⁻³ obtained by means of pellet injection (Fig.2.6.6). This regime is still significantly far from Greenwald limit as mentioned in sec. 2.2. A key question remains open: could an operation with reduced wall recycling and efficient core fuelling by pellets allow achieving higher densities at high current? Experiments on this topic are planned for the next campaign.

2.7 Database and scaling laws

2.7.1 Optimization and validation of a reference RFX-mod database

A validated reference database is an essential tool for scaling studies and also necessary for the entire experimental programme. Efforts have been devoted to encourage a common approach to data analysis that takes advantage of a public depository of validated data and of cross-validation of different diagnostics and models.

A procedure has been developed to trace modifications to pulse files, in order to guarantee that derived quantities are aligned with modifications and to allow retrieving and displaying of older versions. This new procedure takes advantage of an MDSPlus feature, so that different versions of data are identified by their insertion dates.

Other tasks have been identified and have just started along this line: update documents describing on-line programmes (a reference person has been identified for each subtree in the pulse file); maintain and encourage the use of the summary database; favor working groups on specific validation tasks.

A study has been carried out by a working group on the evaluation of Ohmic Power (P_{ohm}) from the available measurements, which has addressed several issues: sensitivity of P_{ohm} estimate on signal filtering and on current and pressure profiles; fluctuations impact on estimate of magnetic energy. It has been assessed that during transient events the

instantaneous Pohn value depends on the filtering interval and it was proposed to include the measured T_e profile in the calculation. Other evaluations of the ohmic input power have also shown that no ‘anomalous’ loop voltage seems to be required to sustain an RFP configuration and that trapped particles play an important role on plasma conductivity also in high temperature RFP devices [Bolzonella08b].

2.7.2 Assessment of RFX-mod scaling laws

Only one proposal in the 2008 experimental programme was specifically dedicated to scaling laws, but many other experiments contributed, in particular extending the plasma current range of operation. Scalings of kinetic energy parameters, like T_e , n_e , poloidal beta and electron energy confinement time have been extended to I_p values exceeding 1.5 MA. It was found that T_e increases linearly with I_p in Clean Mode Control operations (Fig.2.7.1), electron poloidal beta only depends on I/N , not on I_p , and energy confinement time scales well with secondary mode amplitudes (Fig.2.7.2) [Innocente08].

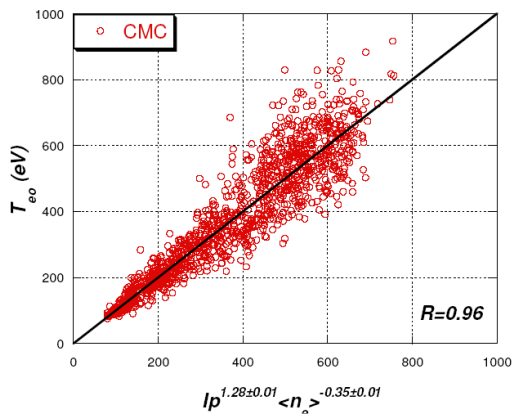


Fig.2.7.1: scaling of central T_e with current and density

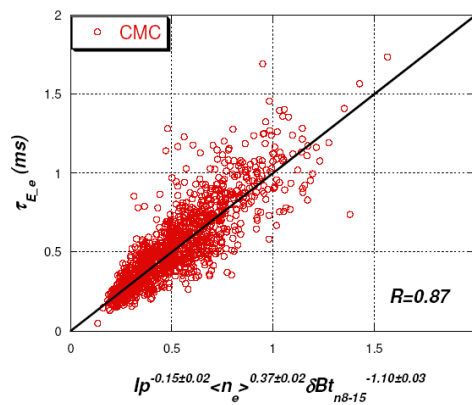


Fig.2.7.2: scaling of energy confinement time with current, density and secondary mode amplitude

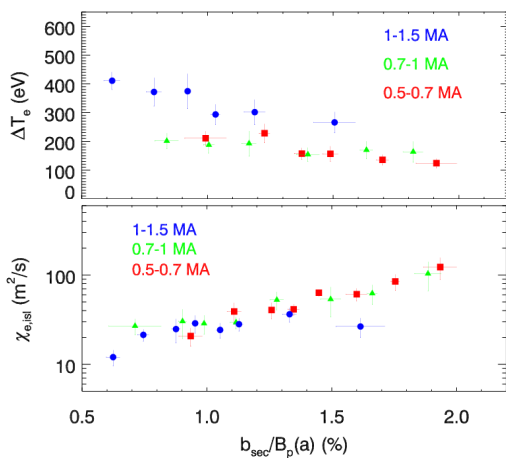


Fig.2.7.3: T_e step and corresponding heat diffusivity of hot island during QSH vs relative amplitude of secondary modes, from Thomson scattering

Other studies focused on scaling of T_e profile characteristics, measured with Thomson scattering, like the steep T_e gradient and corresponding heat diffusivity of the hot island during QSH (fig. 2.7.3) [Alfier08a].

A heat diffusivity model was developed, which well reproduces experimental T_e profiles and produces scaling of confinement properties with magnetic fluctuations [Frassinetti08]. Finally, some effort has been put in trying to find common scaling laws for RFP and tokamak, given the different physics,

taking also advantage from tokamak operation in RFX.

2.8 Neutral beam injector feasibility study

A 25 keV , 50 A, 30 ms pulse Neutral Beam Injector is to be delivered to RFX from the AIST Institute Tsukuba, Japan at the beginning of 2009. A preliminary exercise to predict the fast ion trajectories in the RFX plasma has been performed by means of the test particle code ORBIT. The only possible geometry for the injection of energetic ions is through an equatorial port, which implies that the pitch angle of the particles, with respect to the magnetic field, will be very small, departing from zero due only to the natural divergence of the beam. In such situation, the neutrals ionized on the low field side will become mostly trapped particles, following banana orbits with a very small, sub mm, radial excursion at the very edge to increase and reach several cm towards the plasma centre. Particles that cross the center and are ionized in the high field side will mostly become passing particles. The beam penetration will obviously depend on density and a complete absorption is predicted for a density around $5 \cdot 10^{19} \text{ m}^{-3}$. Confinement of fast particles in RFX-mod is predicted to be of the order of tens of ms. Therefore it is expected that the beam injection will exert little momentum on the plasma and also provide little auxiliary heating as the energy exchange is long compared to the typical energy confinement time of the electrons, or, in different words, as the RFX-mod typical input power is at least ten times higher than the beam power. Confinement improvements as the plasma current is further raised might favorably change such perspective. Instead, the injector will provide a good means to study the confinement properties of fast particles in a RFP, which have been shown in MST to have very interesting properties, with a confinement time much longer than thermal ions.

REFERENCES:

- [Agostini08] Agostini, Cavazzana, Scarin, Serianni, Rev.Sci.Instrum., **77**, 10E513 (2006)
- [Alfier08a] A. Alfier, R. Pasqualotto, G. Spizzo, A. Canton, A. Fassina and L. Frassinetti, Plasma Phys. Control. Fusion **50**, 035013 (2008)
- [Alfier08b] A Alfier, 13th IEA RFP Workshop – Stockholm, Sweden – 9-11 October, 2008
- [Antoni97] Antoni V., et al. Phys. Rev. Lett. **79**, (1997) 4814.
- [Antoni01] Antoni V., et al. Europhys. Lett., **54**, (2001) 51.
- [Bolzonella08a] T. Bolzonella, V. Igochine, et al., Phys. Rev. Lett., **101**, 165003 (2008)
- [Bolzonella08b] T. Bolzonella, P. Innocente, A. Alfier, F. Bonomo, L. Carraro, L. Marrelli, R. Pasqualotto, D. Terranova, “Insights on ohmic input power evaluation in the RFX-mod reversed field pinch”, 35rd EPS Conference on Plasma Phys.
- [Canton08a] A. Canton, S. Dal Bello: ‘Density control in RFX-mod’, 13th IEA/RFP Workshop, Stockholm 2008.

- [Canton08b] A. Canton, S. Dal Bello, R. Cavazzana, P. Innocente, P. Sonato, C. Taliercio, M. Breda: *Density Density control in RFX-mod Reversed Field Pinch Device* 35th EPS Conference, Hersonissos Crete 2008.
- [Cappello92] S. Cappello, R. Paccagnella, *Phys. of Fluids*, **B4** 611 (1992)
- [Cappello04] S. Cappello, *Plasma Phys. Control. Fusion* **46** B313 (2004)
- [Carraro06] L. Carraro et al. 33th EPS Conference Rome Italy 2006 P5.083
- [Carraro08] L. Carraro, D. Terranova et al. 'Particle transport in different magnetic field topological configurations in the RFX-mod experiment' 35th EPS Conference Hersonissos Crete 2008 P-4.019
- [Escande00] D.F. Escande et al, *Phys. Rev. Lett.* **85**, 3169 (2000)
- [Farge92] Farge M. *Annu. Rev. Fluid Mech.*, **24** (1992) 395.
- [Frassinetti08] L. Frassinetti, A. Alfier, R. Pasqualotto, F. Bonomo, P. Innocente, *Nucl. Fusion* **48**, 045007 (2008)
- [Gobbin07] M. Gobbin et al., *Physics of Plasmas* **14**, 072305 (2007)
- [Grando08] L. Grando, G. Manduchi, L. Marrelli, G. Marchiori, et al: "Active control of resonant MHD modes in RFX-mod", 22nd IAEA FEC, Geneva, Switzerland, 2008, proceedings to be published (P9-8).
- [Guo08] Guo S.C., submitted to *Phys. Rev. Lett.* (2008)
- [Igochine08] V. Igochine, T. Bolzonella, et al.: "Externally induced rotation of the resistive wall modes in RFX-mod", 35th EPS Conference on Plasma Phys. Hersonissos, 9 - 13 June 2008, proceedings ECA Vol.32F, P-2.066 (2008).
- [Innocente07] P. Innocente, et al., *Nucl. Fusion* **47**, 1092 (2007)
- [Innocente08] P. Innocente, A. Canton, A. Alfier, R. Pasqualotto, "Scaling studies in RFX-Mod" 13th IEA RFP Workshop – Stockholm, Sweden – 9-11 October, 2008
- [Jachmich00] Jachmich S., et al. in *Proc. 27th EPS Conference on Contr. Fusion and Plasma Phys. Budapest*, 12–16 June 2000 ECA Vol. **24B** (2000) 832-835.
- [Lorenzini07] R. Lorenzini et al., *Nucl. Fusion* **47** 1468 (2007)
- [Lorenzini08a] R. Lorenzini et al., *Phys. Rev. Lett.* **101**, 025005 (2008)
- [Lorenzini08b] R. Lorenzini and RFX-mod team, 50th Annual Meeting of the Division of Plasma Physics – APS, Dallas, Texas, 17 – 21 November, 2008, invited CI1.00002
- [MacLarty92] MacLarty C. S., et al. *Rev. Sci. Instrum.* **63** (1992) 3923.
- [Marchiori07] G. Marchiori, A. Soppelsa, *Fusion Engineering and Design* **83**, 224 (2008)
- [Marrelli08] L. Marrelli, et al: "Advances in MHD mode control in RFX-mod", 35th EPS Conference on Plasma Phys. Hersonissos, 9 - 13 June 2008, proceedings ECA Vol.32F, P-5.065 (2008)
- [Martin07] P. Martin et al., *Plasma Phys. Control. Fusion* **49** A177–A193 (2007)
- [Martin08] P. Martin et al., in *Proc. of the 22nd IAEA Fusion Energy Conference*, 13-18 October 2008, Geneva, Switzerland, OV/5–2Ra

- [Martines08] E. Martines et al., in Proc. of the 22nd IAEA Fusion Energy Conference, 13-18 October 2008, Geneva, Switzerland, EX/P5-26
- [Martini07] S.Martini and the RFX-mod team, Nucl. Fusion **47**, 783 (2007).
- [Mattioli02] M. Mattioli et al., Plasma Phys. Control. Fusion **44**, 33 (2002)
- [Myra06] J.Myra et al. Phys. Plasmas., **13** 092509 (2006)
- [Piovesan08] P. Piovesan et al.' Magnetic order improvement through high current and MHD feedback control in RFX-mod' 35th EPS Conference Hersonissis Crete 2008 O-4.029
- [Pizzimenti08] A. Pizzimenti, R. Paccagnella, Plasma Phys. Control. Fusion, **50** (2008) 065006.
- [Puiatti08a] M.E.Puiatti, P.Scarin, G.Spizzo, M.Valisa, et al., in Proc. of the 22nd IAEA Fusion Energy Conference, 13-18 October 2008, Geneva, Switzerland, EX/P5-05
- [Puiatti08b] M.E. Puiatti: *RFX-mod plans for the next future* 13th IEA/RFP Workshop, Stockholm 2008.
- [Puiatti09] M.E. Puiatti et al. 'High density limit in Reversed Field Pinches' Phys. of Plasmas accepted for publ.
- [Reusch08] J Reusch et al. 'Similarity experiments on RFX-mod and MST standard discharges: Kinetics', 13th IEA RFP Workshop – Stockholm, Sweden – 9-11 October, 2008
- [Scarin08a] P.Scarin et al., in 18th PSI Conf. (Toledo, Spain, 2008), to be published in J.Nucl.Mater.
- [Scarin08b] P.Scarin, M.Agostini, et al., 50th APS, 17-21 November 2008, Dallas
- [Serianni07] Serianni G., et al. Plasma Phys. Control. Fusion **49** (2007) B267
- [Spizzo06] G. Spizzo, et al., Phys. Rev. Letters **96**, 025001 (2006)
- [Spolaore08a] M. Spolaore et al., to be published on Journal of Nuclear Materials
- [Spolaore08b] M. Spolaore, N. Vianello, M. Agostini et al. submitted to Physical Review Letters
- [Terranova08] D. Terranova et al. 13th IEA-RFP workshop, Stockholm, Sweden, 9-11 Oct. 2008
- [Vianello05] Vianello N., et al. Phys. Rev. Lett. **94**, (2005) 135001.
- [Vianello08] N. Vianello, et al: "Turbulence, transport and their relation with magnetic boundary in the RFX-mod device", 35th EPS Conference on Plasma Phys. Hersonissos, 9-13 June 2008, proceedings ECA Vol.32F, O-4.049 (2008).
- [Villone08] F. Villone, Y.Q. Liu, R. Paccagnella, et.al., Phys. Rev. Lett., **100** (2008) 255005.
- [Zanca04] P.Zanca and D.Terranova, Plasma Phys. Contr. Fusion **46**, 1115 (2004)
- [Zanca07] P. Zanca, L. Marrelli, et al., Nuclear Fusion **47**, 1425 (2007).
- [Zanca09] P. Zanca, Plasma Phys. Control. Fusion **51**, 015006 (2009)
- [Zanotto08] L Zanotto et al., 'Similarity experiments on RFX-mod and MST standard discharges: Magnetics', 13th IEA RFP Workshop – Stockholm, Sweden – 9-11 October, 2008, Sweden – 9-11 October, 2008

3 ITER NEUTRAL BEAM INJECTOR

During 2008, the activities aimed to advance the 1 MV Neutral Beam Injector (MITICA), the Ion Source (SPIDER) and the related Test Facility (PRIMA) design have been continued. All these activities have been carried out under EFDA or F4E contracts. An accompanying program aimed to acquire numerical tools to optimize accelerator design and to train personnel to High Voltage and Negative Ion Source research has been carried out.

3.1 NBI Development

3.1.1 Vessels for MITICA and SPIDER

At the beginning of 2008, the activities for EFDA task TW6-THHN-NBD1 have been concluded with the delivery of final reports for the design of the Beam Source and Beam Line Vessels for the ITER NB Injector (fig. 3.1.1). This design was specifically carried out for MITICA Injector, considering top access for maintenance, a RF Negative Ion Source, a SINGAP-MAMuG compatible accelerator, three Beam Line Components with updated cooling headers and a new access layout for beam diagnostic and component monitoring (fig. 3.1.2).

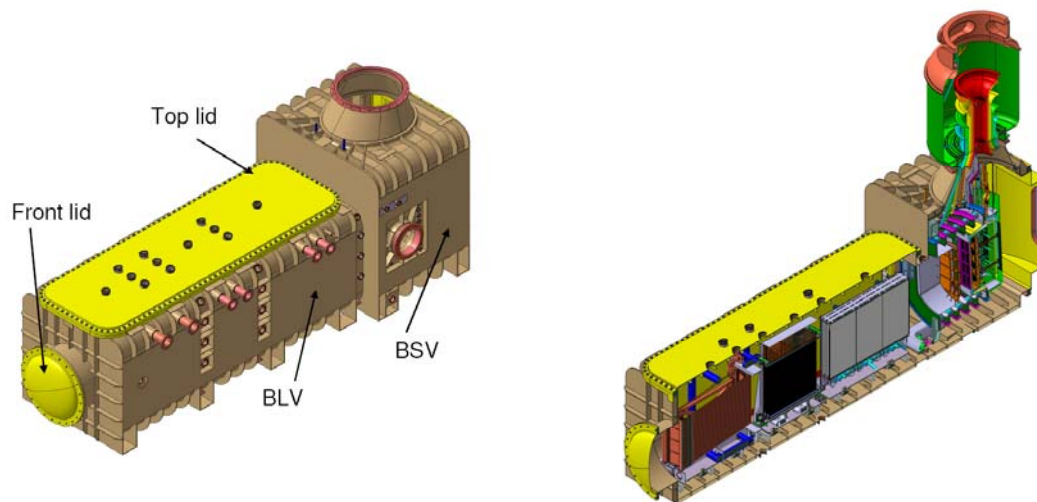


Fig.3.1.1: The NB Injector Vessel (h 5m, w15m) as Fig. 3.1.2: The full assembly of the MITICA NB Injector designed for the MITICA Injector

After delivery of reports and CAD models to EFDA, the activity in 2008 has been devoted to the design of a new vessel for SPIDER.

A cylindrical vessel composed of two longitudinal modules and two torispherical heads has been conceived (see fig. 3.1.3). The cylindrical modules are independently supported and can be translated on rails. The access to the Beam Source and Calorimeters are respectively from the rear and front lids.

The Beam Source is supported inside the vessel by a movable frame that allows for fine adjustments of the Source position as conceptually shown in fig. 3.1.4

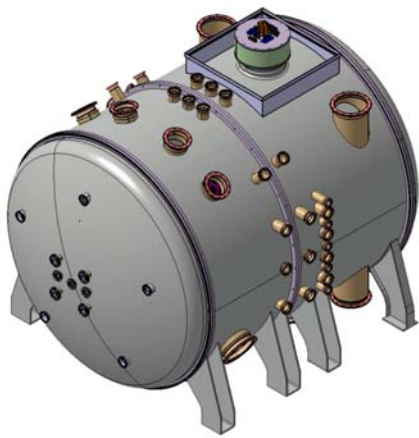


Fig.3.1.3: Isometric view of the SPIDER vessel (h4.5m, w6m)

Following a preliminary design of the vacuum system for SPIDER, the ports for vacuum pumps have been defined and further extension ports have been added to possibly house finger cryopumps inside the vessel.

Diagnostic and inspection accesses have been positioned and dimensioned together with a short pulse calorimeter and long pulse dump to be connected to the front side lid.

A major effort has been dedicated to the definition of supports and interfaces with particular care to hydraulic and electrical insulation requirements. Ceramic insulating rings and vacuum seal flanges with insulated

feedthroughs have been designed both for electrical busbars and signal cables on the top and hydraulic cooling pipes on the bottom.

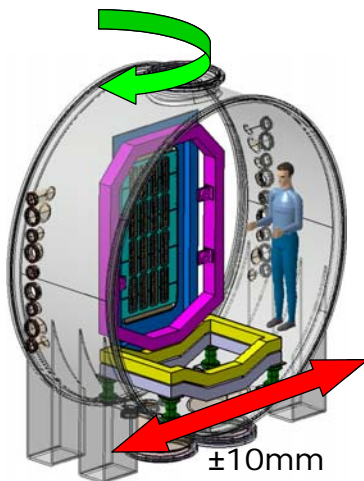


Fig. 3.1.4: Schematic of source support inside the vessel (the ion source is hidden for clarity)

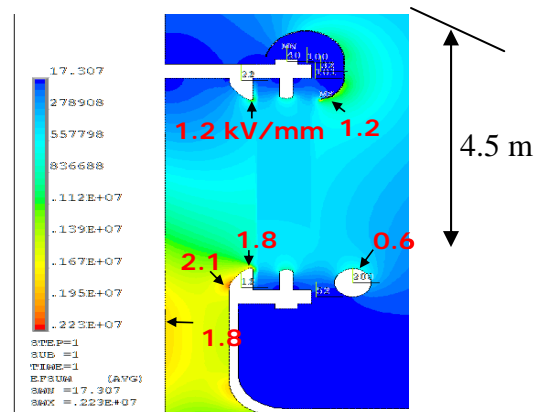


Fig .3.1.5: Electric field distribution around the 100 kV insulated bushing for SPIDER

Detailed electrostatic analyses have been carried out to minimize the electrostatic field strength in the regions of connections (see fig. 3.1.5).

Preliminary contacts with possible manufacturers of particular components as the large ceramic rings and fiber reinforced insulating cooling pipes took place in 2008.

Qualification tests of fiber reinforced plastic pipes for HV insulated water cooling lines are foreseen in 2009 to support the design of both SPIDER and MITICA. The design of the test stand, to be also used for thermo-hydraulic tests of small grid prototypes, has been advanced in 2008 and will be completed in the first part of 2009.

Preliminary mechanical analyses of the vessel evidenced the most critical areas for local displacement and stress, as shown in fig. 3.1.6. Final detailed static and buckling analyses are

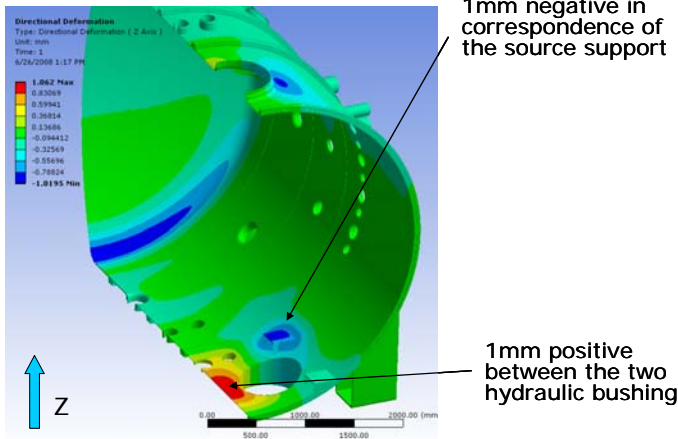


Fig.3.1.6: Deformation contour of SPIDER vessel under vacuum and dead weight load condition

necessarily postponed after the final assessment of the vessel design. In fact the design is still under revision due to the progressive definition of requirements, interfaces and to the design of other in-vessel components as the calorimeters and the electron dump.

It is foreseen to develop the vessel design up to the construction drawing detail. The preparation of

the built-to-print technical specifications is also foreseen during the last part of 2008 and the first months of 2009.

3.1.2 Ion source and Accelerator

At the beginning of 2008 the EFDA task TW6-THHN-NBD1 was concluded with the delivery of the final reports regarding the detailed design of the ion source (fig.3.1.7) and the accelerator for the injector test facility in SINGAP configuration (fig.3.1.8).

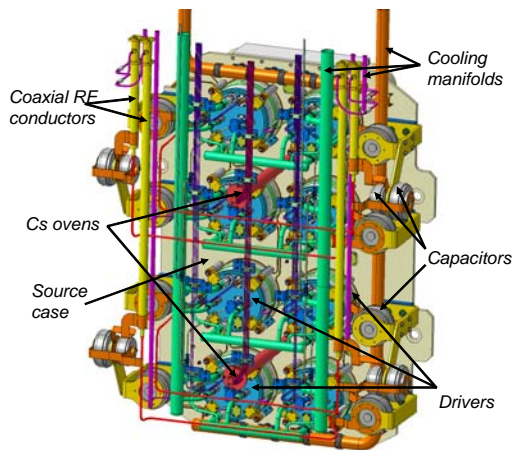


Fig.3.1.7: RF source for full injector facility

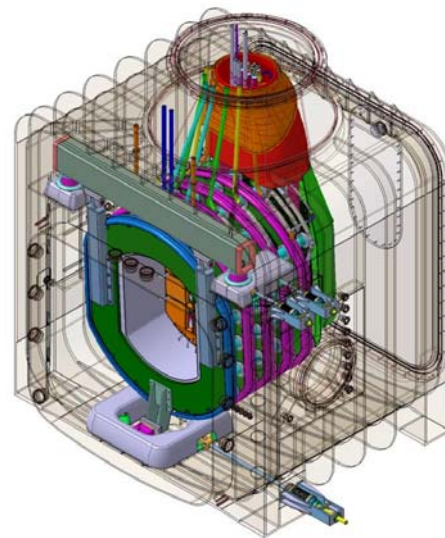


Fig.3.1.8: SINGAP beam source

For the ion source, a reference solution for the most heated parts by back-streaming positive ions was identified and verified with thermo-mechanical simulations. All auxiliary systems were taken into account and revised and the integration within SINGAP beam source was carried out. Preliminary technical specifications were also developed.

For the accelerator, the structure of the beam source has been revised: a new support system has been designed, featuring a top transverse bar with positioning adjustment mechanisms and a lower tilting actuator, that remain in place during ex-vessel maintenance operations on the beam source.

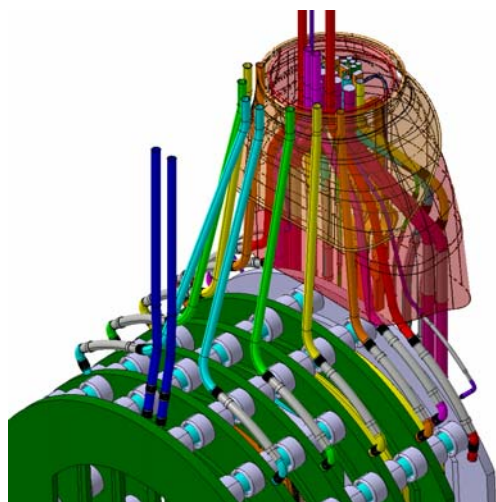


Fig.3.1.9: Connections between beam source and HV bushing

The SINGAP concept for the 1 MV accelerator was developed in detail, with the goal of compatibility and inter-changeability with the MAMuG option.

As a consequence of the beam source vessel modification and the increased space availability, all beam source connections with the bushing were completely revised and a new electrostatic shield has been designed (fig.3.1.9).

Electrostatic analyses and verifications were carried out in order to optimize the design of connection layout and shields between source elements at different potentials.

Thermo-mechanical analyses of the grids were also carried out considering different cooling schemes in order to optimize the mechanical behavior. A double power load deposition has also been taken into account, in coherence with an abnormal electron co-extraction operational scenario (fig.3.1.10).

The ion source and the design of a 100 kV accelerator for the SPIDER beam source has been carried out with the preparation of built-to-print technical specifications and drawings for procurement.

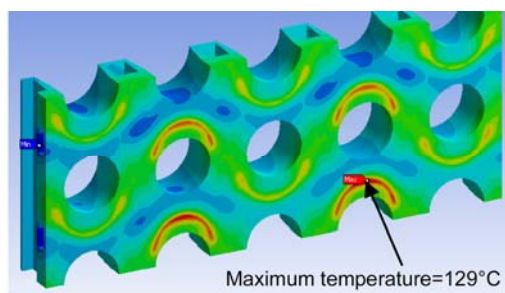


Fig.3.1.10: Thermo-structural analysis of the extraction grid



Fig.3.1.11: RF source for the SPIDER facility

The ion source (fig.3.1.11) was modified in order to simplify parts where the heat load is lower as a consequence of the lower acceleration voltage. Cooling circuits are individually fed from outside of the vessel as much as possible, in order to maximize information from water calorimetry. Items not yet taken into account in the previous design were included, like the bias plate for minimizing co-extracted electrons or the Mo coating for preventing sputtering from internal copper surfaces. A third Cs oven was included at the centre of the source. Critical

manufacturing steps as copper electro-deposition and Mo coating were considered in detail, and the design was optimized in order to minimize possible risks. The design of all parts was developed up to construction drawing detail. The preparation of built-to-print technical specifications has been brought to an advanced stage.

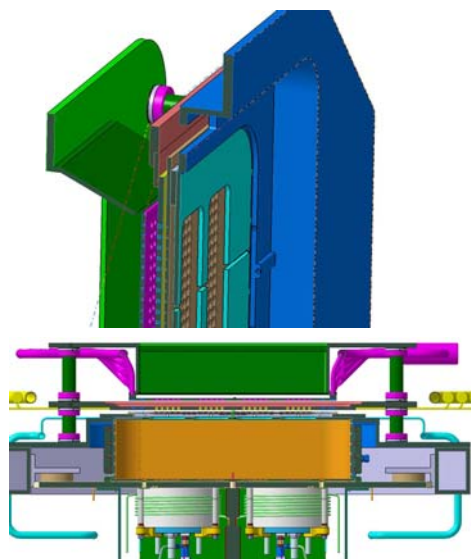


Fig.3.1.12: SPIDER accelerator: horizontal and isometric vertical section

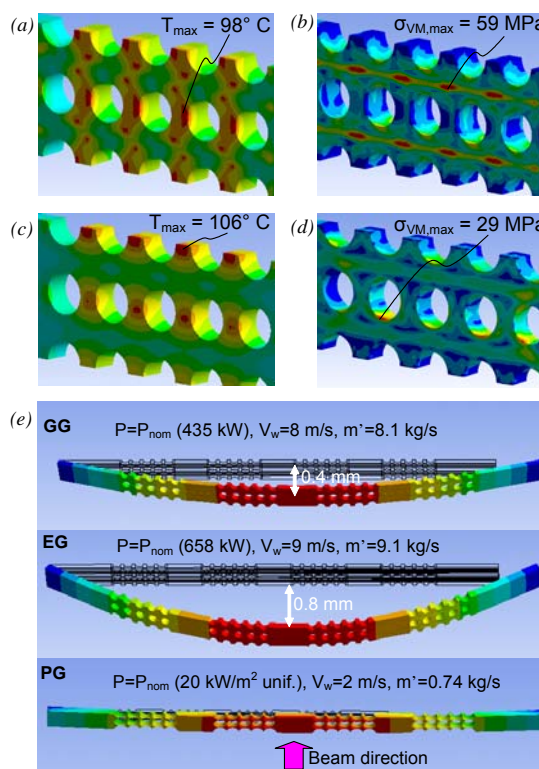


Fig. 3.1.13: Main results of the thermo-structural analyses performed with the ANSYS code on the reference scenario: (a) and (b) Temperature and Von Mises equivalent stress on the EG; (c) and (d) Temperature and Von Mises equivalent stress on the GG; (e) Out of plane deformations of the three grids

The new accelerator for the SPIDER beam source was designed in collaboration with the Indian Domestic Agency (INDA) on the basis of a three grid system (fig.3.1.12): plasma, extraction and grounded grid.

Simulations were carried out in order to optimize the design with regard to all relevant types of functional parameters, as for instance optics, uniformity of magnetic field in the extraction region and hydraulic-thermo-mechanical behavior of the grids (fig.3.1.13).

An example of the modification of the design as a consequence of numerical analyses is the alternative solution proposed for the routing of Plasma Grid current (fig.3.1.14). The supporting frames and the set of cooling manifolds were studied with special attention dedicated to electrostatic issues, manufacture optimization, and (dis)assembly and maintenance efficiency. Integration of diagnostics was developed much further: a complex set of optical accesses was defined to maximize the diagnostic capabilities on main physical phenomena at the edge of the plasma source and inside the accelerator. A large number of Langmuir probes are foreseen in the plasma grid and the bias plate and thermocouples in

every component of the beam source. The system of interfaces and connections was completely redefined with respect to the previous source. Ion source and accelerator are now independently connected to a portal fixed to the lower region of the vessel internal surface. Diagnostic cables, gas and electric power supply are still fed through a bushing on the top part of the vessel, while all high voltage components cooling water pipes are routed through two other bushings located in the lower part of the vessel (fig.3.1.15).

The design of all parts was developed up to construction drawing detail. The preparation of built-to-print technical specifications has been brought to an advanced stage.

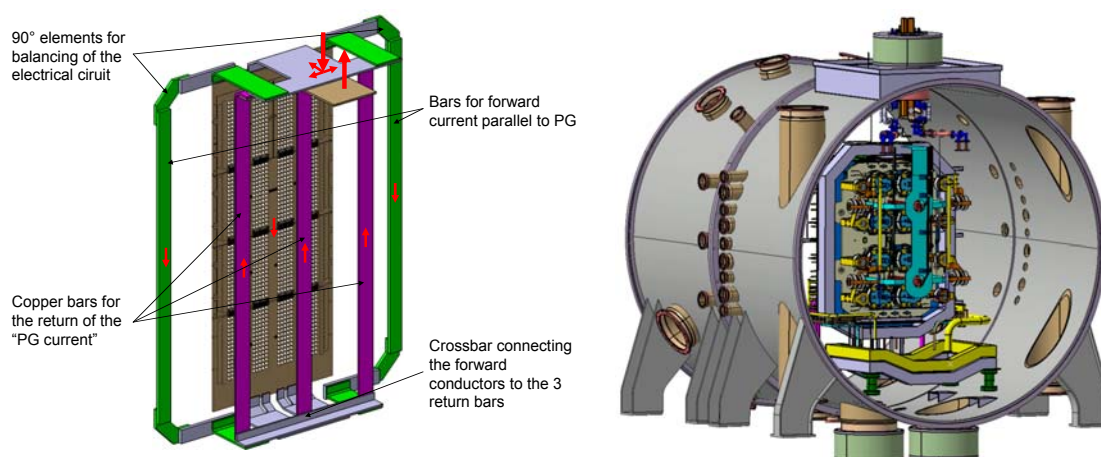


Fig.3.1.14: Alternative solution for the plasma grid current routing Fig.3.1.15: SPIDER beam source interfaces

3.1.3 Power supply

During the first quarter of the year, the Integrated Design Document of the NB Power Supplies (PS) has been completed in collaboration with the Japanese Domestic Agency (JADA), ITER IO and F4E [IDD08]. An analysis of the compatibility of the PS with the requirements related to the beam modulation at full power has been performed [Zanotto08], and the results have been used to check the design. On the basis of the integrated design, the technical annex ("Annex B") to the Procurement Arrangement between EU and ITER for the in kind procurement of the NB PS has been issued.

Following the preparation of the Annex B, RFX continued the collaboration with ITER with the aim of reviewing the Procurement Arrangement documents, in order to have the final version of the tender documents ready to be signed before the end of June.

In parallel, the design of the SPIDER test facility PS has been started. The project foresees a power supply system as similar as possible to the ITER one for the Ion Source and an acceleration power supply system rated for -100kV. A conceptual design of the overall system has been produced, including the transmission lines and the passive protection systems. The design has been discussed and approved by a Review Panel, created on purpose for the SPIDER review process; a conceptual scheme of the SPIDER PS is shown in fig. 3.1.16. The circuit is close to that proposed for ITER, with the source PS installed in an air-insulated Faraday Cage and fed by a -100kV dc insulation transformer. The connection of the PS to the source is

realized with a co-axial, 100kV dc air-insulated transmission line hosting all conductors necessary to feed the source, including 4 RF co-axial lines for the RF antennas. A cross-section of the transmission line is shown in fig. 3.1.17. The external panels, used as return conductors have a twofold advantage: a good

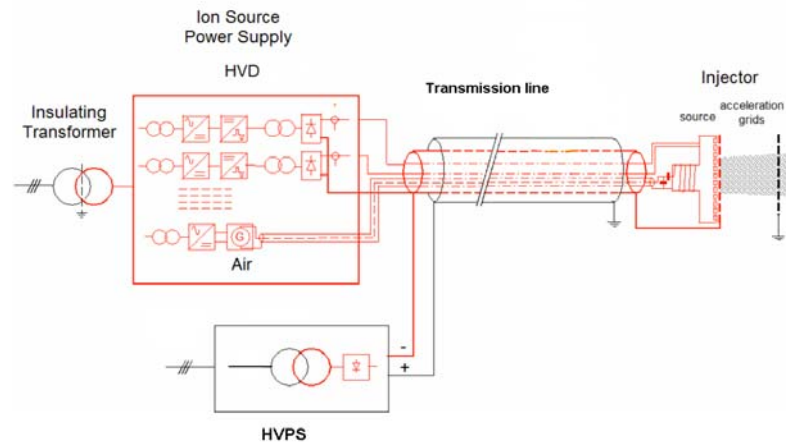


Fig.3.1.16: Conceptual scheme of the SPIDER Power Supplies.

screen against Electro Magnetic Interference (EMI) (the external screen is a double screen) and a cheap solution, since it does not require a high pressure vessel to contain the insulating gas. Analyses have been carried out to determine the most effective protections against the breakdowns. Fig. 3.1.18 shows the provisions to be adopted: a distributed core snubber, a damper resistance in series to the Grounded Grid, a double screen on the HV line, a core snubber and other surge arresters on the -100kV power supplies. A model has been developed and used to check the effectiveness of these provisions as a breakdown of the grids occurs.

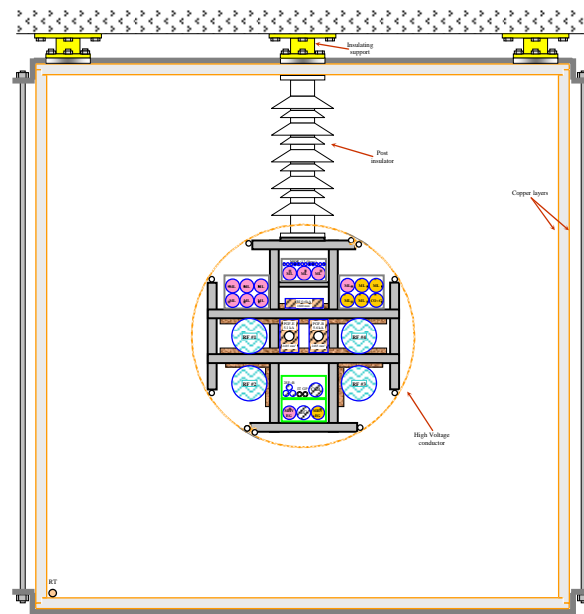


Fig.3.1.17: Cross section of the SPIDER Transmission Line.

Another activity consisted in the preparation of the technical specification for the ISEPS. This specification will be used to procure the source power supplies of SPIDER, ITER NB and

MITICA NB. To support this activity, the model of the PS has been further refined to review the design for the different applications. In particular, the model of the HV network at breakdown has been improved, including a refinement of the ISEPS and of the transmission line, where the effect of the saturation has been accounted for in the core snubber models. The model can be used to determine the over-voltage stress on the PS and, as a consequence, to prescribe specific tests to verify the design of the system before installation on Site.

On top of the ISEPS specification, the specifications of the transmission line and of the High Voltage Deck have been written. The tender processes are foreseen in 2009.

Concerning the SPIDER -100kV power supply, on the basis of the agreement between INDA, ITER and F4E, the responsibility of the conceptual design and of the technical specification has been transferred to INDA. However, RFX has contributed to the activity on the definition of the requirements and of the constraints for the installation in SPIDER. Moreover, RFX is involved on the design review of the Diagnostic Neutral Beam PS, which is similar to the SPIDER PS and will be procured by IN.

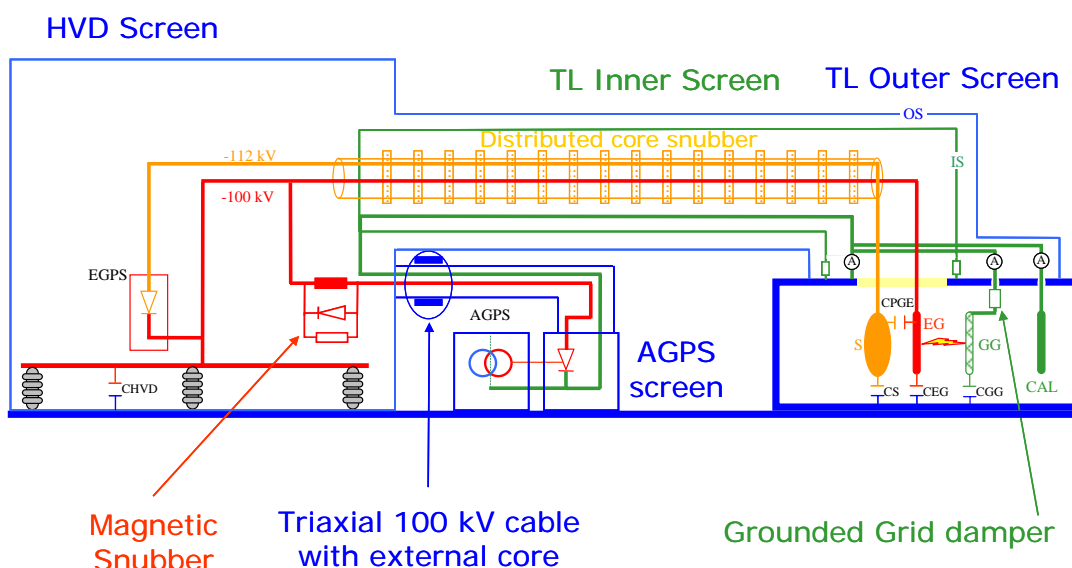


Fig.3.1.18: Conceptual scheme of the passive protection systems

A collaboration between RFX and IPP Garching has started on the development and validation of a Finite Element Model of the RF source. During 2008, a model of the antenna and of the electrostatic screen has been developed and validated against experimental data coming from the BATMAN facility at IPP. Simulations and experimental data showed fairly good agreement; plans for further development of the model, also in the presence of plasma, are ongoing, and a second experimental campaign will be performed next year.

Another activity regarded the development of a damper resistor for ITER and MITICA. The energy deposition on the acceleration grids in the NBI systems as a consequence of arcing due to voltage breakdown is recognized – since the beginning - to be one of the most critical issues affecting NBI performance. Furthermore, the fast voltage and current oscillation (ten MHz range) appearance after the breakdown raises great concern about the Electro Magnetic Interference (EMI) aspect. In the ITER – 1MV NBI, as well as in the MITICA experiment, both these problems will be worse, due to the larger electrostatic energy stored in the huge HV bushing and in the accelerator itself; in fact, simulations carried out with a detailed model of the ITER NBI have shown that the usual Core Snubber solution is not sufficient to keep under control the arc energy and EMI.

For this reason, the installation of a resistor (so called Damper Resistor DR) connecting to ground the last grid of the accelerator (the Grounded Grid) has been proposed. Simulations have proved its efficiency in reducing both the energy and EMI content: for this reason, a task

has been launched to build a DR full scale prototype, to be tested in the ongoing Energy Storage Campaign in the 1 MV test facility in Cadarache.

In 2008 the DR has been designed and built. The resistor is rated for 650 kV/20 kA/1.5 MJ per pulse. It is made of an FRP cylinder, hosting a stack of carbo-ceramic resistors. Three stacks have been prepared in order to test the effect of three different resistor values (20 Ω , 40 Ω , 60 Ω). The DR is designed to be installed under vacuum; the FRP cylinder and the metallic flanges are vacuum tight, so that the resistor stack will be gas insulated (N₂, SF₆ or He). Fig. 3.1.19 shows a picture of the DR assembled

The DR will be also installed for protect ion against voltage breakdown in the 100 kV SPIDER experiment.

3.1.4 Diagnostics

Activities on diagnostics during 2008 have been mainly focused on the Ion Source Test Facility, in order to define all the requirements in terms of parameters to be measured, and to manage the integration into the mechanical design.

The diagnostics can be grouped into a few wide categories as follows: thermocouples (in driver plate, RF drivers, grids), electrical measurements (grid currents and voltages, electrostatic probes, plasma grid filter current), emission spectroscopy (line spectroscopy in source, line spectroscopy of beam, beam tomography, source tomography), absorption spectroscopy (cavity ring-down, laser photodetachment, laser induced fluorescence), radiation measurements (X-ray, neutron), inspection (visible radiation, infrared radiation), mechanical measurements (gas pressure, coolant parameters, residual gas analysis, inlet gas parameters, caesium level). Some of these diagnostics will be described herein.

Spectroscopy allows monitoring key parameters involved in negative ion formation and in neutralisation: temperature and density of electrons, temperature and density of atoms and molecules, density of caesium. Spectroscopic equipment can involve high resolution spectrometers to analyse molecular spectra, in order to evaluate: gas temperature, vibrational temperature, molecular density, and ionisation degree. Low resolution spectrometers can be used for monitoring single outstanding emission lines, such as the Balmer series, caesium lines and doping gas lines (typically N or Ar) and any line due to impurities coming from a vacuum leak; in those cases when real time evaluations (caesium density), occurrence of arcing inside the source or leaks are important, photomultipliers coupled to interference filters might be adopted. CCD arrays, combined to interference filters, can be used to build a tomographic map of certain processes, with the purpose of assessing source symmetry through the detailed space behaviour of Balmer lines. Spectroscopic data interpretation may be quite sophisticated, but significant development has been achieved in the recent past on this subject [Fantz06].



Fig.3.1.19: Damper resistor picture

Cavity ring-down consists in the decay of a short laser pulse injected into the cavity between two highly reflective mirrors. Light losses are due to: leakage through mirrors, scattering, diffraction and photodetachment (photon absorption by negative ions with electron liberation); the last allows the measurement of negative ion density. Nd:YAG lasers at 1.06 μm , with photon energies of 1.2 eV, are commonly used to this end [Bacal08].

Fig. 3.1.20 sketches the geometry adopted for emission and absorption spectroscopy: three horizontal lines-of-sight (LoS) close to the plasma grid are used for cavity ring-down (black lines); the mirrors will be installed in vacuum. Emission spectroscopy is in the visible range, so the same LoS can be shared between cavity ring-down and emission spectroscopy (red lines); the latter will also employ four vertical LoS. Each horizontal line corresponds to four LoS located in slightly different axial positions (Fig. 3.1.20, right hand side); analogously, the vertical lines represent two LoS, axially spaced. The overall arrangement allows investigating top-bottom and left-right asymmetries, as well as axial decays of the parameters. Suitable accesses are also provided in case a finer investigation of source uniformity might be necessary, requiring tomographic analyses (blue fans of LoS).

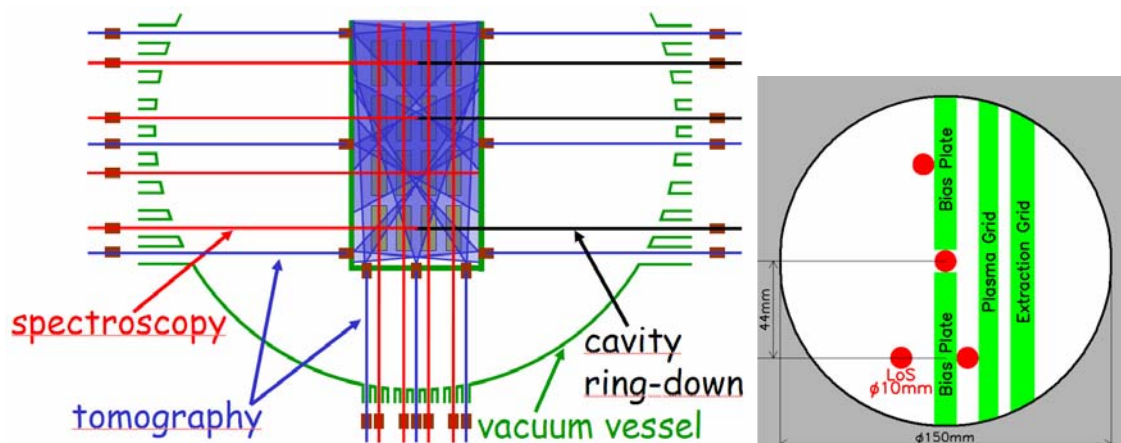


Fig.3.1.20: Arrangement of spectroscopic LoS on a plane parallel to the plasma grid (left) and axially (right).

Electrostatic probes will provide local plasma parameters in the source (electron density, temperature and energy distribution functions). They will be embedded in the bias plate and in the plasma grid. Suitable locations of the probes around the holes in the plasma grid are being decided to obtain information on spatial uniformity. The effect of magnetic fields, negative ions, surface contamination due to caesium and grid operating temperature will be accounted for.

Source efficiency will be studied also in terms of beam parameters. Common techniques include Doppler spectroscopy [Fantz07], applied to the radiation emitted after charge-exchange reactions of the beam with the background gas. The energy distribution of particles gives information about undesired neutralisations, whereas the Doppler width is a measure of the beam divergence. The LoS will be arranged along the beam line so as to allow tomographic reconstructions of the beam position and of the beam uniformity [Cottrel82].

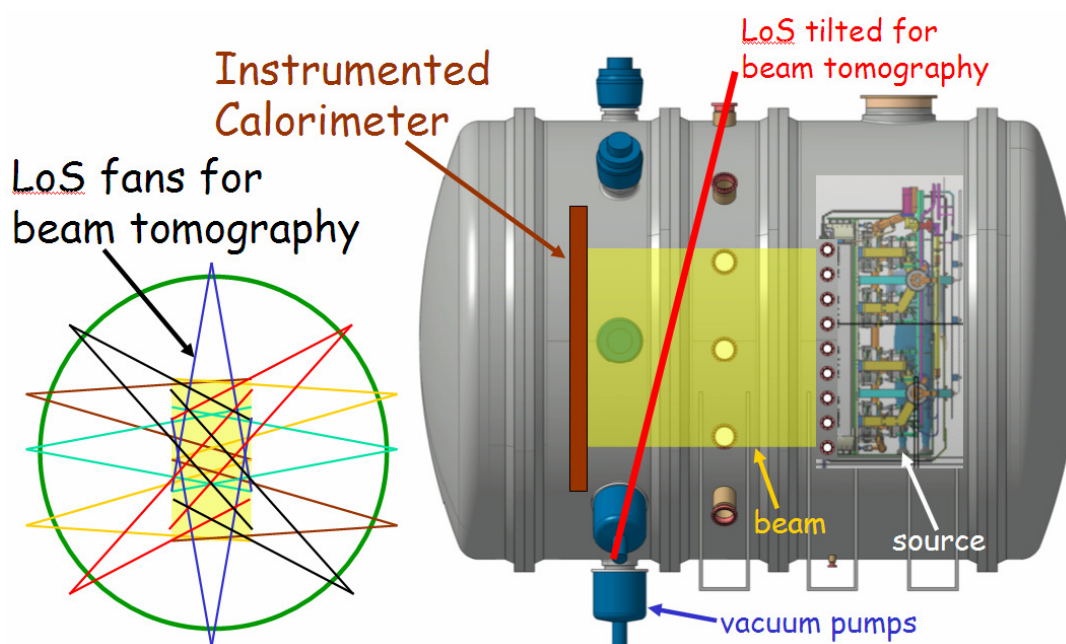


Fig.3.1.21: Arrangement of spectroscopic LoS on a plane parallel to the plasma grid (left) and axially (right).

During short low-power pulses the use of an instrumented calorimeter [Grisham05,Kawai00] is proposed.

The calorimeter will be equipped with thermocouples and will be viewed by infrared cameras in order to investigate beam position and uniformity, thus complementing beam tomography.

The arrangement of the LoS for beam tomography and of the instrumented calorimeter is sketched in Fig. 3.1.21.

3.1.5 Control and Data Acquisition System

In the framework of EFDA task TW6-THHN-NBTF1, the preliminary specification of the architecture of the control, interlock and safety systems of the ITER Neutral Beam Test Facility (NBTF) has been defined. A report of the activity has been delivered to Fusion for Energy, as part of the task deliverables. The activity was carried out in various steps, including the definition of the system functional and non-functional requirements, the definition of a reference layout for the systems, a budgetary estimate and a tentative contract schedule. Scope of the activity was an early definition of the control, interlock and safety systems for the Neutral Beam Injector Test Facility, whereas the control systems of the Diagnostic Neutral Beam and full ITER-size Ion Source Test Facilities were outside the scope of the work.

Fig. 3.1.22 illustrates the preliminary definition of the architecture of the control, interlock and safety system of the ITER Neutral Beam Test Facility. The whole architecture, referred to in figure as NBTF Control, Interlock and safety System Group, can be divided into three systems, each one structured in three tiers to provide personnel and environment safety, machine protection and system management, respectively, following the ITER CODAC philosophy. The NBI Control, Interlock and Safety System is intended to manage the ITER Neutral beam Injector (NBI), i.e. the component under test in the facility. It includes the Plant Safety System

(PSS), the Plant Interlock System (PIS) and the Plant Control System (PCS). The PCS Supervisory System takes care of the automation and monitoring of the injector and is structured into four functional machine subsystems, namely Power Supply, Beam Source, Beam Line and ITER-only. The PCS Data Acquisition Subsystem performs data collection and includes a set of different scientific Diagnostics.

The Aux Control Interlock and Safety System is intended to manage the auxiliary equipment that is needed in the facility to test the injector but is not part of the injector itself. As an example, this system includes the cryogenic system, the cooling system and the vacuum pumping and gas injection systems. The system is structured as the NBI system, to minimize hardware and software development.

The NBTF Control, Interlock and Safety System is intended to supervise the operation of the NBI and AUX systems and is at the highest level in the hierarchical structure of the architecture. As an example, the system will provide the software tools to program and execute an experimental session, to synchronize the facility, to storage and access data. The system is interfaced to the NBI and AUX systems by means of standard hardware interfaces referred to as I&C bridges.

It is worth noting that the system architecture has been also designed to facilitate the integration of the ITER NBI with ITER CODAC, the ITER IT infrastructure providing ITER plant systems management. Specifically, ease of integration with ITER CODAC has been achieved by the use of standard hardware interfaces (I&C bridges) and of the Plant System Host that is the single point, standard plant systems' interface defined by ITER CODAC.

3.2 THE TEST FACILITY

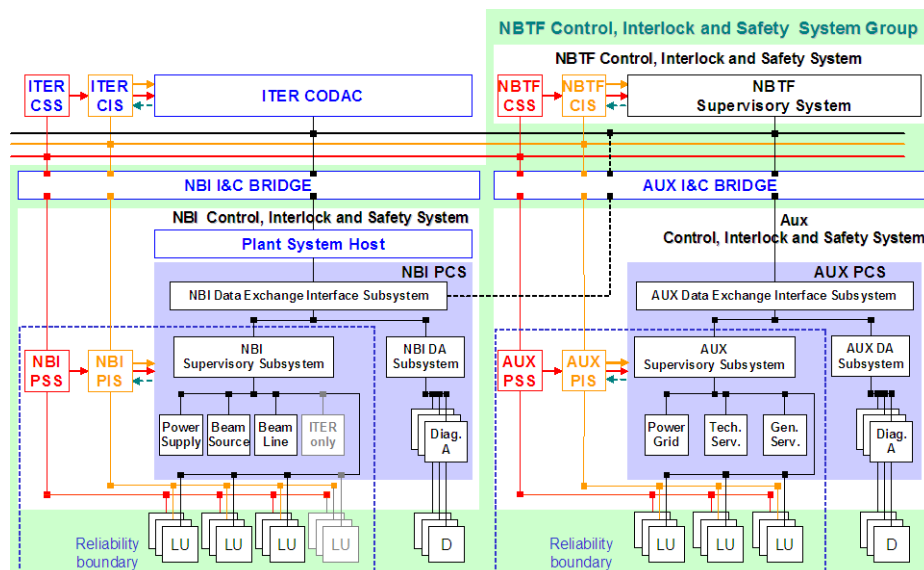


Fig.3.1.22: Preliminary definition of the architecture of the control, interlock and safety systems for the ITER Neutral Beam Test Facility

3.2.1 Auxiliary systems

3.2.1.1 Cooling

The total thermal power to be removed from the two facilities (SPIDER and MITICA) (up to 70 MW) and the power produced by the auxiliary systems have to be rejected to the environment by a Cooling Plant (CP).

The design of the CP has been developed considering the specifications of the ITER Neutral Beam Heating and Current Drive Injector subsequently revised in order to fulfill the updated component requirements [ITER-a, Marcuzzi08]. Furthermore, modifications of the ITER cooling water system [ITER-b] have been considered to reproduce the ITER working conditions in MITICA.

The environmental conditions of the local construction site (Padova) have been analyzed and taken into account for the design of the CP that has not to be reused in the ITER site (Cadarache).

The CP for PRIMA will consist of three main heat transfer systems that exchange thermal power between them, the experiment test facilities and the environment.

The primary heat transfer system (PHTS) will be directly connected to the test facility components and to power supply components; the primary coolant is ultrapure water to which the thermal power produced during experimental operations of the test facilities will be rejected. The secondary heat transfer system (SHTS) will transfer the thermal power of PHTS to the external environment by cooling machines such as cooling towers and dry coolers.

A tertiary heat transfer system (THTS) is also foreseen for some cooling machine circuits (e.g. dry coolers) to avoid coolant freezing during winter. Water basins with large stored energy will be interfaced to the THTS in order to reduce the installed power of heat rejection machines.

The technical specifications for the procurement of the entire cooling plant have been developed including layout drawings and schematics as applicable.

The cooling plant for PRIMA has to fulfill the following functions:

- thermal control of the actively cooled components of SPIDER and MITICA (within ± 20 °C range, ± 2 °C tolerance) by removing the produced thermal power;
- rejection of the thermal power to the environment.

Different phases of the experimental campaigns have been considered in order to determine the CP requirements corresponding to the worst operating scenario: conditioning, full power, shut down.

The coolant flow rates and inlet-outlet temperatures should be measured, acquired and monitored to control the CP and to calculate the exchanged heat fluxes and thermal powers.

Maximum pulse length of the experiments will be 3600 s, but simultaneous operation is only foreseen with reduced pulse duration, expressed by a duty cycle of 1/4.

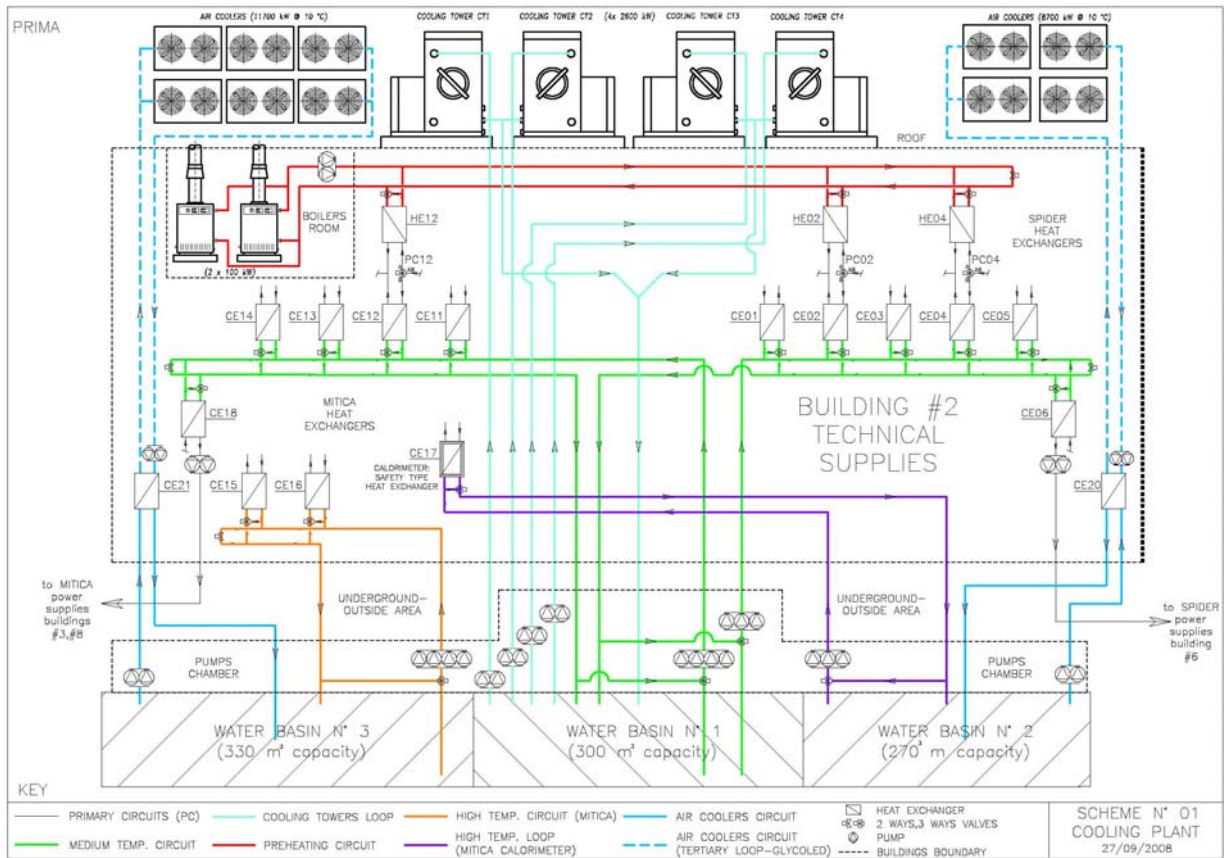
The CP shall provide ultrapure water at specific inlet temperature, pressure and electrical resistivity (minimum $2.0 \text{ M}\Omega \cdot \text{cm}$ for low voltage and power supply components and minimum $10 \text{ M}\Omega \cdot \text{cm}$ for high voltage components) required by each group of components [ITER-a].

Electrochemical corrosion issues shall be taken into account for the design of the cooling circuits. The PHTS will be directly connected to the test facility components that operate at different electrical potentials. High voltage components (down to -1 MV potential) require insulating breaks and voltage insulation also along the water columns.

Continuous water resistivity degradation will occur in the primary cooling loops for dissolved piping materials and components. Then, the primary water will be chemically treated and controlled in a Chemical and Volume Control System (CVCS) to restore the required purification level.

In case of small leak events, the leaking primary circuit will be identified and water shall be evacuated completely from the component and primary loop. For this aim a Draining and Refilling System (DRS) and a Drying System (DS) shall be provided.

The scheme of the cooling plants for PRIMA and SPIDER are shown in fig. 3.2.1 and 3.2.2.



B

Fig. 3.2.1: PRIMA cooling plant

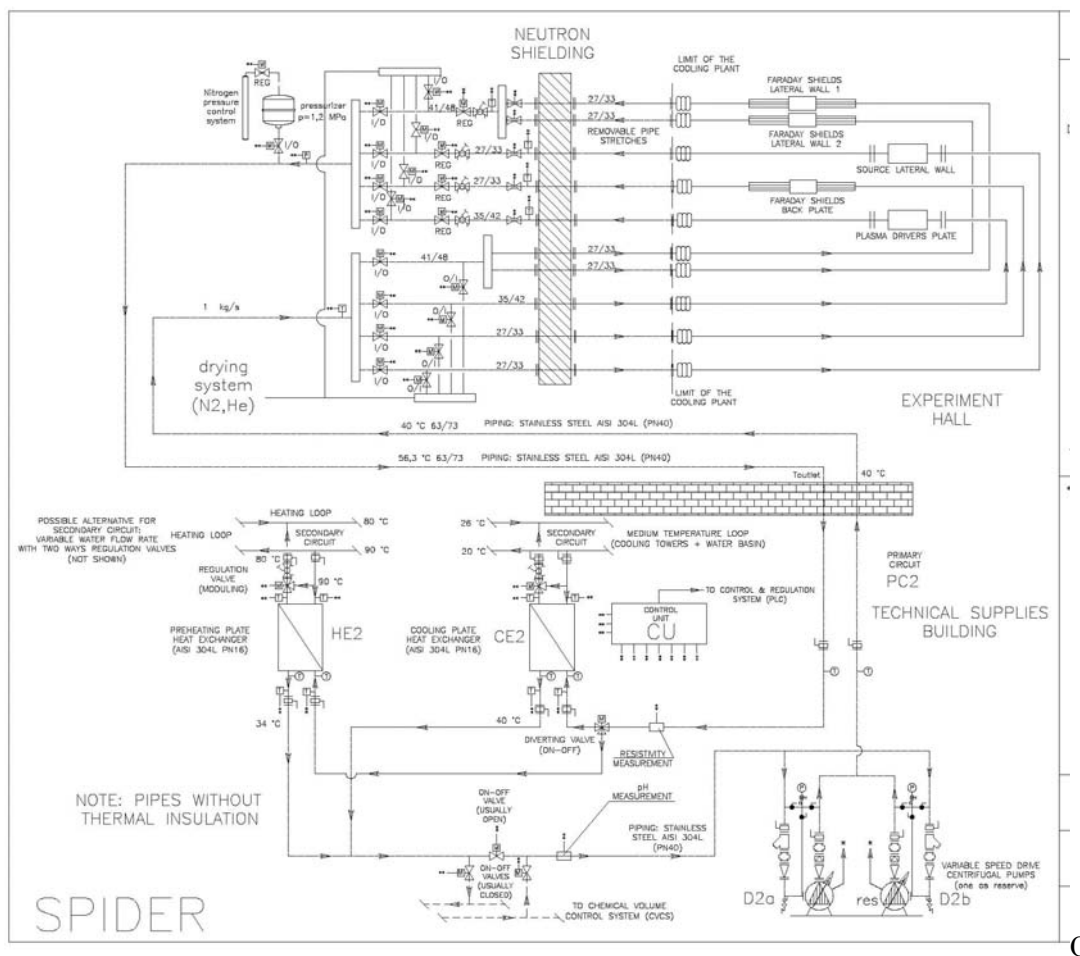


Fig. 3.2.2: SPIDER cooling plant

3.2.1.2 Cryogenics

The 1 MV Neutral Beam Injector Test Facility is equipped with a cryosorption cryogenic pump. During 2008, the following activities have been carried out for the development of the test facility cryoplant and the associated cryogenic process flow:

- Analysis of cryoplant requirements [Fantini08];
- Design review of the external cryogenic system;
- Design of the Helium Purification and Supply system;

The Technical Specification final reports has been issued [Anaclerio08,a], [Anaclerio08,b], [Anaclerio08,c].

The Cryogenic System is common to the whole cryopump system and includes all the equipment needed to provide the required cooling capacity at all temperature levels between 300 K and 4.5 K [Anaclerio08,a]. The helium distribution to the cryopump is obtained via a Proximity Cryogenic System [Anaclerio08,c] providing the link to the helium refrigerators. The Proximity Cryogenic System includes the Distribution Valve Box and the cryogenic piping up to the interface of the cryopump. It distributes the refrigerant to the cryopanel and to the shields [Anaclerio08,b].

In order to reduce the quantity of impurities in the coolant helium and to recover helium during off-normal events, a recovery and purification system is implemented in the cryogenic plant.

The final data concerning the Cryopump heat loads are still under evaluation and therefore some of the technical aspects in the definition of the cryogenic systems are still open.

Considering the uncertainties on cryopump requirements, an assessment of different cryoplant design solutions is ongoing in order to minimize the plant costs and to adapt to possible requirement changes. More details are reported in [Fantini09].

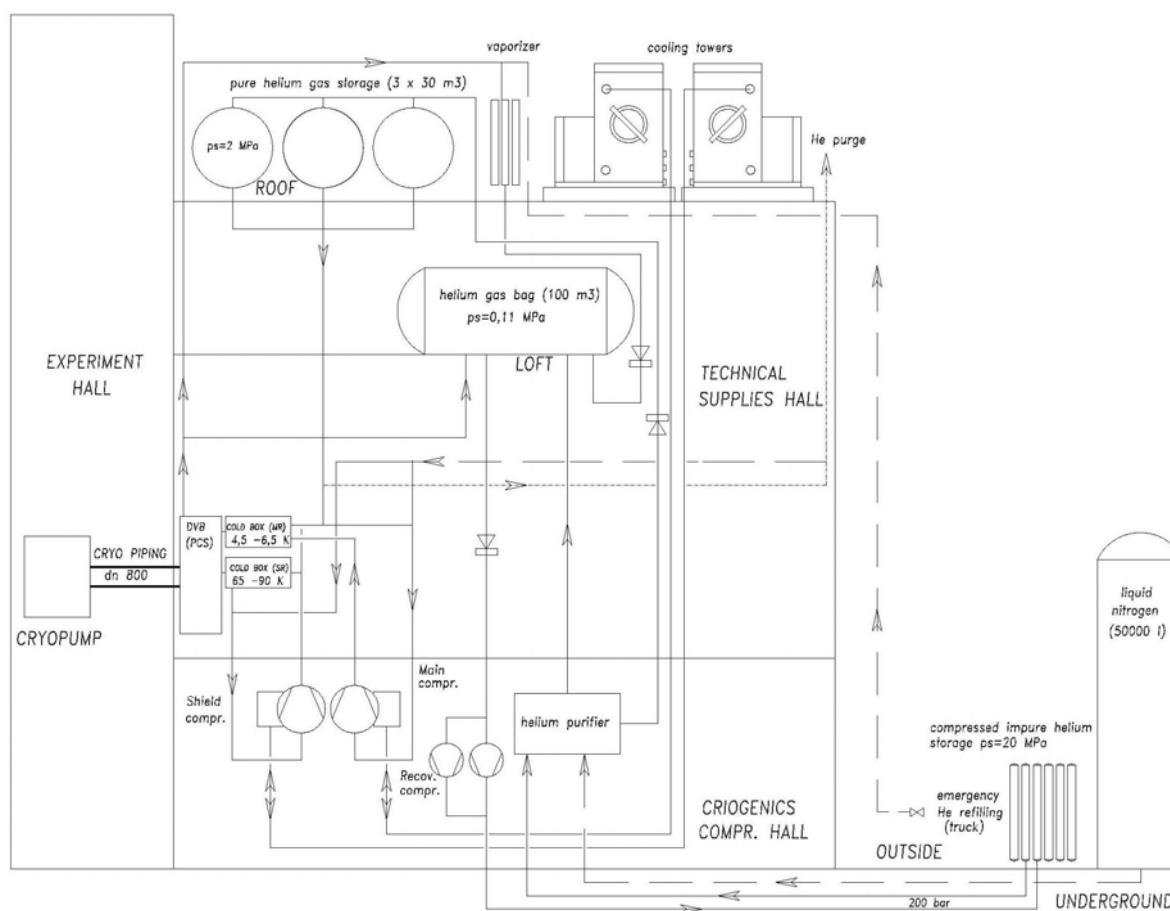


Fig.3.2.3: Cryogenic system layout

3.2.2 Buildings

According to the 2008 Activity Program work has been aimed, to allow starting the infrastructure construction as soon as possible, in order to meet the stringent time schedule related to the start of experiments in the ISTF and with the main injector at the Consorzio RFX site.

The design procedure, according to the Italian law for the public organizations, includes three levels:

- the “preliminary design”, which identifies the general layout of the facility buildings, taking into account the existing available area and the city planning rules;

- the “final design”, a detailed design in which the specific requirements for each hall and the plants that have to be installed inside them are considered. First assessment of the structural analyses and foundations is done together with the design of the civil plants (electrical and thermo-mechanical);
- the “built-to-print” design, with all the information necessary for the public tender.

At the end of 2007, the group of technical offices in charge for the elaboration of the preliminary and final design has been selected.

The preliminary design, started in January, was completed at the middle of May after a complex elaboration in which alternative solutions were examined to optimize the functionality of the buildings, the requests coming from ITER and the need to comply with the available budget.

With respect to the initial layout elaborated in the frame of the 2005 EFDA Contract for the development of the NBI Facility, the new solution is characterized by

- a very limited impact on the existing infrastructure in the CNR Research Area;
- a large experimental hall in which the two experiments (MITICA and SPIDER) are hosted; this solution allows to share among the two experiment the same maintenance area, crane and special area for shielding storage;
- the possibility to better integrate the auxiliary services of the two experiments;
- a separate building for the central control of the experiments, that allows for permanent stay of people with more comfortable features and includes a small meeting room for briefing.
- a layout of the 1 MV SF₆ transmission line, air insulated HV deck, injector and HV transformers reproducing the ITER situation;
- water storage for the cooling system in underground reservoirs.

The “final design” phase was completed on 21 October and at the end of 2008 the draft of the “built-to-print” design of buildings is ready for RFX comments.

In the meantime the authorization process for obtaining the permit to build was started.

The identified solution has the following main features:

- Total area occupied 17.500 mq
- Covered area 7.050 mq
- Available surface for activities 9.170 mq
- Maximum building height 26.4 m

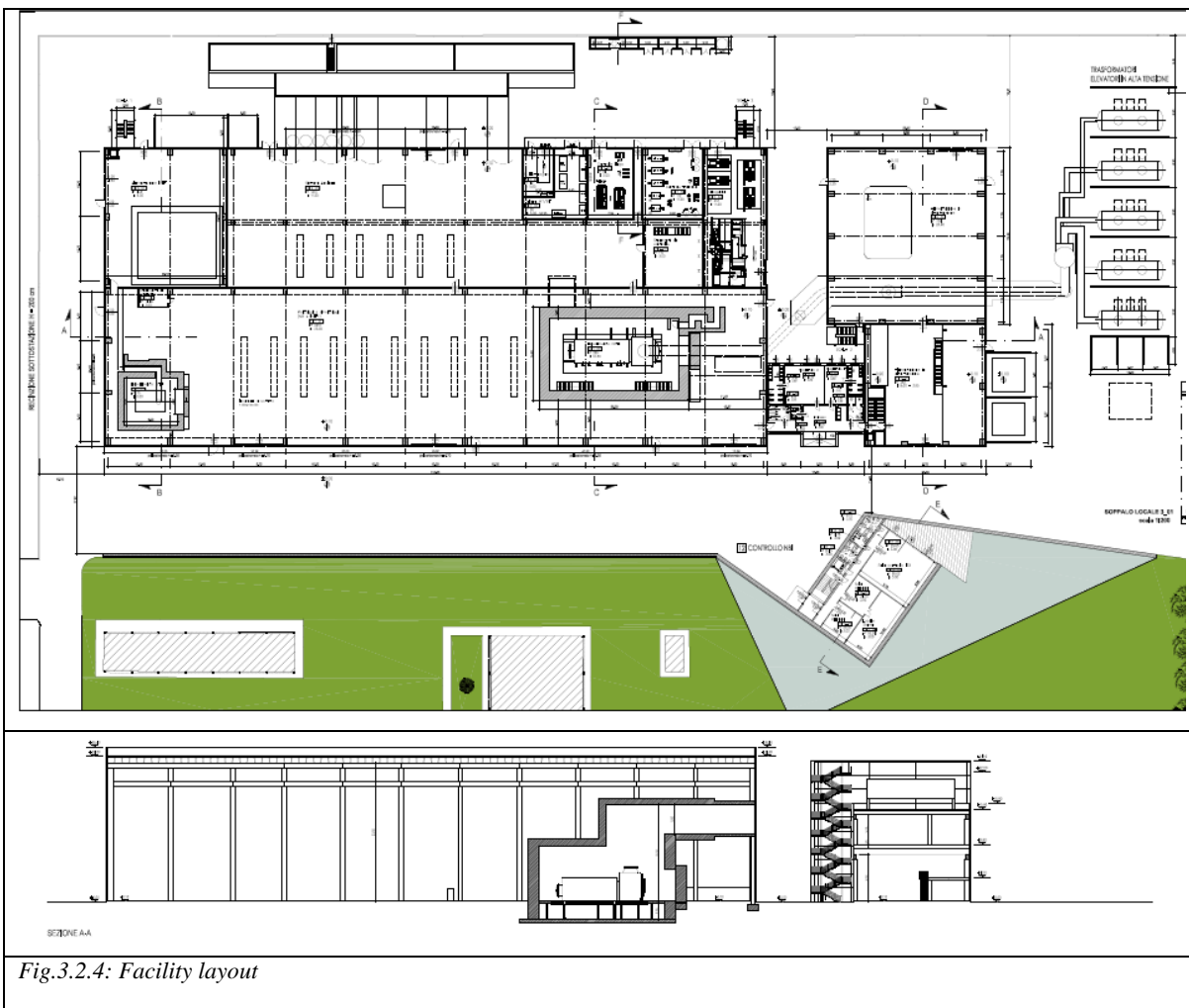


Fig.3.2.4: Facility layout



Fig.3.2.5: The “final design” of the buildings

3.3 NBI Accompanying activities

3.3.1 Modelling

During 2008 modelling of several aspects of the NBI has been carried out: the activities have been mainly devoted to the accelerator for SPIDER; however preliminary simulations for the performance of some diagnostics has been performed as well.

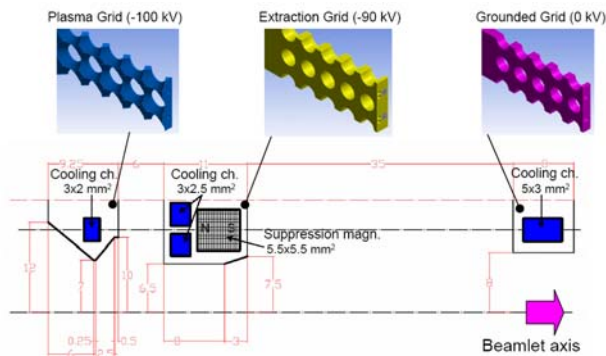


Fig.3.3.1: Design of SPIDER extractor and accelerator.

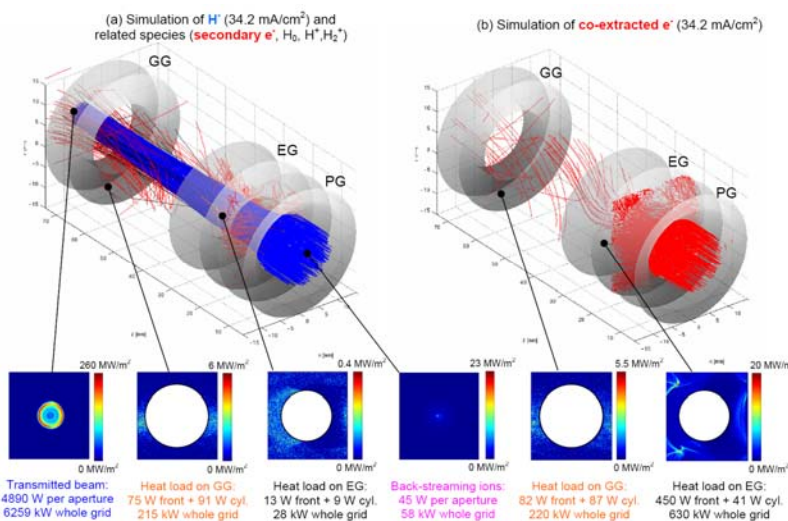


Fig.3.3.2: Beam simulation by EAMCC: particle trajectories and stripping reactions are simulated with a Monte Carlo approach in electrical and magnetic fields. For the grids, heat loads on front surface (front) and on cylindrical part (cyl.) are reported for a single aperture, as well as the load on the whole grid. For transmitted and backstreaming beams, the power corresponding to a single aperture and the total power are reported

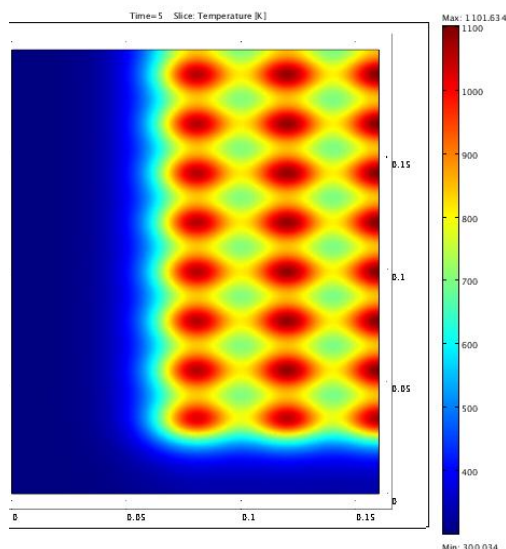


Fig.3.3.3: Front side of the instrumented calorimeter: heat flux 20 MW/m^2 , 5 s, exposure angle 60° .

SPIDER extraction and acceleration regions have been simulated using several codes [Agostinetti08]; in particular, in collaboration with the colleagues from IPR, Ahmedabad, India, the SLACCAD code [Pamela 1991] has been applied to optimise the shape and distances of the accelerator grids on the

basis of optimal optics and stripping reduction. The activity resulted in the geometry of Fig. 3.3.1.

The motion and interactions of particles inside the accelerator, including various processes for secondary particle production, were analysed with the EAMCC code [Fubiani08], which also provides the heat loads on the various grids (Fig. 3.3.2). Based on these results, thermo-structural computations have been

performed to design the proper cooling system for all grids.

The same numerical codes have also been applied to simulate the accelerators of MAMuG, SINGAP and the European 500 kV injector [Antoni08].

Since the magnetic field profile in the source and the accelerator is of great importance for the final features of the beam, a dedicated model has been realised in ANSYS to optimise the magnetic field configuration. A 2D numerical computation has allowed obtaining a substantial reduction of the magnetic field downstream of the accelerator

and a uniform field in the ion source and in the accelerator [Serianni08]. The numerical model is being extended to a full 3D simulation to assess uniformity in the vertical direction and at the boundary.

The equations of a collisional-radiative model have been written for the simulation of the population distribution in the ion source of SPIDER. The model contains electrons, atomic and molecular hydrogen and the corresponding positive ions and negative hydrogen. Several dissociation, excitation and recombination reactions are included. Presently, by means of simplifying hypotheses and of published data, the model has been applied to the evaluation of the spectroscopic signals in SPIDER. In particular, the expected H-alpha signal in the driver, the expansion and the extraction regions of SPIDER has been estimated.

In the COMSOL development environment, thermal analyses have been performed on the best arrangement of the sectors of the short-pulse instrumented calorimeter, intended to measure the beam uniformity in SPIDER. Using carbon fibre composites it will be possible to expose the plates at an angle of 60deg between the normal and the beam direction for some seconds. It has been found, see fig. 3.3.3, that the footprint of the beam is transmitted to the back side of the calorimeter, so that infrared imaging can provide the beam features if the material is sufficiently anisotropic. Electrical simulations have also suggested that, in principle, the effect of secondary emission on the direct measurement of beam current can be reduced.

3.3.2 The small ion source NIO1

A project of a relatively small negative ion source named NIO1 was completed, and some area preparation was begun. Source NIO1 will provide 9 beamlets of H⁻, up to a maximum total ion current of 130 mA at 60 kV, and will be equipped with two rf systems: low power (300 W), broad band and nominal frequency (2 MHz, 2500 W). A scheme of the ion source is shown in fig. 3.3.4.

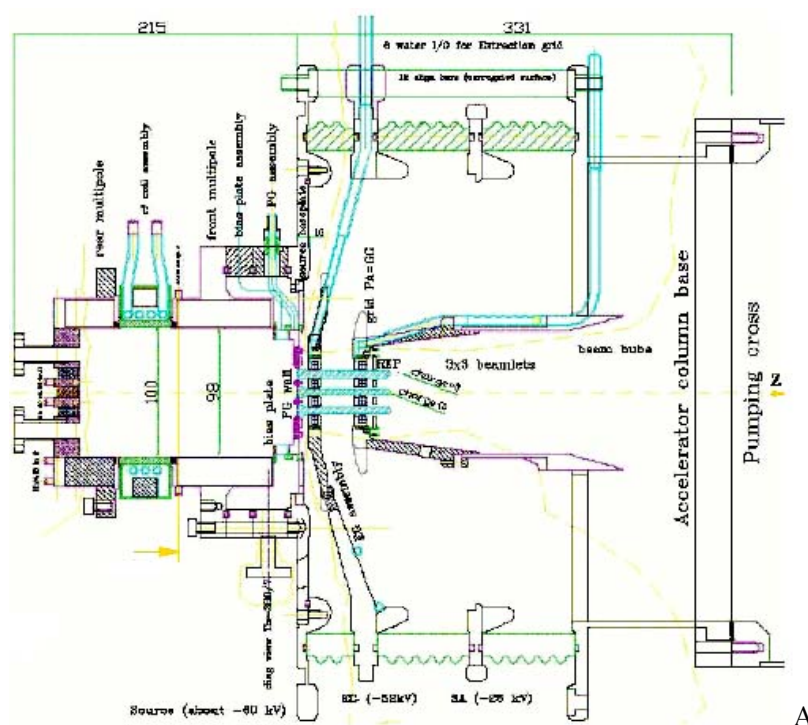


Fig. 3.3.4 Scheme of the RF negative Ion Source NIO1

A first goal of NIO1 is code and modelling verification; to this purpose, an adequate emittance meter and special rf matching are being developed at INFN-LNL. Moreover, handling of cesium and general investigation on materials are being planned.

Modelling activity was focused on improving the BYPO code to include beam losses for neutral collision and space charge compensation in the drift region after the acceleration column. BYPO also includes magnetic field deflection, so it represents an important step in the progress towards a reasonably realistic simulation of major aspect of rf source and acceleration with finite element methods in a multiphysics environment. Other modelling activity of magnetic field, of rf field and of plasma presheath was initiated. Implementation and review of existing atomic databases is well advanced.

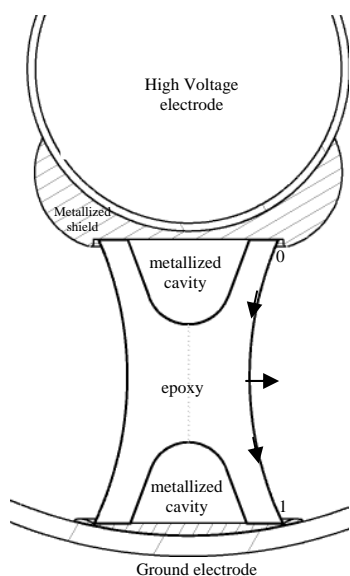


Fig. 3.3.5: Post spacer shape.

3.3.3 High Voltage issues

In 2008 the studies [De Lorenzi08] on the surface charging processes on the epoxy insulators of the ITER NBI SF6 insulated Transmission Line (TL) have been completed.

Electric charging processes of the spacer surface play an important role in the final electric field distribution, and the charge set-up time is of paramount importance to define the voltage testing procedure for the ITER TL, as well as for the gas insulated HV components. These studies were aimed to investigate the effects of the different conductivity properties of the insulator-SF6 system on the surface charge setting-up, and

also to identify a procedure to minimize this charge. Based on the most updated literature, two

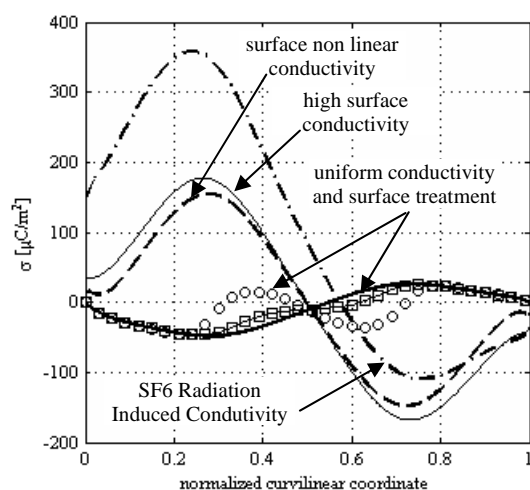


Fig. 3.3.6: Surface charge density along spacer for different conductivity combinations

simulation tools have been developed: the first consisting of a quasi-static non linear model for epoxy spacers based on the finite element code ANSYS™, the other consisting of a spacer profile optimization package, whose kernel is based on a genetic algorithm. The numerical tools have been applied to post and disk spacer models of the TL; in particular, the optimization package has been used on the disk spacer.

Figures 3.3.5, 3.3.6 and 3.3.7 show for the -1MV post spacer the electric charge

distributions for different combinations of the epoxy bulk, epoxy surface and SF6 conductivity and the related setting up time. These results indicate how large can be the variability of electric charge (a factor of 5) and setting-up time (factor $>10^3$), highlighting the importance to

keep under control the bulk and the surface conductivity. The effect of the SF6 conductivity enhancement due to ionizing radiation, a very unusual - but expected in ITER- operating condition for Gas Insulated Lines, has been found to be dramatic in terms of charge accumulation. As far as the charge setting up time is concerned, the minimum time is of the order of some hours (except in the case of high surface conductivity), giving a clear indication for the testing voltage time, which should be not less than five hours.

On the basis of the equation governing the charge accumulation on the spacer surface

$$\frac{d\sigma}{dt} = \gamma_i \cdot E_{in} - \gamma_g \cdot E_{gn} - \nabla \cdot (\gamma_s \cdot E_\tau)$$

being γ_i , γ_g , γ_s the epoxy, gas and surface conductivities and the normal and tangential components E_{in} , E_{gn} , E_τ of the electric field, an optimization software has been developed to obtain a profile minimizing both the normal electric field and the gradient of the tangential field. The tool has been applied to the disk spacer of the Transmission Line.

Fig. 3.3.8 shows the modification of the profiles and figure 3.3.9 shows the charge accumulation

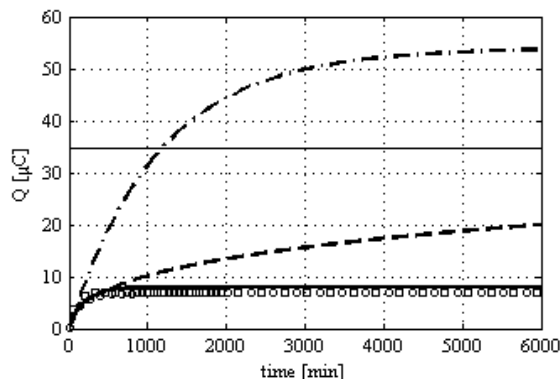


Fig. 3.3.7: Time evolution of the electric charge (absolute value)

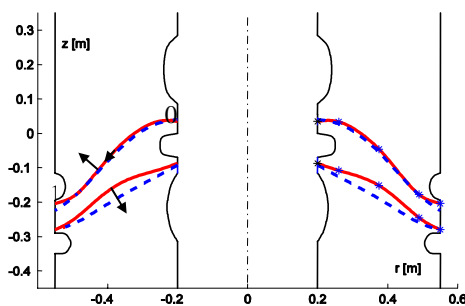


Fig. 3.3.8: Contours of the axial cross-section of the disk spacer: optimized (solid), reference (dashed).

before and after the optimization.

The optimization results efficient only in the cases in which the bulk conductivity dominates, i.e. the cases indicated in fig. 3.3-5 as *uniform conductivity* and *surface treatment*; in other terms, the optimization is effective if the charge surface density does not exceed 40-50 $\mu\text{C}/\text{m}^2$. Instead, if the surface charge exceeds this value (i.e. when the surface or SF6 conductivities prevail over the bulk one), the optimization process could produce even larger surface

charging, as shown for the cases indicated as *surface non linear conductivity* and *SF6 RIC*. Again, the control of the conductivity plays a key role in the spacer design.

3.3.4 Participation to the operation of NBI Test Facilities

During 2008 RFX personnel has participated to the operation of the NBI facilities in Naka (JAEA) and Garching (IPP).

3.3.4.1 Participation to the operation of NBI in Naka Test Facility

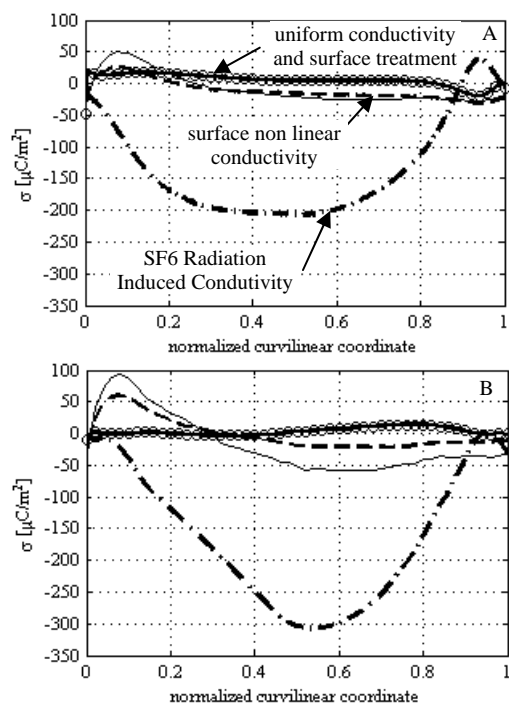


Fig. 3.3.9: Charge accumulation for different conductivity combinations for the reference (A) and optimized (B) profile

Two physicists have participated to the test of the SINGAP accelerator adapted to the 1MV Test Facility in Naka. The data have been analyzed by developing and applying a 0-D model which describes the effect of the secondary particles (positive ions due to ionization and electrons due to stripping and collision of ions with the grid surface). The results have been benchmarked with the results of a 1D numerical code. Experimental campaigns have been carried out to compare pulses in SINGAP configuration with the same ion source arc power, background pressure and acceleration voltage as in a previous campaign with the accelerator in MAMuG configuration. As a result it has been found that secondary electrons produced by back-streaming ions impinging on the grids result in currents and heat load on the acceleration grid larger than those observed in MAMuG

configuration. The results have contributed to the analysis performed to compare the two concepts, showing that the MAMuG concept is preferable to the SINGAP one.

Following this experimental campaign, an engineer has been sent to participate to the following experimental campaign with MAMuG configuration and related High Voltage test of components.

The activity has been focused on the participation to MAMuG experiments with particular emphasis on high voltage conditioning, measurements and related operational issues.

The participation to the experimental campaigns has allowed a better understanding of the high voltage issues and a practical experience with the components and techniques used to prevent breakdown inside the MAMuG accelerator. Further activities have been concentrated on the validation, by experimental results, of a Montecarlo numerical code (EAMCC) applied to simulate the the results of the SINGAP accelerator: an example is given in Fig. 3.3.10.

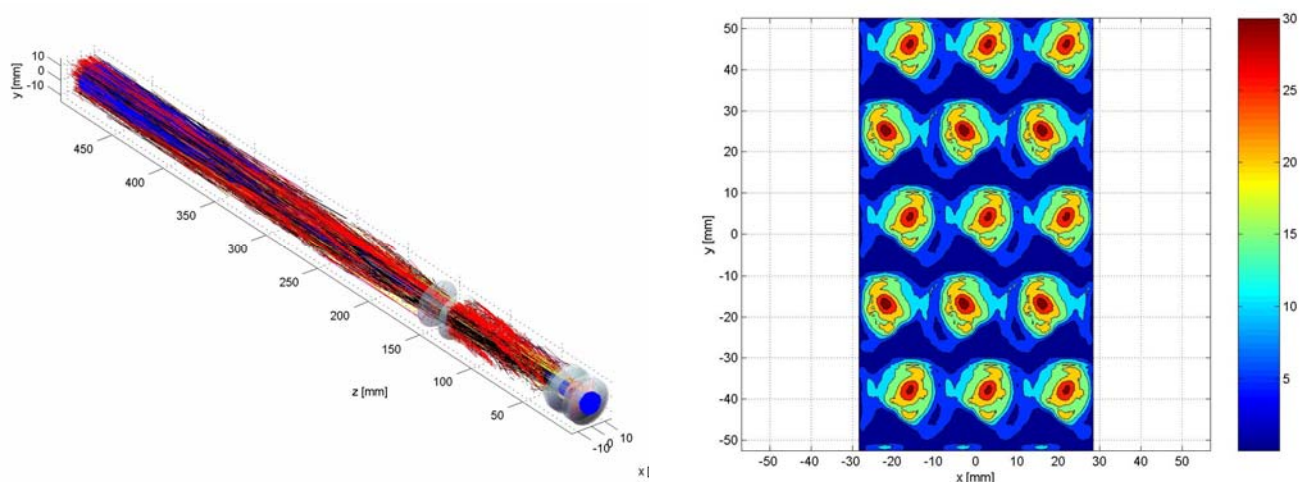


Fig. 3.3.10: Beam optics(electron and negative ion trajectories) and related thermal load on the grids in the case of SINGAP as obtained by the EAMCC Montecarlo code.

3.3.4.2 Participation to the operation of Ion Source in Garching Test Facility

Three engineers have been sent to participate to the operation and test of the power supply of the BATMAN negative ion source. Scope of the activity has been the measurement of voltage and current at the radio-frequency coil of BATMAN. The measurements have allowed benchmarking the model for the power supply developed for the ITER negative ion source with the experimental results. In particular the equivalent electrical parameters for the radio-frequency coil have been used to validate a finite element electromagnetic model currently under development.

REFERENCES

- [Agostinetti08] P. Agostinetti, et al., Proc. 1st Int. Conf. on Neg. Ions, Beams and Sources, 10-12 Sep. 2008, Aix-en-Provence, France
- [Anaclerio08,a] G. Anaclerio, F. Fantini, R. Pengo, RFX-NBTF-TN-095, EFDA Task: TW6-THH-NBTF1-ITER Neutral Beam Test Facility Task deliverable: 4.5 Cryoplant of NBTF Cryopump Part 2/4 : The Main Refrigerator (2008)
- [Anaclerio08,b] G. Anaclerio, F. Fantini, R. Pengo, RFX-NBTF-TN-096, EFDA Task: TW6-THH-NBTF1-ITER Neutral Beam Test Facility Task deliverable: 4.5 Cryoplant of NBTF Cryopump. Part 3/4 : The Shield Refrigerator (2008)
- [Anaclerio08,c] G. Anaclerio, F. Fantini, R. Pengo, RFX-NBTF-TN-097, EFDA Task: TW6-THH-NBTF1-ITER Neutral Beam Test Facility Task deliverable: Cryoplant of the NBTF Cryopump. Part 4/4 : The Proximity Cryogenic System (2008)
- [Antoni08] V. Antoni, et al., invit. contr. at 18th Int. Toki Conf., 9-12 Dec. 2008, Toki, Japan
- [Bacal2006] M. Bacal, Rev. Sci. Instrum., 71, 3981 (2000)
- [Cottrell82] Cottrell G A 1982, J. Phys. E 15 432

[De Lorenzi08]: A. De Lorenzi, P. Bettini, L. Grando, A. Pesce, R. Specogna, IEEE Transactions on Dielectrics and Electrical Insulation, under publication.

[Fantini08] Fantini, RFX-NBTF-TN-094, EFDA Task: TW6-THH-NBTF1-ITER Neutral Beam Test Facility Task deliverable: 4.5 Cryogenic system of NBX Cryopump.Part 1/4: Requirements (2008)

[Fantini09] F. Fantini, G. Anaclerio, O. Barana, F. Fellin,R. Pengo, Progress on the Design of the cryogenic plant for the ITER Neutral Beam Injector Test Facility in Padova, SOFT 25th Symposium on Fusion Technology, Rostock, Germany (proceedings, to be published in Fusion Engineering and Design), (2008).

[Fantz06] Fantz U et al 2006, Nucl. Fusion 46 S297

[Fantz07] Fantz U et al 2007, Plasma Phys. Control. Fusion 49 B563

[Fubiani08] G. Fubiani, et al., Phys. Rev. Spec. Topics Accel. Beams **11**, 014202 (2008)

[Grisham05] Grisham L 2005, IEEE Trans. Plasma Sci. 33 1814

[ITER-a] ITER Design Requirements and Guidelines (DRG2), Neutral Beam Heating & Current Drive System and Diagnostic Neutral Beam, G A0 GDRD 3 01-07-19 R 1.0, www.iter.org.

[ITER-b] ITER Configuration Control Board 1, ITER Design Change Requests 64, 154 and 159, www.iter.org.

[Kawai00] Kawai M et al 2000, Rev. Sci. Instrum. 71 755

[Marcuzzi08] D. Marcuzzi, M. Dalla Palma, M. Pavei, B. Heinemann, W. Kraus, R. Riedl. Detail design of the RF Source for the 1 MV Neutral Beam Test Facility. SOFT 25th Symposium on Fusion Technology. September 15-19, 2008. Rostock, Germany.

[Pamela91] J. Pamela, Rev. Sci. Inst. **62**, 1163 (1991)

[Serianni08] G. Serianni, et al., poster at 18th Int. Toki Conf., 9-12 Dec. 2008, Toki, Japan

4 DIAGNOSTICS

4.1. RFX Diagnostics

The work plan for 2008 entailed the re-commissioning of old RFX diagnostics, i.e. the FIR polarimeter and the microwave reflectometer, the upgrade of other ones, such as the SXR tomography and the edge probes, and the development of new measurements, such as the edge T_e and n_e from intensity ratio of He spectral lines and the q profile from the ablation clouds of Li or H pellets. Most activities were completed as planned and some provided the first plasma measurements, e.g. the FIR polarimeter, the laser blow-off and the edge T_e and n_e from He lines. In the case of the diagnostic NBI, despite the completion of the planned activities, plasma measurements are still lacking, but a strategy to pursue useful results could be envisaged. Other diagnostics made significant progress and could get some preliminary results, such as the reflectometer and the q profile measurement from pellet ablation cloud. In some cases the work was limited to a design level. Moreover the new DESO diagnostic was developed in addition to the original planning.

4.1.1 FIR Polarimeter

The strong effort dedicated in 2008 to this diagnostic allowed to obtain the first measurements. The laser system has been completely revised: the internal mirrors of the CO₂ high power laser were replaced with new components, obtaining an optimized output in terms of wavelength, emission power and spatial mode; the good coupling of the CO₂ beam and the FIR laser has been restored; the FIR cavity has been carefully aligned, obtaining a good FIR spot with an output power of about 100 mW. The optical line from the laser system to the machine (about 30 m long in dry atmosphere of N₂ gas to avoid FIR laser absorption by water vapor) has been realigned. The automatic calibration system of the diagnostic has been set up and successfully tested. This allowed to operate 5 polarimetric chords, measuring the magnetic field of RFX-mod plasmas since June 2008. The first measurements showed that the new mechanical design is very good, since they are no more affected by mechanical vibrations. On most of the chords the signal to noise ratio (SNR) is now below the 10% target value. Figure 4.1.1 shows an example of

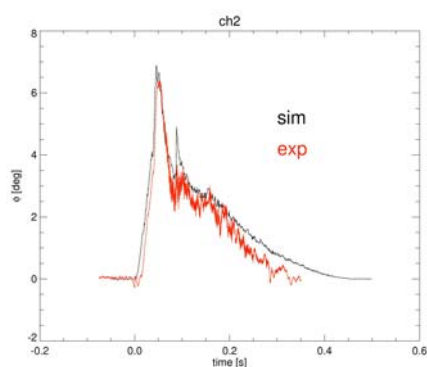


Fig.4.1.1: rotation of the polarization angle for chord #2 (red line) and expected one from μ &p simulation (black line). Shot #24934.

measurement of chord #2 for a 1.3MA shot. The work and the results obtained highlighted that a further improvement of the SNR could be achieved: in fact, the new focusing path of the FIR laser beam requires a 1.5m long propagation of the beam in free air inside the laser room and, despite the effort to condition the air of the room, the residual humidity causes a reduction of the laser beam power, and hence of the signals at the detectors, up to 70%. To overcome the problem, a new containing box for the laser beams with a powerful air conditioning system has been

designed and ordered. In this way we expect to reduce the attenuation of the FIR beam to less than 10% over the focusing path.

4.1.2 Microwave reflectometer

The Ka band of the reflectometer ($f: 26\div 40$ GHz, $n_e: 0.9\div 2\cdot 10^{19}\text{m}^{-3}$), has been installed and put into operation on RFX mod. First measurements show strong microwave reflection when the plasma density exceeds the critical value ($f_{pe}^2 = e^2 n_e / (4\pi^2 \epsilon_0 m_e) > f_{\text{microwave}}^2$) as expected. The signal post processing needed to extract the relevant physical information is in preparation. It is planned for year 2009 to put into operation the other 4 bands. In this way, the fast time evolution of a 5-point density profile will be available.

4.1.3 Soft X-Ray (SXR) diagnostics

4.1.3.1. New horizontal SXR camera

A new version of the horizontal manipulator of the soft x-ray (SXR) tomography has been designed between 2006 and 2007. This camera, based on the wide experience of the past years on RFX and MST, will substantially increase the spatial resolution of the tomography, adding a total of 65 channels organized in three rows. Different beryllium foils will be installed in two rows so that different energy spectral ranges could be measured simultaneously in the same plasma shot: these data will allow to follow the temporal evolution (up to 100 kHz) of the plasma SXR emission and electron temperature profile with high accuracy.

Most of the electronics (acquisition) has been already purchased; two prototypes of amplifiers have been tested, defining the final version of the amplification stage. The various parts of the diagnostic (mechanics, supports etc.) have been built during this year, but the final assembly of the new SXR camera and the installation in RFX-mod will occur in the next year.

4.1.3.2 SXR Multifilter

This diagnostic supplies the core T_e from SXR measurements using the two-foil technique. Presently 4 photodiodes are used to measure the SXR flux from the plasma. The cones of sight defined by the diodes surface and the pinhole are almost overlapped two by two but in the presence of a more emissive structure, like in QSH or SHAx, a systematic error appears in the calculated T_e since each diode “sees” the SXR structure differently from all the others due to the partial overlapping of the cones of sight. This error is further complicated in the case of rotation of the island. It is planned to upgrade the diagnostic, going from 4 to 6 channels arranged in a more favorable way for this type of measurement. In addition, new beryllium foils will be installed in order to extend the T_e measurements to almost all types of RFX-mod plasmas. This modification started with the design of a new support of the photodiodes, while keeping all the external mechanical parts.

4.1.4 Edge measurements

4.1.4.1 Temperature and density profile from thermal He beam

In 2008 a new diagnostic called Thermal Helium Beam (THB) has been installed in RFX-mod

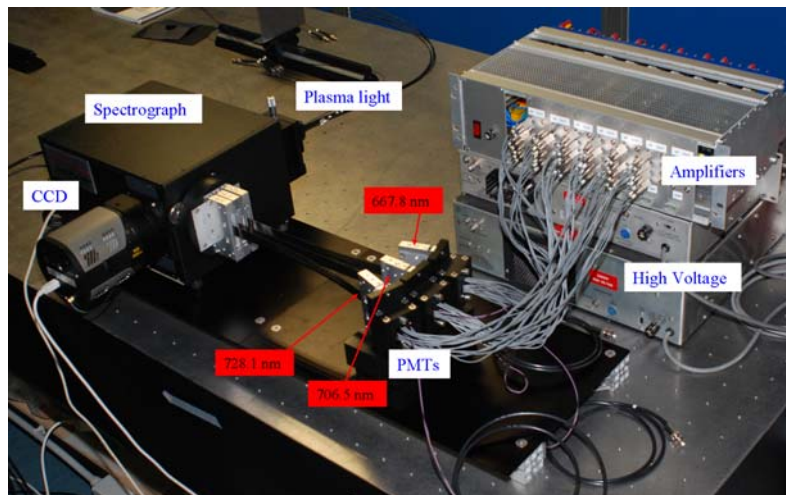


Fig.4.1.2: layout of the Thermal Helium Beam Polychromator for the measurement of T_e and n_e edge radial profiles

for the measurement of the edge radial profiles of electron temperature (T_e) and density (n_e) and their time evolution [Scarin08]. This is a development of the old THB previously installed at RFX experiments [Carraro00]. A Helium atomic beam is injected into the plasma edge and its optical emission on the three lines $\lambda_1=667.8\text{nm}$, $\lambda_2=706.5\text{nm}$ and $\lambda_3=728.1\text{nm}$ is observed. The light is collected from eight different radial positions, from 0 to 35 mm with a spatial resolution of 5 mm. In figure 4.1.2 the layout of the diagnostic is shown. The light collected in the 8 different radial positions enters the spectrograph used as polychromator. The three lines $\lambda_1, \lambda_2, \lambda_3$ can be observed by a CCD camera with a time resolution of about 100 μs , or with three multianode photomultipliers (PMTs) that allow a higher time resolution (up to 10 μs). In figure 4.1.3 there is an example of the results obtained with the THB and the CCD cameras (during the 2008 campaigns the THB has been used in this configuration): the time evolution of the edge radial profiles of T_e , n_e and P_e is shown.

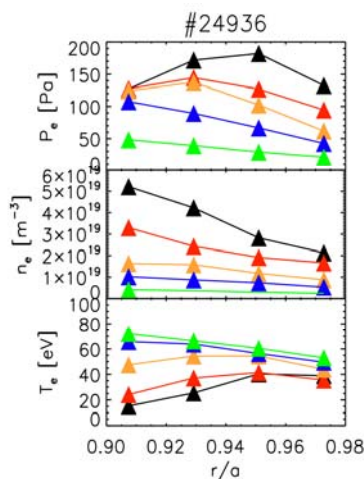


Fig.4.1.3: edge profiles measured with THB. Different colors refer to different time instants

4.1.4.2 Laser Blow-Off system

At the end of 2008 the PMTs have been installed for the measurements of the three Helium lines. After the calibration and the tests, the diagnostic in this new configuration has been coupled with the RFX-mod machine and first plasma signals have been collected.

The Laser Blow-Off system has been installed and aligned. The same laser used for the edge Thomson scattering diagnostic has been used, with a beam splitter allowing the simultaneous activation of the two systems. The first injections into the plasma have been carried out ablating a Nickel target, as Nickel is a well-suited impurity for transport studies in a plasma characterized by the RFX-mod electron temperature and density. Different target thicknesses

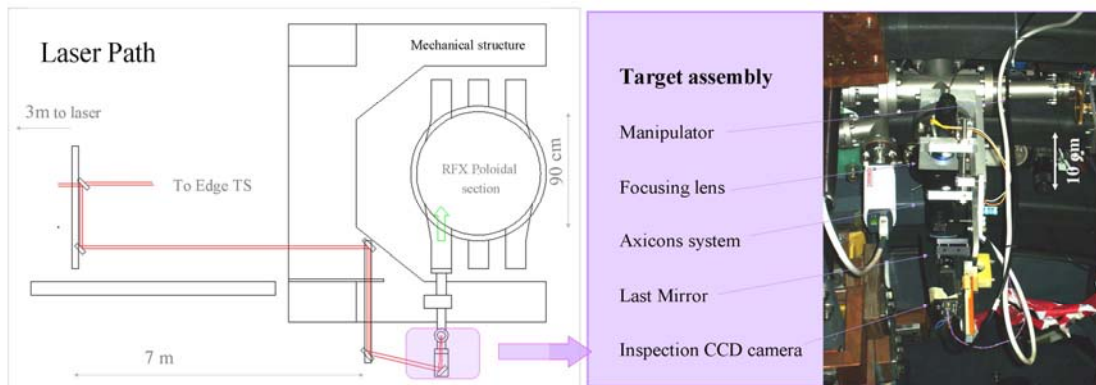


Fig.4.1.4: schematics of the laser path for laser blow-off injections in RFX-mod (left) and detail of the target assembly (right).

and optic configurations have been tested in order to optimize the Nickel ablation. The first results obtained for the impurity transport parameters are reported in section 5.2.8.

4.1.4.3 Plasma density measurement in the edge region

During this year the diagnostic “triple Langmuir probe” placed at 82° toroidal position at r=459 mm was updated from several point of view. The temperature measurement was completed with the plasma density and plasma potential measurements.

The probe measurement circuit has been completely renewed and the range of temperature measurement has been doubled. Furthermore a system for protecting the electric circuit from the plasma arcs has been tested and installed.

The acquisition system is now based on optical fibers: the acquisition sampling frequency has been improved and is presently set at 5 MHz.

The effect of magnetizing winding currents up to 50 kA on optical transmitters have been concentrated by suitably positioning them close to the vacuum vessel.

4.1.4.4 Arc-less power supply for ion saturation measurements

The activity performed in 2008 has led to the development of a power supply, to be used for ion saturation current measurements with Langmuir probes, capable of interrupting the current when an arc develops. A prototype of the protection circuit has been built. On the basis of the results of laboratory tests, some improvements are being carried out to test the prototype on real plasma using the fixed triple probe.

4.1.5 Diagnostic Neutral Beam: T_i and B measurements

An increase of the optical etendue has not allowed to detect Charge Exchange signals, as the collected radiation remains severely dominated by a strong passive component. Simulations

carried out by means of Von Hellermann's code suggested to investigate the emission of O VIII rather than C VI. The O VIII line at 6068 Å has been therefore monitored with the highly luminous and high resolution spectrometer but no sign of active signal has been found. Rather, the passive emission has provided first evaluation of the ion temperature in the plasma core. In fact, transport simulations of O in RFX suggest that O VIII should be emitting in the plasma core. However, both the uncertainties on the impurity transport coefficients and the geometry of the measurement do not allow a precise evolution of the radial position of the measured ion temperature. T_i results to be around 50% of T_e at intermediate density, becomes similar to T_e at high density, while in the interesting region of low density, where strong QSHs develop, the O emission is far too low for a Doppler broadening evaluation. Detailed simulations of the energy equipartition processes via the code Riport have not been completed so far. A comparison with the MST case suggested to try the UV emission lines, which have a larger effective charge exchange cross section. This led to ask Von Hellermann to include the calculation of such lines in his code and, in parallel, to design a new layout of the diagnostic, as the spectrometer cannot any longer be kept far from RFX in order to compensate for the signal losses along the optical fibers. These measurements will be tried on RFX at the end of the 2008 campaign. Also, as a result of the comparison exercise, also MST can now be simulated by means of the same code, which will add useful information.

H α measurements provided a very weak beam emission signal that will be used for a first attempt to yield an estimate of B_t in the center. However the weakness of the signal confirms that the injector current needs to be restored at least to its original value (2.5 equivalent A) and that a smaller divergence of the beam should be sought for, possibly by changing the extraction grids.

4.1.6 Impurity pellet injector and q profile measurements from ablation cloud

The design of the pellet injector interface to the RFX-mod has been completed and the order for its construction has been placed. It is expected that the injector will be installed in January 2009. At the same time important preparation activities have been completed: the Lithium handling and pellet preparation tools have been developed, and experimental tests have been performed to estimate the vacuum pumping requirements needed to limit the injection of pellet driver gas into the RFX-mod vessel. The system has been also optimized improving the sabot loading parts, to improve its reliability and to reduce running manpower requirements.

Taking advantage of the new fast CMOS camera, the first measurements of the safety factor profile, $q(r)$, in RFX-mod have been performed by observing the ablation cloud of frozen hydrogen pellets launched by the cryogenic injector. The cloud angle has been measured (Fig.4.1.5a) and the measured radial profiles agree with those computed with the toroidal equilibrium model (Fig.4.1.5b). These first measurements prove the possibility to effectively measure the safety factor profile with good precision by this technique. The spatial resolution and the precision of the measurement will be improved the next year by using the Lithium pellet injector thanks to the lower pellet speed and the larger cloud length.

4.1.7 Desorption measurements

During 2008 the subject of density control, intended as the capability to operate the machine at a desired plasma density, has been thoroughly addressed. Two main aspects have been pointed out. On the one side, it has been found that the gas flow produced by the fueling system, made of piezo-electric valves used in pulsed way, is not reproducible if operated without precaution. In particular, if a sequence of openings is performed, the valves proved to progressively increase their flow with a difference between the first and the last shot of the sequence that can reach 50%. Nevertheless, after 4-5 pulses, a regime behavior, characterized by a 10% maximum spread of the flow in the following pulses, proved to be reached, but only if the sequence is not interrupted for more than half an hour. On the other side, due to the full graphite first wall, it was found that in RFX-mod the issue of density control is strongly connected to the capability to control the H₂ particle content in the wall itself. In fact, during operation, the plasma density is entirely sustained by particle fluxes coming from the wall.

In order to allow a precise fuelling and a better density control during operation, a new

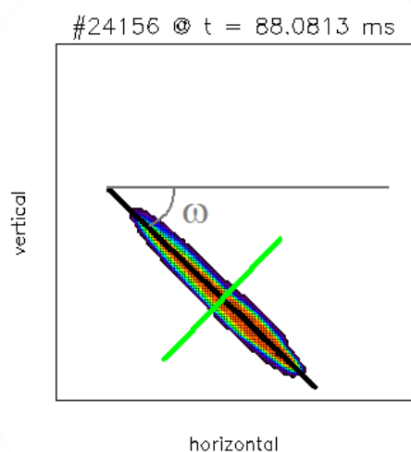


Fig.4.1.5a: fast CMOS camera image of the hydrogen pellet ablation cloud.

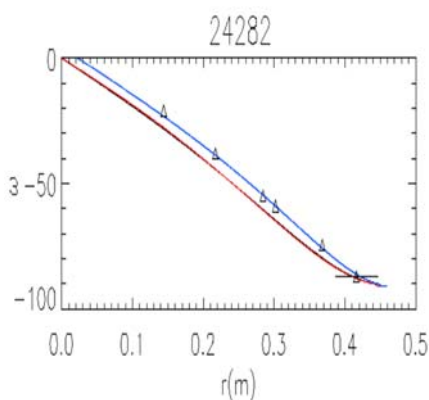


Fig.4.1.5b: comparison of the measured cloud angle (triangles) with those from toroidal equilibrium model (blue line) and cylindrical models (red and black lines).

diagnostic system, named DESO (DESOrption diagnostic), has been implemented during this year on RFX-mod [Canton08a]. By means of a series of dummy openings before each RFX-mod shot, the system keeps the piezo valves in a working state in order to assure the reproducibility of their flow. Moreover, by processing the time evolution of the in-vessel pressure, DESO computes both the total number of particles that are supplied to the discharge by means of the valve system and the total number of particles that are outgassed from the wall and extracted from the vessel after each shot by the pumping system. DESO measurements, coupled to data coming from other diagnostics (masses of the injected pellets from the injector system, particles removed from the wall during He GDC's from a mass spectrometer), allowed to compute three parameters that characterize the status of the wall [Canton08b]: the Desorption Factor (Des%), defined as the per cent ratio between the particles extracted after the end of the pulse and the total fuelled ones in that shot, the particles left in the wall after each shot (DeltaPart), defined as the difference between the total fuelled

particles and the outgassed ones (in case of He GDC the extracted particles are also subtracted), the total number of particles stored in the wall since the last baking or

boronization procedure (TotPart), computed as the sum of DeltaPart for all the shots since the treatment. It was found that, for a specific shot, Des% describes the capability of the wall to absorb particles in that shot, and that it influences the I/N values obtained in the discharge more than TotPart: in particular a not absorbing wall (Des%>100%) forces a I/N to the value $2 \times 10^{-14} \text{Am}$, likely corresponding to the maximum sustainable density. The analysis of DeltaPart behavior, conversely, has shown that normal operation in RFX-mod stores particles in the graphite at almost each shot, and that we have not yet found an effective way to prevent particle accumulation in the wall.

4.2 Diagnostics for ITER

4.2.1 In-vessel magnetic sensors

The development of in-vessel magnetic equilibrium sensors for ITER has been continued in the framework of the EU activities on ITER magnetic diagnostics. A cluster of Associates (CRPP, ENEA/RFX, CEA, CIEMAT) is being formed to answer to calls for grants issued by F4E. Equilibrium sensors are essential for machine control and plasma diagnostics. Pick-up coils made of Mineral Insulated Cables (MIC), which have been widely used in JET and in other tokamaks so far, are considered inadequate to this purpose, in view of the spurious signals due



Fig.4.2.1a: ceramic-filled pick-up coil after curing process

to Radiation-Induced and Thermally-Induced Electromotive Force (RIEMF/TIEMF) effects which are expected to produce unacceptable measurement drift during long plasma pulses [Vayakis05, Vermeeren08, Vila07]. Since the pick-up coils are still considered the most simple and reliable magnetic sensors suitable to the harsh ITER in-vessel environment, it was decided to develop new pick-up coils with the following guidelines:

- using low-RIEMF/TIEMF materials (such as pure metals with reduced extraneous materials)
- reducing the thermal gradients caused by radiation heating, by improving the equivalent thermal conductivity to the vessel

A first approach for the sensor design originated from previous experience with fluid ceramic fillers (at RFX and JET) and is based on a winding made of flexible ceramic- or glass- coated conductor, "impregnated" with fluid ceramic in order to improve the overall thermal conductivity and dielectric properties of the winding pack (fig. 4.2.1a and b). The conductor material is also expected to provide a lower RIEMF/TIEMF sensitivity with respect to winding packs made of MIC, which constituted the ITER reference design. An impregnation system, based on an impregnation chamber connected to a vacuum system was specifically designed

and a dozen of prototypes were built with ceramic coated wires using different winding procedures and different impregnation procedures. The prototypes were then tested to assess the fabrication process and the reliability.

The tests have proved that a wire winding is a viable technological solution, but also that the reliability of the electrical insulation made of flexible ceramic is critical. More recent tests on coils made with "POZh" wire, which is a high-temperature resistant cable with tight braided fibre-glass insulation, produced in the Russian Federation have given better results. However, the thermal behaviour of the ceramic-filled coil and the outgassing rate can be a critical issue too.

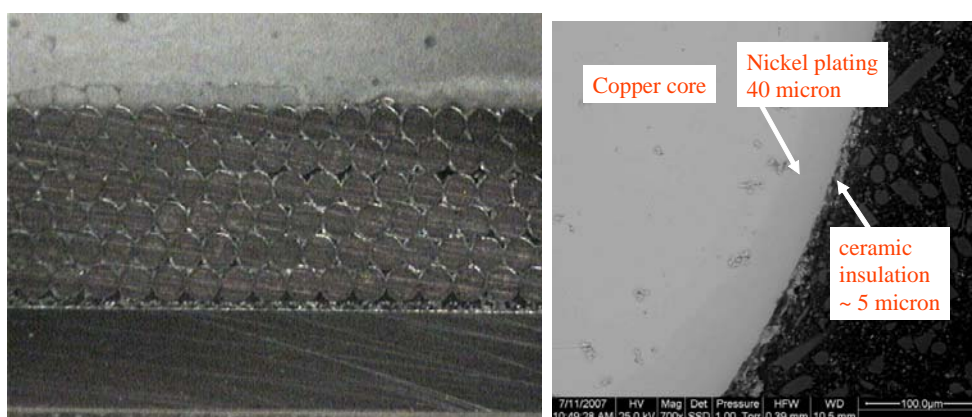


Fig.4.2.1b: micrographic image of a ceramic-filled coil section (left) and SEM analysis of ceramic-coated wire (right)

The second approach for the sensor design is based on ceramic-substrate micro-circuit technology LTCC (Low Temperature Co-fired Ceramic), which has been used in special purpose electronic applications such as aerospace, telecommunication and defense. In this case, the sensors are constituted by a stack of ceramic-layers with printed metallic lines, high-pressure laminated and fired in one or more steps to obtain a single object (fig. 4.2.1c and d). Lines on different layers are connected by metallic vias. The result is a compact, highly reliable circuit. The materials are vacuum and high-temperature compatible. A first set of 6 prototypes with 10 layers of Ag conductors was built and tested with very good results. The tests have shown that the LTCC sensors are suitable to meet the ITER requirements both in terms of compatibility as in-vessel components (chemical composition and outgassing rate) and in terms of measurement performances (signal bandwidth, dimensional stability, low stray area, low thermal gradient). Final reports for EFDA contract TW5-TPDS-DIASUP5 (EFDA 05-1347 D2.2) and task agreement TW5-TPDS-DIADEV D2a have been submitted and approved by EFDA. Reports for contracts TW6-TPDS-DIADES and TW6-TPDS-DIASUP12 part I are in progress and will be completed in the first months of 2009.

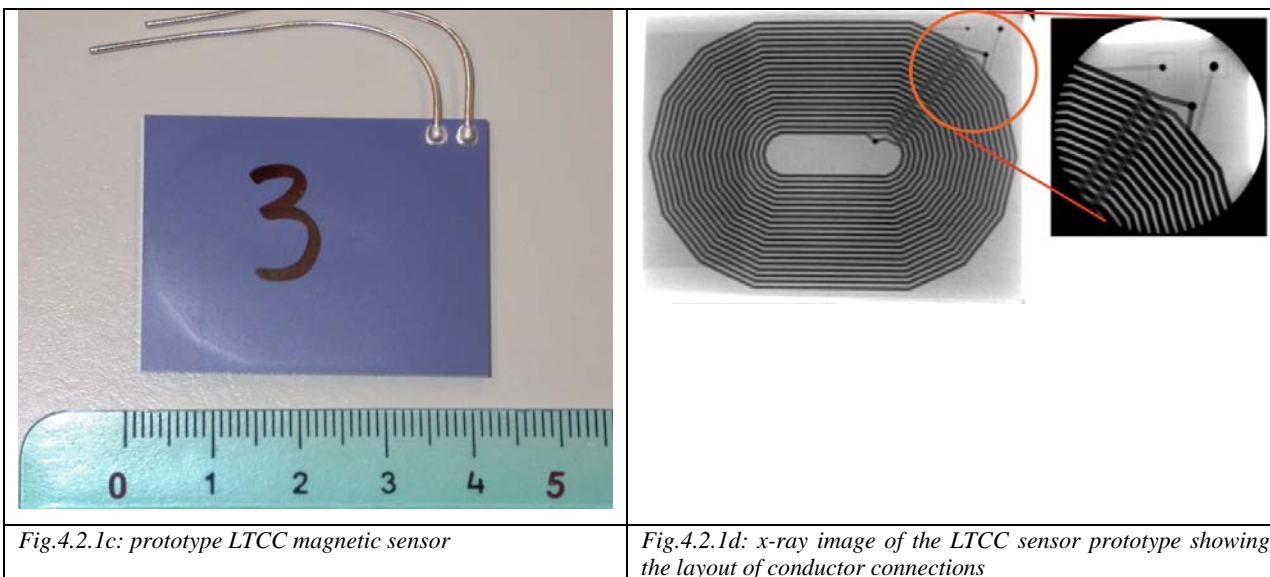


Fig.4.2.1c: prototype LTCC magnetic sensor

Fig.4.2.1d: x-ray image of the LTCC sensor prototype showing the layout of conductor connections

4.2.2 Core LIDAR.

RFX has contributed to develop the specifications of the ITER core LIDAR diagnostic, participating to a cluster of EU Fusion Associates, coordinated by UKAEA. The task EFDA/06-1442 was concluded in February 2008, with the delivery in due time of the draft final report [Pasqualotto08].

According to the Work Breakdown Structure defined in the Thomson Scattering (Core LIDAR) Project Management Plan, RFX took responsibility of the Work Packages: NIR Detectors and Calibration System.

A conceptual design of the Near Infrared (NIR) detectors was produced, assessing potential capabilities and availability of NIR detectors to cover the spectral range 850-1100 nm and beyond. Finding a suitable NIR detector is an essential condition to use only Nd:YAG lasers for TS measurements in all Te expected ranges. Otherwise a doubled Nd:YAG will be required for lower Te values. The work started in 2007 with a) an investigation of published documentation

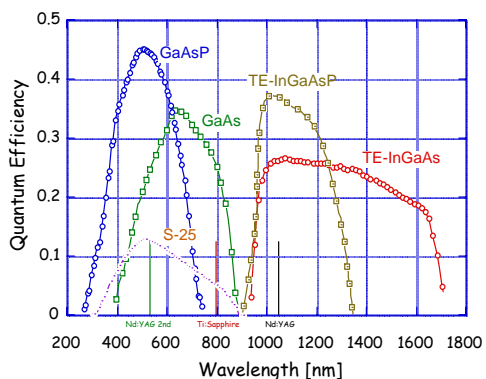


Fig. 4.2.2: spectral QE of two types of TE photocathodes, available in commercial detectors, compared with that of the photocathodes of visible LIDAR detectors

on Transferred Electron (TE) photocathodes and a preliminary assessment of their suitability for core LIDAR detectors; b) negotiation with the Intevac company of a possible development program for procurement of suitable TE photocathode detectors. The work has been concluded in 2008 with a) the performance simulation of the system with the inclusion of TE detectors; b) the review of wider range of studied technologies for NIR detectors and assessment of their applicability; c) the assessment of suitability of available technologies for NIR Lidar detectors (in particular the comparison between two main

approaches: MicroChannel Plates and Intensified Photodiodes); d) contacts with a wider range of manufacturers to investigate manufacturing capabilities and availability to R&D; e) the definition of a strategy ahead for procurement and proposal of development program [Walsh08]. A list of R&D proposals were produced for this purpose and with the perspective to continue the work, participating to a formalized cluster of Associations, still led by UKAEA, to answer to F4E calls.

The other main task of RFX was to assess possible calibration methods: a) use a micro retroreflector array or a Lambertian white diffuser installed on the shutter in front of the first mirror and back-illuminated through the collection optics from an external source, as a method for relative calibration; b) use Thomson scattering measurements from dual wavelength laser sources as a method for relative calibration, and specifically to measure both the electron temperature and the transmission of collection optics. Feasibility and limitations of the latter method have been investigated with a simulation. Also for the further development of proper calibration methods, a set of R&D tasks have been proposed for future work.

A project management plan for procurement of the NIR detectors, with proposal of a time plan and estimate of required resources, has been produced.

4.3 Diagnostics for JET

4.3.1 High Resolution Thomson Scattering (HRTS) for JET

In 2008 the HRTS project for JET has been successfully completed. In 2007 the project was extended by one year to solve the only still outstanding problem, i.e. the high risk to damage the input optics by the laser beam. Because of this, after completion of the experimental campaign in March 2007, the HRTS laser beam was not allowed to propagate any more through the existing beam path. To mitigate the risk and re-gain permission to operate, a new input path has been designed, tested and installed early in 2008. Some protection systems

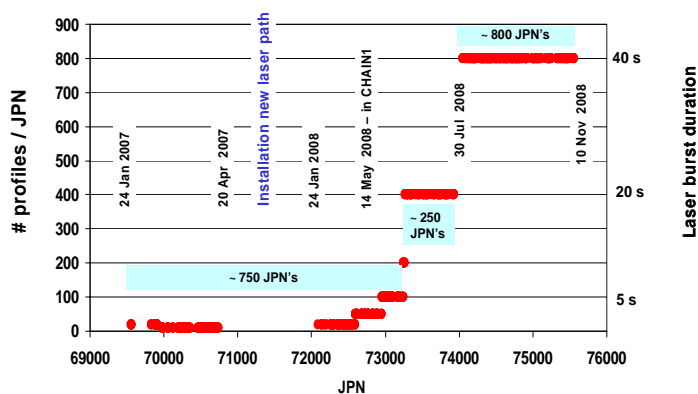


Fig. 4.3.1: operation of HRTS on JET in 2007-08: number of temperature and density profiles measured for each Jet pulse (JPN), from a safe limit of 10 to the final default value of 800.

have also been developed and installed, to detect anomalous laser behaviours and to interlock the system. Among them a monitor of the laser beam profile, which acquires and analyses in real time each laser pulse and shut down the laser if the peak power is too high.

Also the acquisition system has been brought to full performance by installing more fibre optic delay lines, thus increasing the

number of points in the profiles from 37 to 61.

The HRTS has then been operational during the entire 2008 experimental campaign, gradually increasing the laser burst duration up to 40s, equivalent to 800 profiles measured during a JET discharge (fig. 4.3.1), with 20 Hz repetition rate and 1.5 cm spatial resolution, fully meeting the requested specifications. The spatial resolution has been further increased by sweeping the plasma position, which has allowed resolving more in detail the edge transport barrier (fig. 4.3.2).

Data acquired in 2008 have been successfully used in several physics studies.

4.3.2 Magnetic coils

The enhancement of the Magnetic diagnostic system for the JET-EP programme had the main aim of improving the accuracy of the reconstruction of the plasma equilibrium and the performance of the real time feedback control of the plasma shape. The whole diagnostic system consists of both in-vessel and ex-vessel sensors, subdivided into several sub-systems, for a total of a hundred new magnetic sensors.

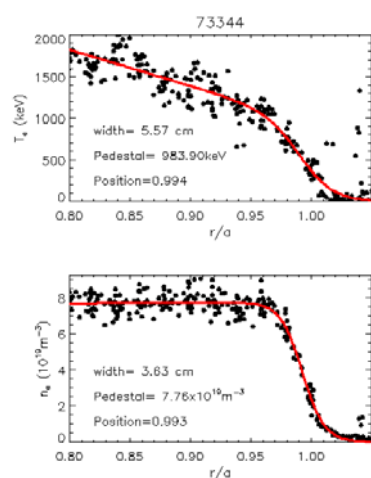


Fig. 4.3.2: T_e and n_e profiles from HRTS, sweeping plasma position (pre-ELM selection)

The project has been managed since 2002 in the framework of a number of EFDA-JET Orders and Notifications, under the joint responsibility of Consorzio RFX and Consorzio CREATE, in close collaboration with the JET Operator and CRPP. The activities during 2008 were mainly dedicated to signal validation and functional commissioning of the in-vessel subsystems installed during the 2007 shut-down.

The assessment of the performance of the new coils was carried out verifying the consistency of experimental signals

with reconstructed signals, obtained by using equilibrium codes based firstly on independent existing magnetic measurements and then integrated with the new signals.

The validation of the new signals was completed successfully, even though during the commissioning a few probes evidenced on erratic behaviour, which seems to be related to malfunctions of in-vessel connections; understanding the cause of this malfunction still requires further investigation. The overall functional commissioning demonstrated that the information provided by the new coils allows a more precise reconstruction of regions not covered by previous measurements, in particular the upper region for high triangularity and high elongated plasmas [Peruzzo08]. This demonstration represents the achievement of the goal of the project, which is planned to be formally completed by the end of 2008.

REFERENCES

- [Canton08a] A.Canton, S. Dal Bello, et al., 35th EPS Conference on Plasma Phys. Hersonissos, 9 - 13 June 2008, proceedings ECA **32F**, D-1.002 (2008).
- [Canton08b] A.Canton, S.Dal Bello, 13th IEA/RFP Workshop, October 9-11, 2008, Stockholm.

- [Carraro00] L. Carraro, G. De Pol, et al., *Plasma Phys. Control. Fusion* **42**, 1 (2000).
- [Pasqualotto 08] R. Pasqualotto, L. Giudicotti, EFDA Report n. EFDA06-1442: TW6-TPDS-DIADES, 15-02-2008.
- [Peruzzo 2008] S. Peruzzo, R. Albanese, V. Coccoresse, S. Gerasimov, N. Lam, F. Maviglia, I. Pearson, P. Prior, A. Quercia, and L. Zabeo, "Installation and commissioning of the JET-EP magnetic diagnostic system", presented at the 25th Symposium on Fusion Technology, 15-19 September 2008, Rostock, Germany; to be published on *Fusion Engineering and Design*.
- [Scarin08] P. Scarin, M. Agostini, et al., 50th APS, 17-21 November 2008, Dallas.
- [Vayakis05] G. Vayakis, Sugie et al., "Radiation-induced thermoelectric sensitivity (RITES) in ITER prototype magnetic sensors", *Rev. Sci. Instrum.* Vol. **75**, No **10** (2005).
- [Vermeeren08] L. Vermeeren and R. Weber, "Induced voltages and currents in copper and stainless steel core mineral insulated cables due to radiation and thermal gradients", *Fusion Engineering and Design* **82** (2007).
- [Vila07] R. Vila , E.R. Hodgson "TIEMF in unirradiated Cu cored MI cables: Microstructure" *Fusion Engineering and Design* **82** (2007) 1271–1276.
- [Walsh08] M.J. Walsh, K. Beausang, M.N.A. Beurskens, L. Giudicotti, T. Hatae, D. Johnson, S. Kajita, E.E. Mukhin, R. Pasqualotto, S.L. Prunty, R.D. Scannell, G. Vayakis for the ITPA Thomson Scattering Working Group, "Performance Evaluation of ITER Thomson Scattering Systems", paper IAEA-CN- IT/P6-25, "22nd IAEA Fusion Energy Conference", 13-18 October 2008, Geneva, Switzerland.

5. THEORY AND MODELLING

In 2008 the qualitative and quantitative improvement of confinement in RFX-mod was an incentive to study the RFP with low magnetic chaos, both to develop its theoretical description and to interpret its experimental features. A noteworthy fact was the implementation of a new version of the PIXIE3D code enabling extended MHD modeling; it is suitable for parallel computing and features an optimized preconditioner. Since confinement improves when the magnetic boundary becomes more axis-symmetric, new efforts led to a better understanding of the clean mode control of this boundary. Tokamak micro-turbulence codes were modified and used to address the experimental regimes where magnetic chaos no longer rules anomalous transport. However codes computing collisional particle dynamics in RFP magnetic fields still proved to be useful.

5.1 Magnetohydrodynamics

5.1.1 Implementation at RFX of the PIXIE3D code

During 2008 the first serial version of the PIXIE3D code, previously implemented at RFX, has been successfully benchmarked against the SpeCyl code on results for 1D and 2D reversed field pinch and tokamak solutions in cylindrical geometry and force free conditions. PIXIE3D is designed to address extended MHD modelling including energy balance, generalised Ohm's law, and toroidal geometry. In the second part of 2008, as a second step in our collaboration with L. Chacon (ORNL), a second version of PIXIE3D has been implemented at RFX. The updated version is suitable for parallel computing. This version, whose numerical results show a perfect agreement with the previous one, has been used to complete the 2D benchmark with the SpeCyl code and to start the benchmark extending its application to fully 3D solutions. First 3D RFP simulations, with dissipation parameters in the range which is predicted to lead to QSH conditions by SpeCyl, have been performed with PIXIE3D. The solution provided by the latter code does agree with the former: a QSH regime is indeed found, with the same preferred helicity and the same helical field amplitude as the SpeCyl one [Bonfiglio08a]. The activity with the parallel code PIXIE3D has been possible thanks to the new architecture for high

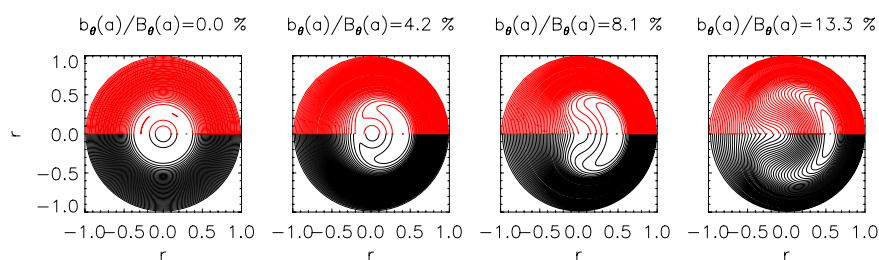


Fig.5.1.1: 2D benchmark between PIXIE3D and SpeCyl: evolution of the helical flux function ψ when a tearing mode dynamics is simulated. The initial condition is an unstable axisymmetric equilibrium, while the final one corresponds to the nonlinearly saturated helical equilibrium, after the expulsion of the magnetic separatrix. Red contour levels are resulting from a simulations by PIXIE3D, black ones come from the omologous simulation by SpeCyl: there is a clear agreement between the two.

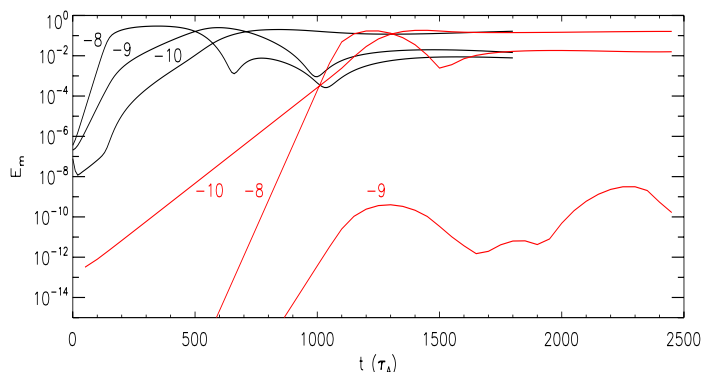


Fig.5.1.2: 3D benchmark between PIXIE3D and SpeCyl: temporal evolution of the magnetic energy of $m=1$ modes (n value indicated next to each curve) for SpeCyl (black) and PIXIE3D (red). With the same dissipation parameters, both codes predict a QSH regime with the same preferred helicity. The saturation amplitudes of the dominant mode are also the same.

performance parallel computing, which has been implemented at RFX in 2008. In fact, as users involved in High performance computing (HPC) activities, we have now at RFX a parallel computing system which is, for the time being, composed by two linux machines equipped by 16 numerical processors each. Considering that a 3D parallel run of PIXIE3D, with the strictly necessary mesh resolution, takes weeks to be completed, and considering also that PIXIE3D is not the only parallel code used at RFX, we consider the present HPC facility at RFX just a starting point and strongly support future extensions. Examples of evolution of the helical function and of magnetic energy of $m=1$ modes are shown in fig. 5.1.1 and 5.1.2.

Concerning other MHD studies done in 2008, the work on ultra-low q simulations with SpeCyl, which began in 2007, was completed and led to a publication [Bonfiglio08b]. A study on OPCD simulations, aiming at clarifying the mechanism of QSH triggering by OPCD action observed in the experiment, is also under way [Bonfiglio08c].

5.1.2 Tokamak disruptions and vertical displacement events

In 2008 the activity regarding the EFDA task /05-1335 TW5-TPO-ASYVDE (Asymmetric VDE modeling for ITER) has been completed and in April the final report has been delivered to EFDA. The simulation work has been carried out in full 3D geometry using the nonlinear resistive MHD code M3D. Interesting cases of non symmetric VDE's for ITER reference and advanced scenarios have been obtained.

The simulations have confirmed that the toroidal peaking factor (TPF) and halo fraction (hcf) (i.e. the ratio of the normal current going to the wall to the total toroidal plasma current) are within the limits of the ITER construction specifications : $TPF \cdot hcf < 0.75$ [Paccagnella08].

5.1.3 RWMs in toroidal geometry with realistic 3D walls

The activity on theoretical modeling of RWMs continued in 2008 with the validation of the CarMa code and the determination of 3D effects of the wall on RWM stability (see the section on Integrated tokamak modeling activity).

5.1.4 Modeling of active rotation of the RWM by external control

In order to study the physics of RWM dynamics and to define a new strategy of the mode control, the new theoretical model has been proposed for the active control on the rotation of the RWMs in RFX-mod by application of the complex gain [Bolzonella08]. Since the RWM mode rational surface is outside the plasma, the usual torque theory is not appropriate. The new model provides a dispersion relation for a cylindrical RFP plasma taking into account the effects of the resistive wall and feedback system, and simulates the experimental control procedure. The obtained dispersion relation gives the rotation frequency of the RWM under the active control by the complex gain, which is in agreement with the experimental results as shown in fig. 5.1.3.

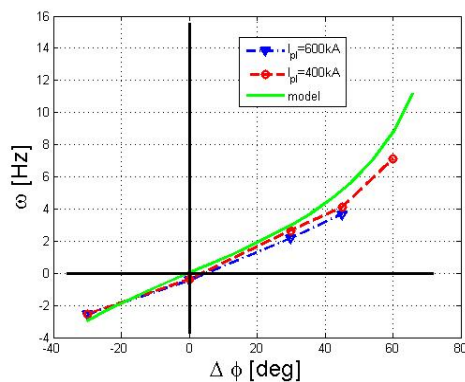


Fig.5.1.3: Dependence of the mode rotating frequency on the phase angle of the complex gain

5.1.5 Feedback control on tearing modes

A general analysis of the CMC feedback on the RFP dynamo tearing modes has been done [Zanca08]. A single resistive shell is considered, with the active coils placed outside. The radial field variation across the shell is taken into account. The model describes the evolution of several tearing modes at the same time, under the viscous torque due to the fluid motion and the electromagnetic torque developed by the image currents induced onto the shell, by the feedback currents, and by the non-linear interaction between different tearing modes. The CMC feedback is shown to prevent the tearing modes wall-locking: regardless to the amplitudes at the resonant surfaces, tearing modes rotate with edge values very close to those they would have in the presence of an ideal shell in the place of the resistive shell. It is demonstrated that the feedback (for given gain values and shell characteristics) does not fix the absolute value of the edge radial field, but the

ratio $\hat{b}_a^{m,n} \equiv \left| \frac{b_r^{m,n}(a)}{b_r^{m,n}(r_{m,n})} \right|$. In terms of $\hat{b}_a^{m,n}$ and power required to the coils, the feedback performance improves increasing the shell time constant τ_w , until saturation is found at $\tau_w \approx 100\text{ms}$: in the example shown in figure 5.1.4, the control radius is set at the inner surface of the shell, $r_f = r_{wi}$. With a standard PD controller the feedback cannot decrease $\hat{b}_a^{m,n}$ below the ideal-shell values even moving the control radius at the plasma edge: $r_f = a$. This means that the lower limit for $\hat{b}_a^{m,n}$ is determined by the plasma shell proximity.

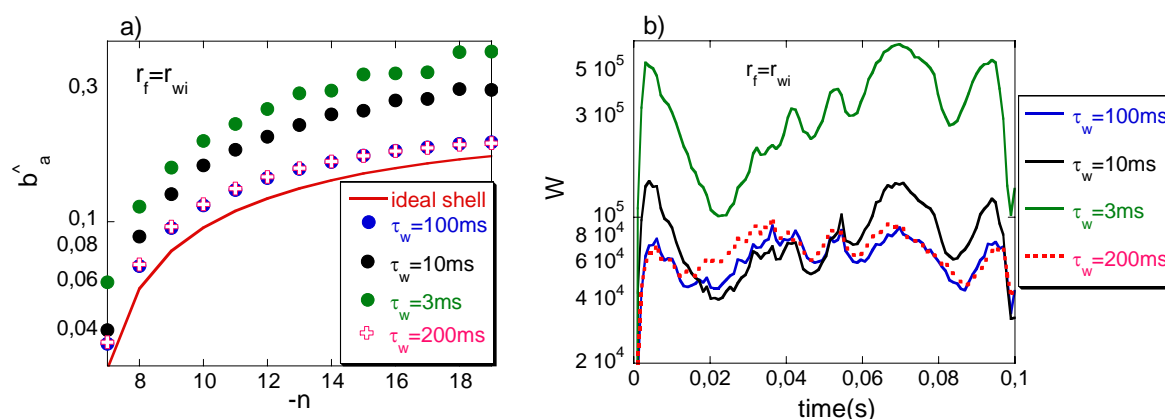


Fig.5.1.4: a) Edge radial field normalized to the resonant surface amplitude for the $m=1$ modes; the red line are the values obtained with an ideal shell in the place of the system resistive-shell+feedback. b) Maximum power required to the coils. Note the logarithmic scale in the y-axis.

5.1.6 0D and 1D models with a phenomenological term for the dynamo effect

A 1D time-dependent model for the magnetic field profile evolution in RFX-mod has been developed. The model is based on the solution of the magnetic field diffusion equation, supplemented with an additional term which takes into account the effect of the dynamo electric field. This term has been modeled by an alpha-dynamo approach, adopting two different proportionality constants between dynamo field and magnetic field for the poloidal and toroidal components [Guo97]. The model has been shown to be able to reproduce with sufficient accuracy the multiple helicity RFX-mod discharges, including the current-rise and current-decay phases.

A 0D time-dependent model of the behavior of the plasma current in RFX-mod and of the currents in the main windings (toroidal field winding and magnetizing winding) has been developed. The model is based on that developed by Sprott [Sprott88], with some refinements to take into account the peculiarities of RFX-mod, such as the return current in the F-coils and the fact that the toroidal field coils power supplies are current-controlled during most of the discharge. A computer code solving the resulting evolution equations has been written. The model is now being tested against experimental data

5.1.7 Response to applied perturbations

An analysis of experiments done by applying $m=0$ non axi-symmetric perturbations through the toroidal field coils in RFX has been done by using a linear model for reconstructing the coils magnetic field. In this way the plasma response to the applied perturbations has been evaluated. It has been established that, at least at shallow reversal, the plasma responds in a stable way to the perturbation. It has also been shown that the measured $m=0$, provided that the applied component is subtracted, can be essentially accounted by the nonlinear coupling of two adjacent $m=1$ modes. This is only partially true when a dominant helicity is present in the plasma [Pizzimenti08].

5.2 Transport

5.2.1 Impurity transport

Ni transport analysis inside the QSH hot structure has been attempted, by reconstructing the RFX-mod radiation pattern after a Ni LBO injection with the available collisional-radiative impurity diffusion model [Mattioli02]. Due to the strongly varying plasma conditions (including poloidal and toroidal asymmetries in the Te profile due to the helical geometry) the Ni transport parameters evaluations obtained are not fully reliable. Preliminary results indicate that the observed Ni emission time evolution depends more on the electron temperature evolution (i.e. on the energy content of the island) rather than on strong differences in the Ni transport properties inside the thermal island. Ni emission data have been reasonably reproduced using for both the MH and QSH phases the same transport parameters ($D \sim 10\text{-}20$ m²/s in the plasma centre) [Carraro08].

5.2.2 Fluid transport: RIPORT

The two one-dimensional codes RFXPORT and RITM have been coupled, in order to obtain a self-consistent simulation of the plasma discharge [Predebon et al, submitted to Plasma Phys. Control Fusion]. In its original form, RFXPORT solves the MHD equations assuming an Ohm's law with a Spitzer like resistivity and a dynamo term, together with the main gas transport equations; on the other hand, RITM solves the transport equations for the main particle species and each impurity ion state, working out the necessary atomic processes. The integration has been realized keeping the first code as equilibrium and main gas transport solver, while the second one is used to compute the neutral/impurity related quantities in the continuity and heat balance equations, e.g. the densities of neutrals and impurities, the radiation power losses and the effective charge profile. The code has been conceived so as to include various transport models. Those currently implemented are based on the quasi-linear representation of the magnetic field diffusivity, with the aim to describe the evolution of the chaotic multiple helicity states of the RFP configuration.

The code has been applied to some experimental scenarios, and in particular for the characterization of the RFX-mod plasma discharges close to the Greenwald density limit [Puiatti et al, submitted to Phys. Plasmas], which usually show highly radiative layers at the plasma edge and considerably hollow density profiles.

5.2.3 Microturbulence as a supplementary source of transport

The reduction of large-scale macroscopic MHD modes in the core allows for other sources of turbulence, till now secondary, to emerge. This was an incentive to implement at RFX three different codes enabling the simulation of electrostatic microturbulence.

The first one is the TRB code [Garbet03], a fluid code for the nonlinear study of electrostatic core microturbulence (ITG and TEM modes) that incorporates a closure mimicking Landau damping, a kinetic effect. This latter feature is important since Landau damping was shown to

make ITG modes more stable in the RFP than in the tokamak. The code was modified to fit RFP geometry and provided first results of ITG growth rate estimates [Eps08a].

The gyrokinetic flux-tube code GS2 [Kotschenreuter95] has been imported with a dual purpose. First, in the framework of the collaboration with JET, the aim is to investigate the reduced accumulation of high-charge ions in H-mode in the presence of radiofrequency heating, cf. [Puiatti06]; the role of microturbulence in such an experimental context is analyzed for trace impurities, in order to find the related transport coefficients to be compared with the experimental results. Second, the code is used to identify the microinstabilities playing a major role in the RFP configuration, in cases characterized by a scarcely chaotic magnetic field; first attempts have been carried out to investigate the conditions under which ITG-TEM driven instabilities take place, and to compare their overall effect on particle/heat transport with the tokamak counterpart.

Edge microturbulence has been tackled numerically by using a 2-dim code for the study of curvature-driven electrostatic turbulence. It was developed, following the pattern in [Naulin06]. The code produces long-time simulations of turbulent fields (vorticity, temperature, density), whose statistical properties are to be compared against experimental data, especially from GPI probe (this work is in progress). Edge turbulence has been investigated also with simple analytical phenomenological models, in order to provide rationale for statistical patterns occurring. Results appearing in [Sattin08].

A broader issue concerns the formalism itself that has to be used in order to mathematically quantify transport, regardless of the underlying drive: the diffusive versus anomalous transport paradigm. Further work was performed to make more precise the limits of validity of the fractional diffusion and of the advection-diffusion models. At the occasion of an invited talk about this topic at the 35th European Physical Society Conference on Plasma Physics, a pedagogical version of the work published last year has been published. It includes new elements further exhibiting the strength of the advection-diffusion model [Eps08b].

5.2.4 Linear gyrokinetic theory on ITG and TEM modes in RFP configuration

As an extension of the work in 2007 about the linear threshold of ITG mode in RFP configuration, the kinetic ITG theory (adiabatic electrons) has been applied to the RFP plasmas in RFX-mod. A typical RFX-mod discharge has been analyzed based on the profiles of density, temperature and $q(r)$ measured in experiment. The results on the threshold are obtained and shown in Figure 5.2.1, where the threshold values expressed by temperature gradient scale lengths $L_{Ti_c}(r)$ are plotted as a function of the normalized minor radius r/a . The observed electron temperature profile $T_e(r)$ and corresponding gradient scale lengths $L_{Te} (\approx L_{Ti})$ are also plotted. The high temperature region in the center area is the hot helical core produced by the non-linear development of the dominant mode ($m=1, n=7$) during the QSH phase. The figure shows that near the edge of the hot helical core, the temperature profile is steep enough to match the threshold value at which the ITG mode can be driven to be unstable. In addition,

such type of temperature slope can also be found near the plasma edge where the temperature cools down near the vacuum vessel [1].

The effect of the trapped electrons on the ITG mode and on the Trapped Electron Mode (TEM) were also investigated in the RFP configuration and preliminary results are available. The trapped electron response in RFP configuration is derived from the gyrokinetic equation, and the corresponding numerical code was created. To start with, the collisionless case is

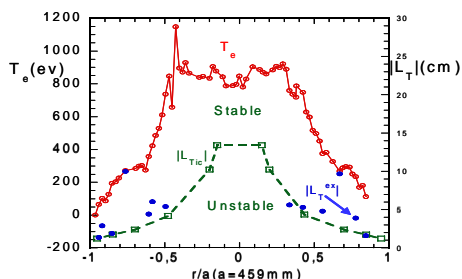


Fig.5.2.1: Ion Temperature Gradient mode stability threshold for ion temperature gradients assumed to be equal to electron temperature ones in SHAx regimes of RFX-mod.

numerically analyzed. The results show that, in comparison with the adiabatic electron case of the ITG mode, the effect of the trapped electrons is rather small, which gives only a small modification on the values of the ITG stability threshold (a little bit higher than the case without trapped electrons)

The TEM instability is studied by taking into account the trapped electron response and the ion kinetic effects. The preliminary results (collisionless) in RFP plasmas have been obtained. The TEM mode is driven by the

precession resonance of the trapped electrons ($\omega \sim \langle \omega_{de} \rangle$) and propagating in the electron diamagnetic drift direction. It is found that, in very peaked density gradient regions, TEM in a RFP plasma is unstable even without temperature gradient; however, for flat density profile, the TEM instability requires a steep electron temperature gradient.

5.2.5 Classical collisional transport theory

Classical collisional transport theory is developed under the assumption of uniform magnetic field and small gradients, so that proportionality between generalized forces and gradients can be established. However these assumptions are often not satisfied. Neoclassical transport theory takes into account the curvature of magnetic field, in the hypothesis of existence of magnetic surfaces, while turbulent transport theory investigates the influence of collective mechanisms on transport. In either theory it has been found that spatial non-uniformity greatly influences the transport coefficients. Moreover this is well confirmed experimentally. In order to better understand the relation between gradients and transport, the problem has been faced from the basic classical level. First results indicated that “classical” diffusion and electric conductivity strongly depend on pressure gradient and velocity shear. In fact these “classical” transport coefficients could be greatly enhanced or depressed or even could be reversed in sign, indicating better or worse confined plasma configurations. These results have been reached using stationary one-fluid and electric current equations, without the usual small gradient approximations. Diffusion and conductivity coefficients are introduced in these equations

writing flux and current density in term of density gradient and electric field respectively and then found as solutions of coupled algebraic equations.

5.2.6 FLiT for magnetic perturbation

The FLiT code has been extended to describe particle orbits. This was done by solving the guiding center equations in the toroidal flux coordinate used to solve the Newcomb's equation for the eigenfunctions of the first order magnetic perturbations. For the sake of numerical

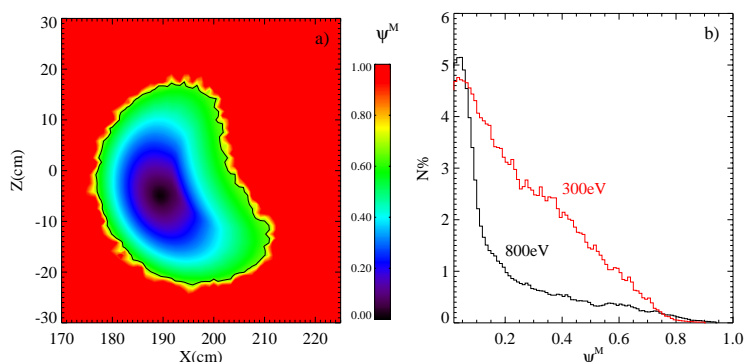


Fig.5.2.2: a) Helical magnetic flux ψ^M reconstruction on a poloidal cross section (normalized). b) Particle density distribution for two simulations at $T=300\text{eV}$ (red line) and $T=800\text{eV}$ (black line).

flexibility, the higher order formulation of the guiding center motion developed by R.G. Littlejohn has been used [Littlejohn81]. Littlejohn formulation allows the presence of stationary and time varying magnetic and electric fields and implicitly conserves particle energy.

The inclusion of collisions is now underway by solving the stochastic differential equations equivalent to the Fokker-Plank-like equation of the five-dimensional phase-space distribution function of particles guiding centers. For the pitch angle and energy scattering parts of the collisional term those developed by A. Boozer and G. Kuo-Petravich [Boozer81] have been used. Instead the classical diffusive part of the collisional operator has been evaluated by computing the second order correction to the gyro-averaged collisional operator in presence of spatial gradients on the distribution function.

5.2.7 Characterization of test particle transport in RFX-mod plasmas in QSH and SHAx regimes

RFX-mod plasmas at high current ($1-1.5\text{MA}$) are often in a Quasi Single Helicity (QSH) regime characterized by a dominant mode with helicity $(1,-7)$ and a low level of secondary modes. Thus, a significant fraction of the plasma volume is not anymore axial-symmetric but helically deformed. In such a condition particle and energy transport needs to be investigated in this new geometry. To this end the guiding center code ORBIT [White84] has been implemented with a new routine in order to evaluate the ion and electron diffusion coefficients in Single Helicity plasmas (SH, without secondary modes) [Gobbin_2007]. During the last year the code has been further modified to deal also with QSH (with secondary modes too) and Single Helical Axis (SHAx [Lorenzini08], i.e. QSH with a separatrix expulsion) plasmas. The same method described in [Gobbin07] has been applied to determine the helical flux ψ^M associated to the computed magnetic surfaces. For a given position of a particle, the corresponding ψ^M univocally

defines the helical surface it crosses. A map of ψ^M on a poloidal cross section is shown in Fig. 5.2.2(a).

In the following the main results obtained from the numerical investigation are reported.

5.2.8 Diffusion coefficients

A set of test particles with random pitch angle $\lambda = \cos(\theta)$, θ being the angle between the particle velocity \mathbf{v} and the field \mathbf{B} , are deposited inside the helical structure and diffuse out of it subject to collisions. Particles are considered lost when they cross the helical loss surface labeled by $\psi^M=1$; they are then injected back in the helical axis position, in such a way to keep constant the particle number during the whole simulation. Information on transport is obtained from the stationary spatial distribution, computed with respect to the helical poloidal flux ψ^M relative to the topology of the reference helical equilibrium. In Fig. 5.2.2(b) the ion and electron density distributions for $T= 300$ and $800eV$ are reported. While the former (red line) is almost linearly decreasing, the latter is not characterized by a linear trend. This non-diffusive behavior at high temperatures is mainly a consequence of the reduced plasma collisionality (which is proportional to $T_e^{-3/2}$). Similar simulations have been performed at different temperatures for ions and electrons. Estimation of the diffusion coefficients give: $D_{i,QSH} \sim 1 \div 4m^2/s$ for ions and $D_{e,QSH} \sim 0.8 \div 3m^2/s$ for electrons, in the temperature range $T \sim 300 \div 1200eV$, for the same level of secondary modes ($N_s \sim 1.05$). In a pure Single Helicity regime ($N_s=1$) we obtain $D_{i,SH} \sim 0.5D_{i,QSH}$ and $D_{e,SH} \sim 0.1D_{e,QSH}$. These values are much lower than those measured in Multiple Helicity plasmas where $D \sim 30m^2/s$.

5.2.9 Effects of secondary modes on diffusion coefficients.

Transport simulations have been performed for different levels of secondary modes ($N_s \sim 1 \div 1.5$). In SH condition: $D_{i,SH} \gg D_{e,SH}$ so that an ambipolar electric field should be considered to equate the fluxes between electrons and ions. The same holds for significant level of secondary modes ($N_s > 1.1$), where instead $D_{e,QSH} \gg D_{i,QSH}$, since the small electron mass increases the sensitivity to magnetic perturbations. But, for the typical values of secondary modes in RFX-mod best performances ($N_s \sim 1.02 \div 1.1$) we have $D_{i,QSH} \sim D_{e,QSH}$, even without any ambipolar electric field.

5.2.10 Trapped and passing particle diffusion

The reason of the non-diffusive behavior, shown in Fig. 5.2.2(b) for the particle distribution at high temperature, can be understood by analyzing the pitch of the lost ions. Most of them are in fact trapped with a pitch close to zero. This is explained by considering that at very low collisionality (high temperatures) passing ions are only affected by the residual chaos and by a small thermal drift due to their non-zero temperature. Thus their transport is very low since they follow the helical magnetic field lines inside the helical structure and perform many

toroidal turns until a collision deflects them from their initial orbit. On the other hand, even in a very low collisionality regime, trapped particles diffuse across the helical magnetic structure due to *banana* and *superbanana* orbits. Numerical simulations show that the ratio of the diffusion coefficients using only passing (D_{pas}) or trapped particles (D_{trap}) is about $D_{pas} / D_{trap} \sim 0.01$, thus confirming that the latter give the main contribution to transport inside the helical structure.

5.2.11 Application to a database of experimental plasmas

Several experimental QSH and SHAX plasmas have been investigated by transport simulations. In particular we have estimated the ion diffusion coefficients and their scaling with parameters proportional to the energy of the dominant and of the secondary modes. Analysis show that the computed D_i increase with the ratio secondaries/dominant modes and in SHAx states they are close to the values obtained in ideal SH simulations. A further decrease of the secondary modes could still allow reducing the electron diffusion coefficients D_e and thus the global transport in the helical structure.

5.3 Current drive and heating by electron cyclotron

In collaboration with R. Bilato (IPP Garching) and D. Farina (IFP-CNR Milano) a study of electron cyclotron heating and current drive in RFPs has been initiated. As a result of this assessment, a possible mechanism of wave absorption through a conversion mechanism of the wave to an electrostatic Bernstein wave has been found. Full wave simulations carried out by F. Volpe (Un. Madison Wisconsin) and A. Koehn (Un. Stuttgart) have predicted an encouraging 55% wave absorption in RFX-mod at 1 MA current [Bilato08].

5.4 Trapped particles

During 2008 a first step toward a comprehensive assessment of the role of trapped particles in Reversed Field Pinch has been undertaken. The work involved focusing on this topic partial studies obtained with different theoretical tools already available at the laboratory. In fact, the main effort has been devoted to provide a closer comparison of the results obtained with different approaches. Presently the main conclusion is that the fraction of trapped particles is of the order of 30-40 % in an RFP like RFX-mod, and that neoclassical transport appears to be the main source of particle transport (one order of magnitude larger than classical one) when achieving the low-chaos SHAx regimes.

REFERENCES

- [Bilato08] R. Bilato et. al. "Feasibility of Electron Bernstein Wave Coupling via O-X-B Mode Conversion in the RFX-mod reversed field pinch device", to be submitted to PPCF
- [Bolzonella08] T. Bolzonella, V. Igochine, S. C. Guo, D. Yadicin, M. Baruzzo, and H. Zohm; PRL 101,165003 (2008)

- [Bonfiglio08a] D. Bonfiglio, L. Chacon and S. Cappello, poster contribution for the 50th APS DPP meeting, Dallas (2008).
- [Bonfiglio08b] D. Bonfiglio, S. Cappello, R. Piovan, L. Zanotto and M. Zuin, *Nucl. Fusion* 48, 115010 (2008).
- [Bonfiglio08c] D. Bonfiglio, S. Cappello, M. Gobbin, G. Spizzo, poster contribution for the 50th APS DPP meeting, Dallas (2008).
- [Boozer81] A. Boozer and G. Kuo-Petravich, *Plasma Phys.* 24, 851 (1981)
- [Carraro08] L. Carraro et al. 'Particle transport in different magnetic field topological configurations in the RFX-mod experiment' 35th EPS Plasma Physics Conference 2008
- [Eps08a] M. Gobbin, et al, "Numerical studies of particle transport in RFX-mod low chaos regimes" (poster at the 35th EPS Plasma Physics Conference, 9-13 June 2008, Hersonissos, Crete)
- [Eps08b] D.F. Escande, F. Sattin, *Plasma Phys. Control. Fus.* 50, 124023 (2008)
- [Garbet03] X. Garbet, et al., *Phys. Rev. Lett.* 91, 035001 (2003)
- [Gobbin07] M. Gobbin et al., *Phys. Plasmas* 14, 072305 (2007)
- [Gobbin08] M. Gobbin, L. Guazzotto, S. C. Guo, I. Predebon, F. Sattin, G. Spizzo, P. Zanca and S. Cappello, to appear in *Journal of Plasma and Fusion Research Series* (contributed paper to International Congress on Plasma Physics 2008 – Fukuoka – Japan)
- [Guo08] S.C. Guo, *Phys. Plasmas*, to appear in *Physics of Plasmas* Dec. 2008
- [Guo97] S. Guo, C. Lo Surdo, R. Paccagnella, *Nucl. Fusion* 37, 1147 (1997).
- [Kotschenreuter95] M. Kotschenreuther et al. *Comput. Phys. Commun.* 88, 128 (1995)
- [Littlejohn81] R.G. Littlejohn, *Phys. Fluids* 24, 1730 (1981)
- [Lorenzini08] R. Lorenzini et al., *Phys. Rev. Lett* 97, 02005 (2008)
- [Mattioli02] M. Mattioli et al. 'Experimental and simulated VUV spectra from the JET tokamak and the reversed field pinch RFX' *Plasma Phys. Control. Fusion* 44 33 (2002)
- [Naulin06] O.E. Garcia, et al, *Phys. Scr.* T122, 104 (2006)
- [Paccagnella08] R. Paccagnella, H. Strauss, J. Breslau, "3D MHD VDE and disruptions simulations of tokamak plasmas including some ITER scenarios", submitted to *Nucl. Fusion*
- [Pizzimenti08] A. Pizzimenti, R. Paccagnella, "Mode coupling studies in the RFX-mod reversed field pinch", *Plasma Phys. Contr. Fusion*, 50 (2008) 065006.
- [Puiatti06] M.E. Puiatti et al. *Phys. Plasmas* 13 042501 (2006)
- [Sattin08] F. Sattin, et al, "On the statistics of edge fluctuations: comparative study between various diagnostics techniques and fusion devices" (submitted); F. Sattin, et al, "About the parabolic relation existing between the skewness and the kurtosis in time series of experimental data" (submitted); F. Sattin, et al, "Fluctuations and power spectra in edge plasmas" (in preparation); P. Scarin, et al, "Measurements of characteristic pressure profile lengths and comparison to turbulence scale lengths in RFX-mod edge" (poster at the 50th APS Conference, 17-21 November 2008, Dallas, Texas)

[Spagnolo07] S. Spagnolo, Tesi di laurea del corso di laurea specialistica in Fisica, Facoltà di Scienze MM. FF. NN., Università di Padova, a.a. 2007-2008.

[Spizzo06] G.Spizzo, S.Cappello, A.Cravotta, D.F.Escande, et al., Phys. Rev. Lett. 96, 025001 (2006).

[Sprott88] J. C. Sprott, Phys. Fluids. **31**, 2266 (1988).

[White84] R.B.White and M.S.Chance, Phys. Fluids 27, 2455 (1984)

[Zanca04] P.Zanca and D.Terranova, Plasma Phys. Control. Fusion 46, 1115 (2004).

[Zanca08] P. Zanca, 'Avoidance of tearing modes wall-locking in a reversed field pinch with active feedback coils' to be published in Plasma Physics Controlled Fusion (2008).

6 TOKAMAK PHYSICS

Despite the large and successful effort on the RFX experiment, Consorzio RFX has also significantly contributed to Tokamak physics studies, with experiments or data analysis mainly on JET and ASDEX Upgrade. Research subjects have regarded MHD studies and control and transport issues, in the core and in particular at the edge, as well as tests of disruption prediction models. Specific subjects on edge turbulence and transport that could not easily be investigated elsewhere have been carried out on ALCATOR C-mod and CASTOR. Contacts have also been established with JT60 SA for collaborative RWM studies in support of the power supply procurement.

6.1 ASDEX Upgrade

6.1.1 *Measurement of Toroidal Alfvén Eigenmodes by means of SXR tomography*

The internal structure of Toroidal Alfvén Eigenmodes (TAE) and of other fast particle-driven modes is being studied in ASDEX-Upgrade (AUG) in collaboration with IPP scientists. A fast soft x-ray tomographic diagnostic with 2MHz sampling rate and 0.5MHz bandwidth is being used to this aim. This allowed measuring the radial profile of multiple TAEs destabilized by fast ions accelerated through Ion Cyclotron Resonance Heating in AUG. A comparison with predictions of the linear MHD code CASTOR and the gyrokinetic code LIGKA found good agreement with the experiment in different plasma conditions [Piovesan08_1].

Similar studies also revealed the existence of a new fast particle-driven instability, the so-called Sierpes mode, which has been shown to be a particular type of Beta Induced Alfvén Eigenmode (BAE). Since its structure is very core-localized, this mode could not be detected before, based on external magnetic measurements only. This instability plays a significant role in the fast ion transport, as shown by measurements of the fast ion losses made by a new type of detector with high frequency resolution [García-Muñoz08_1]. The Sierpes and the TAEs act synergistically to enhance fast ion losses. In fact, as shown by the soft x-ray reconstructions, the eigenfunctions of the two modes overlap around mid-radius, which cause the ions displaced by the Sierpes to be eventually expelled by the TAEs [García-Muñoz08_2].

Important information on the mechanisms responsible for fast ion transport induced by high-frequency modes has been given by correlating the mode amplitude measured in the core through soft x-ray tomography with the fast ion losses detected at the edge. A clear nonlinear dependence between the two was found, which suggests that a diffusive type of mechanism is at play in these experiments [Piovesan08_2].

6.1.2 *Use of insertable magnetic probes for electrostatic and magnetic fluctuations.*

During 2008 a new insertable probe, designed and constructed in collaboration with EURATOM-ÖAW, EURATOM-IPP and EURATOM-RISØ Association has been installed on Asdex-U tokamak. This probe, whose scheme is shown in figure 6.1.1, contains six Langmuir probe pins of graphite by which the radial fluctuation-induced transport of particles and momentum can be measured from a simultaneous determination of the poloidal and radial

electric field components together with the density estimated from ion saturation current. A triple pick-up magnetic coil is inserted in the probe, and is located 2 cm behind the more protruding pin. With this coil all the three components of magnetic field fluctuations can be measured. The probe has been mounted on the fast reciprocating mid-plane manipulator in order to explore the Scrape Off Layer region, and used in several AUG shots, in ELMy H-Mode configuration, in order to get information on the current filaments, which are believed to be associated with ELM events.

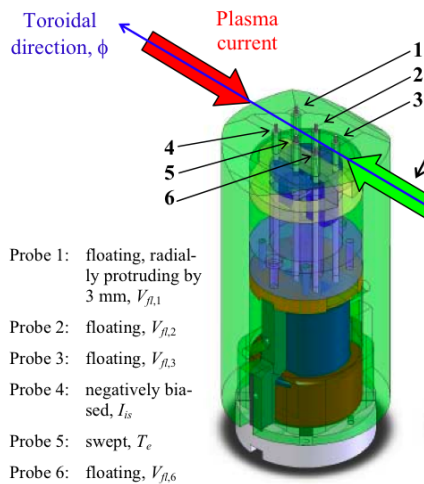


Fig.6.1.1: Schematic drawing of the probe head. The probe pins are numbered with probe 1 protruding by 3 mm from the other probes. In the toroidal and poloidal directions the distance between the probe pins is 10 mm, respectively.

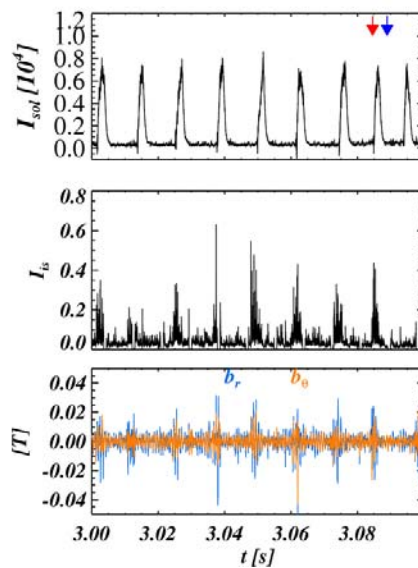


Fig.6.1.2: Temporal evolution of: (a) current in the SOL, (b) Ion saturation current, (c) magnetic signals b_r and b_θ from the radial and poloidal sensor coils, respectively.

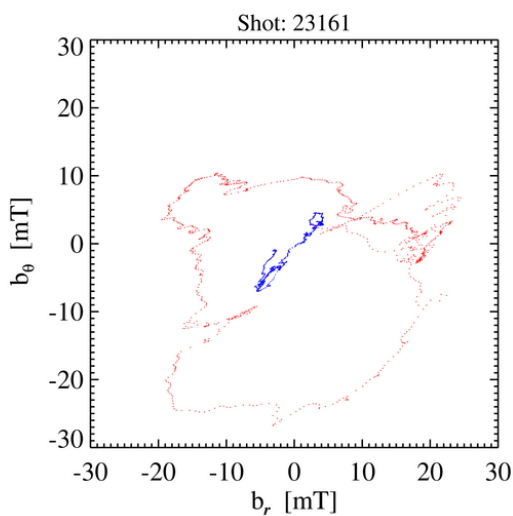


Fig.6.1.3: Hodograms of the poloidal and radial magnetic signals, b_θ and b_r for the time intervals shown by the arrows in the respective colors in Fig. 6.1.2: red arrow during an ELM interval, blue arrow in during an inter-ELM interval.

The appearance of an ELM in front of the probe can be easily recognized by a local fast enhancement of the ion saturation current measurement. This behavior gives a precise trigger of the ELM, occurrence particularly useful when we deal with very localized measurements, and is in any case well synchronized with the current collected on the divertor plate, which is a clear sign of ELM's occurrence (see fig 6.1.2).

Associated to the ELM appearance also strong magnetic activity can be observed, which is believed to be due to magnetic field line aligned current filaments. The hodogram of the perpendicular components of the magnetic field can highlight the

filamentary nature of these magnetic perturbations. The hodograms are reconstructed by plotting the trajectory of the magnetic field in the b_r - b_p plane. Two examples of these hodograms are shown in figure 6.1.3, referring to two different time intervals, corresponding to ELM (red point), and ELM-free (blue point) phases: the two intervals are indicated with the same color scheme also in figure 6.1.2. The presence of a closed loop during the ELM phase is a possible indication of a current filament mainly aligned in the toroidal direction, whereas in the inter-ELM phase magnetic fluctuations appear almost linearly polarized.

6.1.3 Prediction of disruptions

This activity has been carried out in collaboration with the University of Cagliari.

The disruption prediction tools developed for JET have been also applied to ASDEX Upgrade, aiming at integrating the predictor in the local real control system. A neural network based system could deteriorate its performance during the operational phase, as it may face new plasma configurations with features completely different from those included in the training database. To off-line test the predictor, a new set of pulses containing both disruptive and safe pulses has been selected from AUG experimental campaigns between October 2004 and June 2007 along with a criterion proposed in [Cannas08], each shot being visually inspected so as to discard VDEs disruptions and shots with corrupted parameters. In addition an algorithm to automatically correct wrong density measurements has been developed. A further visual analysis allowed classifying the disruptions induced by the killer-gas.

Test results show the worsening of the performance of the original predictor. Thus, a statistic analysis of predictor input parameters belonging to the new data set has been performed in order to verify the presence of new plasma features. The comparison of the statistical distributions of old and new databases does not highlight significant differences, which could justify the deterioration of the predicting performance of the original system when fed with the new pulses. Finally, a new neural network predictor has been built using the new data base both for training, validation and test. The performance of the new predictor is comparable with that of the old predictor. These results confirm the crucial importance to update any data based predictor in presence of plasma configurations not used during the training phase.

A combined prediction system composed by a Neural Network predictor and a Locked-mode trigger is presently under investigation on ASDEX Upgrade. A comparison between the prediction times accomplished by the NN predictor during the off-line test and those attained by the locked-mode trigger during the on-line tests has been performed shot by shot. This comparison will be useful to understand which of the two predictive systems is more suitable for the different types of disruptions and the different operational spaces.

6.2 JET

6.2.1 Effect of ICRH injection on impurity transport

One session was prepared and performed on 22 August at JET with the aim of studying specific

aspects of the known pump out effect that the application of central electron heating exerts on impurities. This mechanism is of particular relevance in a fusion reactor as well as in ITER, where impurity accumulation, especially of heavy metals or of elements injected ad hoc to create a radiation shield, such as N or Ne or Ar, is not bearable. However such mechanism is not yet fully understood. Turbulence simulation has not been able so far to reveal what type of instability can drive impurities out of the plasma core in the specific conditions in which experiments have been carried out at JET. To heat electrons, ICRH applied to H minority (around 4-5%) was chosen. The ICRH power was scanned from 0 to 3 MW, setting two values per shot. In each shot one laser pulse was used to inject either Ni or Mo and two short puffs of a mixture of Ne and Ar were used. In particular the aim was to determine the minimum amount of power that is able to flatten the impurity profile. Attempts to couple more ICRH power failed. Data analysis is ongoing. While the general trend is confirmed, differences in the Ni behavior in discharges with similar radio frequency power seem to provide means to discriminate the possible role of other parameters such as, for example, the safety factor. The analysis consists of the determination of the impurity transport parameters and, in a second step, of the simulation of the discharges by means of the transport code JETTO and the quasi linear turbulent transport code GS2, the latter in collaboration with IPP Garching.

6.2.2 Study of Resistive Wall Modes in proximity of beta limits

Scientists from Consorzio RFX participated in 2008 to JET experiments dedicated to the “Assessment of beta limits in the advanced tokamak scenario”, within the Task Force Scenario 2. During the nine experimental sessions dedicated to this proposal, in particular, expertise on MHD mode analyses was provided by the RFX scientists on site.

The aim of these experiments is to identify the maximum beta achievable before performance-limiting MHD instabilities, such as tearing modes and/or Resistive Wall Modes (RWM), develop. An important target is in particular to describe in detail the dependence of this beta limit on the shape and time evolution of the safety factor and/or of the pressure radial profiles, which are the two main quantities that were varied in experiments. This knowledge is important, in particular, to develop scenarios in which the above limits may be overcome and higher performances may be accessed.

Among the various issues that are being investigated within this proposal, the activity of the RFX scientists is focusing in particular on data analysis on the following topics [Challis08]: the precise nature of the β -limiting modes, which is not yet fully clear at the moment; the interplay between internal transport barriers and MHD modes; and the study of the Alfvénic activity, in particular Alfvén cascades, which can give precious information on the evolution of the safety factor profile in the first part of the discharge.

Moreover, based on experience gained in this activity, new experiments at higher toroidal magnetic field have been proposed by Task Force S2, to be completed between the end of 2008 and the first campaigns of 2009, which will be also supported by RFX scientists. This refers in

particular to the experimental proposal, “AT scenario: high power, confinement and stability studies at 2.3 T”.

6.2.3 Development of a new analysis tool for radial localization of tearing mode

In 2008 a new software tool which computes the coherence phase and amplitude between the signal coming from fast magnetic coils and the ECE signals has been implemented. In general, the square module of coherence between two fluctuation signals gives the information of how much the two signals are correlated, and its phase can become useful to extract other information. If one of the two signals is a punctual measure of the electron temperature in the plasma, and the other is a magnetic signal coming from coils placed outside the plasma, the radial profile of the phase of coherence between these two signals can flag the presence of a magnetic island. For this reason, by studying the radial position of phase inversions in coherence, the position of the magnetic island can be inferred. Since the magnetic island is intrinsically associated with a resonant tearing mode, it is possible to obtain important information about the plasma q profile. In the code the largest modes in Fourier space are tracked during the whole magnetic time window by a tracking algorithm, which is able to make

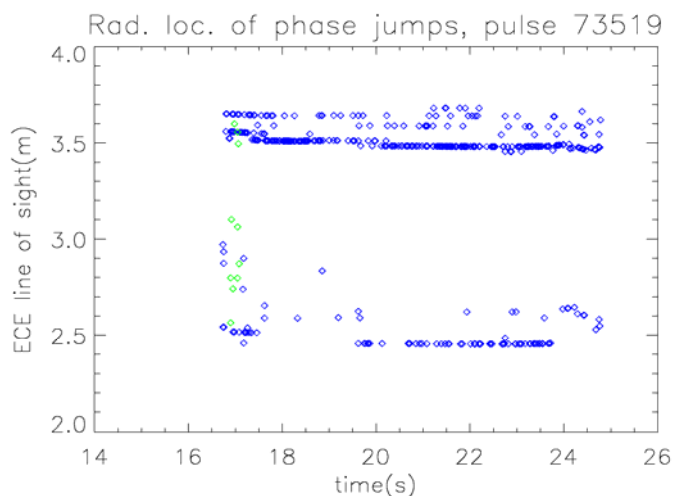


Figure 6.2.4: Example of temporal evolution of $n=2$ (blue) and $n=3$ (green) mode radial location on the $kk3$ line of sight.

a preliminary selection on the possible modes used for correlation calculation. After the mode tracking step, the coherence phase and amplitude between the two signals are calculated, the calculation is performed for each mode in a narrow frequency band around the mode ($\sim 1\text{kHz}$), which is moving in time following the mode frequency behaviour. The output of this process is the radial profile of coherence phase and amplitude for

the whole acquisition window of $kk3f$ (in the range in which modes are present). Then the radii in which a phase difference around π (phase inversion) is present are stored for each profile, giving the temporal evolution of the radial position of tearing modes.

The code has been tested on several high power JET pulses, and the results are encouraging for the accurate description of tearing mode’s radial location and for the large amplitude of the reconstruction window. An example is shown in Fig 6.2.4. The whole process is also totally automatic; this feature makes it suitable to be run inter-pulse, in the first or second JET analysis chain. Other efforts are ongoing to build a graphical interface, and to connect the code to the PPF system, with the aim of making it available among the JAC analysis codes.

6.2.4 Prediction of disruption

This activity has been carried out in collaboration with the University of Cagliari.

The performance of a disruption predictor based on Multilayer Perceptron (MLP) neural network has been improved by using the Support Vector Machines (SVM). The developed predictor [Cannas07] is able to perform both prediction and Novelty Detection (i.e., to recognize pulses belonging to plasma configurations never presented to the neural network during the learning phase). It is crucial to develop a system able to measure the reliability of the predictor output and to automatically update it in the case of plasma configurations not used during the training phase. Recently, a new Kernel Machine, called Geometrical Kernel Machine (GKM), has been proposed to predict disruptive events at JET [Delogu08]. Such algorithm automatically determines both the number of neurons and the synaptic weights of a MLP neural network with a single hidden layer. The resulting network is able to classify any finite set of patterns defined in a real domain. The prediction problem has been here modeled as a two classes classification problem. The geometrical interpretation of the network equations allows us both to develop the disruption predictor and to manage the so called ageing of the Kernel Machine. In fact, using the same Kernel Machine, a novelty detection system has been integrated in the predictor, increasing the overall system performance. The GKM used as novelty detector is able to justify many of the missed alarms and false alarms of the predictor as they are recognized to belong to unexplored regions of the operational space. The developed predictors (SVM and GKM) are suitable to be used in real time at JET.

6.2.5 ELM dynamics studies

Also this activity has been carried out in collaboration with the University of Cagliari.

Determining whether ELM dynamic is chaotic or random is crucial to correctly describe the ELM cycle. An additional motivation of interest in this topic is that chaos can be controlled even without any knowledge on the system model. The dynamic characteristics of 8 ELM time-series data from JET have been investigated [Camplani08]. Characteristic parameters, such as the Hurst exponent and the Maximal Lyapunov Exponent, have been evaluated. Hurst exponents are greater than 0.85 for all the time series suggesting a deterministic process, and the Maximal Lyapunov Exponent is positive for some of them. Due to the exiguity of the database, to the shortness of the time series and to the presence of noise, the obtained results do not allow concluding whether ELM time series are definitely chaotic or not, but they are found to be consistent with the hypothesis of chaotic dynamics. Further analysis will be carried out with additional methods to explore the presence of deterministic chaos.

6.3 ALCATOR C-mod

6.3.1 Analysis of turbulence imaging data

In 2008 the collaboration with the Alcator C-mod tokamak has continued, in the wider frame of the comparison of edge turbulence between RFX-mod and tokamak experiments [Sattin08].

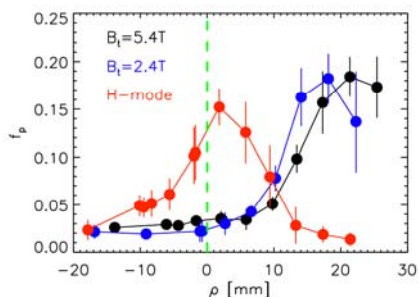


Fig.6.3.1: Packing fraction of the edge structures for L-mode discharges (two different toroidal magnetic fields) and H-mode discharges (red points). $\rho=0$ is the radial position of the separatrix.

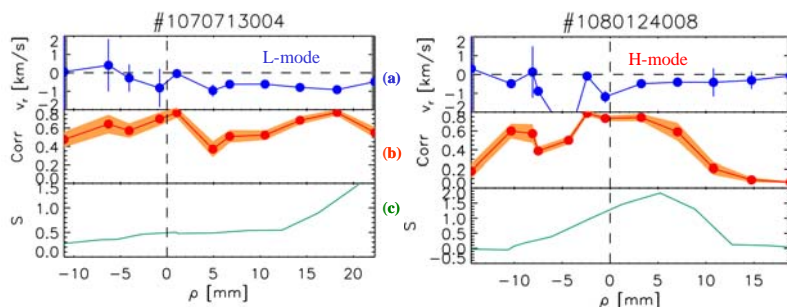


Fig.6.3.2: (a) radial velocity of edge fluctuations; (b) correlation between radial GPI chords; (c) skewness of GPI fluctuations. Figure at left refers to L-mode discharge, at right to H-mode one. All the quantities are plotted as a function of ρ , the distance from the separatrix.

Like in RFX-mod, also in Alcator C-mod there is a Gas Puff Imaging diagnostic to measure plasma edge fluctuations and in particular edge turbulence. In particular, the difference in the edge turbulence between L-mode and H-mode plasmas has been studied, and the research in this field is ongoing yet. In this way the impact of the edge turbulence in the onset and sustainment of H-mode regimes is studied. In fact, also in the NSTX tokamak a difference in the edge turbulence between the two regimes was previously found [Agostini07]. In figure 6.3.1 the packing fraction f_p

(area occupied by coherent structures) is shown as a function of the distance from the separatrix for L- and H-mode discharges. In the L-mode, regardless of the value of the toroidal magnetic field, f_p increases beyond the separatrix, indicating that the edge structures,

probably born near the separatrix, evolve outward increasing their dimension. Instead in the H-mode, f_p reaches its maximum value at the separatrix, showing a clearly different behavior. Another difference between the two regimes is shown in figure 6.3.2. In L-mode the radial velocity (a) of the edge fluctuations (outward) is about twice with respect to the H-mode near and outside the separatrix. Also the skewness (third order momentum of the PDF) has a different behavior in the two regimes (c). For both regimes and in all the radial positions explored, skewness assumes positive values, indicating the presence of mainly positive (with respect to the average) bursts in the GPI time series.

6.4 CASTOR

6.4.1 Measurement of plasma potential and diffusion coefficient at the edge

The “ball-pen probe” is a novel electric probe for the direct measurement of the plasma potential which has been developed at IPP-Prague, with contributions from Consorzio RFX, and tested on the CASTOR tokamak. In particular, Consorzio RFX has given a substantial contribution in developing a model to interpret floating potential power spectra measured with this probe and use them to derive an estimate of the plasma diffusion coefficient [Brotankova06, Brotankova08]. A version of this probe especially developed for RFX-mod, in

order to explore its ability to work properly in a low magnetic field regime, has been jointly built and successfully tested at the end of 2006. A new experimental campaign has been carried out at the end of 2007. The aim of this new campaign was to overcome some limitations that had been found in the first set-up, mainly using a larger sweep voltage so as to clearly detect both the ion and electron saturation currents, and adding to the sweeping voltage a bias derived in real time from a floating electrode. The data analysis has been carried out in the course of 2008, studying both the resulting plasma potential profiles and the fluctuation data with the aim of deriving the diffusion coefficient. It has been shown that, while in some shots a reliable outcome is obtained, in some other cases no reasonable result can be derived. A comparison of the analysis outcome with radial magnetic field measurements in the probe proximity has been carried out. While a definitive conclusion is hard to be drawn, due to the lack of a magnetic field measurement on the probe itself, it seems reasonable to think that the influx of electrons into the wells where the electrodes are housed is influenced by the local edge structure, in particular by the presence of the $m=0$ islands which characterize the RFP edge. This is also in agreement with recent findings obtained in RFX-mod, which suggest that also the local temperature and density gradients are strongly affected by the $m=0$ islands. These results do not invalidate the possibility of using the ball-pen probe at low magnetic fields, but simply call for a precise knowledge of the local magnetic topology.

6.5 JT60 SA

6.5.1 *Analysis of RWM in support of the procurement of the power supply*

In support to the procurement of the in-vessel coils power supply for JT-60SA, analyses of existing data and plans for new experiments on RFX-mod have been agreed with the JT-60SA group. In particular on the active RWM control subject, new investigations were planned addressing the mode rigidity issue. A joint experimental proposal has been written and first vacuum tests of new active coil control software have been executed in 2008. When implemented on plasma discharges, the new software will take advantage of the flexibility of the RFX-mod control system and will allow the control of selected RWM instabilities with different (reduced) coil configurations while keeping optimal control of any other source of error fields in the discharge. In this way an experimental investigation about the minimum coil configuration for RWM control can be carried out in a fully controlled and well diagnosed environment.

6.6 FAST

FAST has been officially presented in 2008 to the Fusion Facilities Review Panel set up by the EU Commission. Consorzio RFX has contributed to the effort that has led to such presentation. The capability of providing an ITER relevant environment in an integrated way, that is by achieving simultaneously the normalized values for all the relevant parameters, has been highlighted, as this is considered a key characteristic of a satellite machine that should

accompany ITER during its life. FAST, in the present form, would be an ideal machine to study the physics of fast ions in reactor relevant plasmas as well as to envisage techniques to control the plasma-divertor interaction, especially those associated to ELM's. Fast ions would be generated by external heating systems, primarily via ICRH radiation but possibly also through a Neutral Beam Injection based on a negative ion source. The study of the optimization of ICRH power coupling represents a further important commitment for FAST as 30 MW have to be coupled in a relatively small device in order to achieve the reference H-mode scenario. Contribution has been given also to the presentation of FAST to other European Associations. At RFX, detailed simulation work has been limited in 2008 to adapting previous evaluations, such as for the stability of Resistive Wall Modes, to the evolving ideas for plasma equilibrium. Adaptation work of certain diagnostics to a pulse duration extended to 170 seconds has been postponed to late 2008 - early 2009.

REFERENCES

- [Agostini07] M. Agostini, S.J. Zweben et al. *Phys. Plasmas*, **14**, 102305 (2007)
- [Brotankova06] J. Brotankova, E. Martines et al., Proceedings of the 33rd EPS Conference on Plasma Physics, Roma, 19 - 23 June 2006 (European Physical Society, 2006), Vol. 30I, P-2.195.
- [Brotankova08] J. Brotankova, E. Martines et al., *Contributions to Plasma Physics* **48**, 418 (2008)
- [Camplani08] M. Camplani, B. Cannas, A. Fanni, P. Sonato, M.K. Zedda, E. Solano, JET-EFDA contributors, "Dynamic behaviour of type I and type III Edge localized modes in the JET tokamak", 35th Eps Conference on Plasma Physics, 9-13 June 2008, Crete, Greece.
- [Cannas07] B. Cannas, R. S. Delogu, A. Fanni, P. Sonato, M. K. Zedda and JET-EFDA contributors, "Support Vector Machines for disruption prediction and novelty detection at JET," *Fusion Engineering and Design*, **82**, Issues 5-14, October 2007, pp. 1124-1130.
- [Cannas08] B. Cannas, A. Fanni, G. Pautasso, G. Sias, P. Sonato and ASDEX-Upgrade Team, "Criteria and algorithms for constructing reliable data bases for statistical analysis of disruptions at ASDEX-Upgrade", 25th Symposium on Fusion Technology (SOFT), 15-19 September 2008, Rostock, Germany, accepted for publication on *Fusion Engineering and Design*.
- [Challis08] C. Challis, et al., "High beta-N development at JET for steady state regimes", oral contribution, W69 IEA Workshop on Development of high beta-N scenarios for ITER, San Diego, USA (2008)
- [Delogu08] R. Delogu, A. Fanni, and A. Montisci, "Geometrical Synthesis of MLP Neural Networks," *Neurocomputing*, **71**, Issues 4-6, January 2008, Pages 919-930.
- [García-Muñoz08_1] M. García-Muñoz, et al., *Phys. Rev. Lett.* **100**, 055005 (2008)
- [García-Muñoz08_2] M. García-Muñoz, et al., 22nd IAEA FEC, Geneva, Switzerland, paper IAEA-CN-165/EX/6-1 (2008)
- [Piovesan08_1] P. Piovesan, V. Igochine, et al., *Nucl. Fusion* **48**, 065001 (2008)

[Piovesan08_2] P. Piovesan, et al., P30, 10th IAEA Technical Meeting on Energetic Particles in Magnetic Confinement Systems, Kloster Seeon, Munich, paper P30 (2007)

[Sattin08] F.Sattin, M.Agostini et al., submitted to Plasma Phys. Control. Fusion

7 INTEGRATED TOKAMAK MODELING

The Integrated Tokamak Modelling is a taskforce of EFDA which has the aim of integrating different software modules for plasma simulations within an user friendly system but with a high flexibility in order for the system to be able to adapt itself to future changes in operating system architectures and data communication technologies. This integration requires both software engineering and physical model developments. The activity of Consorzio RFX in 2008 within ITM is reported in the following paragraphs.

7.1 *Infrastructure Support Project*

In 2008, the activity has been mainly devoted to the development of the Universal Access Layer (UAL) (taskITM-08-CPD-T4). This software layer represents the unique interface to data in the ITM simulations and has been currently ported to the following language platforms: Fortran90, C++ and Java.

Besides the development of the language-specific libraries, the work in 2008 has been dedicated to the integration of the UAL with KEPLER, the simulation framework which is going to be used for ITM activities and to the development of memory mapped data access to improve simulation performance. Work in 2008 was dedicated to the implementation of a single computer solution. It is foreseen to extend this to a distributed architecture and to the integration of HDF5 data management system into the UAL. Even if MDSplus represents the main data system of the UAL, this new feature will allow exporting data files to sites where HDF5 is being used as the data interface; to the development of the required infrastructure for managing data files, such as procedures for building directory trees and for re-directing data flow in a standard way when running simulation on the ITM Gateway.

7.2 *Equilibrium and stability*

The code FLOW, which solves the MHD equilibrium in presence of flow, has been benchmarked against the CHEASE code for tokamak and RFP equilibria. New important diagnostics such as the bootstrap current, the trapped particle fraction etc. have been added to the code.

A considerable effort have been done in 2008 to understand the constraint for the integration of this code under the ITM platform, accessible through the ENEA-Portici server. A version of the code that can be compiled and run on this server is now available.

7.3 *Nonlinear MHD and RWM*

The CarMa code which solves the stability problem in presence of 3D passive structures for the RWMs have been used to predict the RWM growth rates in the RFX-mod device. Significant effects of the non axi-symmetric wall has been found [Villone 2008] on certain modes and a good agreement with the predictions of other codes has been established for the axi-symmetric wall case. This comparison work represents an important validation of the code.

Preliminary discussion of the structure/organization of the data for running CarMa within the ITM infrastructure has initiated.

7.4 Impurity Transport

During 2008 the implementation and benchmarking of the ‘superstages’ description of heavy impurities in the integrated transport codes at JET has been done.

A library of new routines accessing and interpolating the ADAS data (for unbundled or bundled impurities) has been successfully tested for both SANCO and EDGE2D.

Now JETTO/SANCO and EDGE2D codes can run simulations with all kinds of impurities. In the case of EDGE2D, heavy impurities, such as Tungsten, can be simulated only if they are bundled into a reasonably small number of superstages.

REFERENCES

[Villone 2008] F. Villone, Y.Q. Liu, R. Paccagnella, et.al., “Effects of three-dimensional electromagnetic structures on resistive-wall-mode stability of reversed field pinches”, Phys. Rev. Lett., 100 (2008) 255005.

8 ENGINEERING

This chapter summarizes first the engineering activities carried out on the RFX machine during 2008. Most activities have been driven by the intention of extending machine operation up to a plasma current of 1.5MA and beyond. The most resource demanding activity has been the upgrade of the energy transfer system of the poloidal circuit, which was necessary to open the possibility of interrupting magnetizing current as high as 50kA. Other activities have been necessary to monitor the machine stresses due to high current operation and to improve machine protection against unexpected plasma termination, which, if not properly controlled, at high plasma current can be dangerous for the integrity of the machine. Efforts were also spent to upgrade the computational capability of the offline RFX calculation clusters, to cope with the ever increasing demand of running numerical codes. Minor activities were developed to install a back-up electric machine measurement system and to enhance the video monitoring system of the experimental halls.

As far as the engineering collaborations with other laboratories are concerned, JET-EP2 support has been given also during 2008, while the activity for the AUG in-vessel coils enhancement continued with limited effort. The engineering activities for the Broader Approach are reported in sec. 9.

8.1 Activities for high current experiments in RFX mod

8.1.1 Upgrade of the energy transfer system

The energy transfer system has been upgraded, in order to withstand more demanding conditions deriving from the increase in the magnetizing current I_M up to 50kA.

The system, composed of four identical sections, is based on dc-current breaking units and includes, as main components, the vacuum breakers PTSO (two tubes in series per section, see Fig. 8.1.1 for a description of the system before the upgrade); the breakers perform the task of interrupting the current with the help of a counterpulse capacitor bank (PTCB), which zeroes the current and extinguishes the arc.

In the past, experiments were carried out at RFX to develop a vacuum circuit breaker unit for the protection of the ITER superconducting coils [Bonicelli05].

During the tests, the vacuum tubes (contact diameter 12cm, named D12), showed an unexpected limit in the specific energy I^2t dissipated in the closed contacts, before opening: when the threshold of 2.3GA²s is exceeded, the probability of having current re-strikes or interruption failures increases

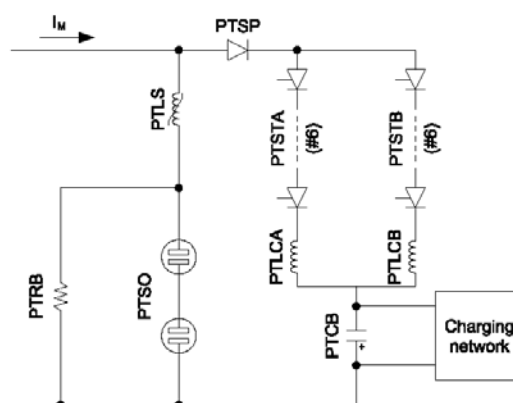


Fig. 8.1.1: the former RFX energy transfer system (one section).

dramatically and in some cases even welding of the contacts can occur.

The tubes used in RFX were similar to those tested for ITER, but with a smaller surface (contact diameter 10cm, named D10); supposing that the aforementioned limit scales with the contact area, it yields that the I^2t is lower than $1.6\text{GA}^2\text{s}$ for tubes D10. For a typical RFX pulse with $I_M=40\text{kA}$, the I^2t before opening results approximately $1.5\text{GA}^2\text{s}$: this means that the D10 tubes were likely to be very close to their maximum performance and therefore would be inadequate for a magnetizing current of 50kA .

Even the D12 tubes alone would not be able to withstand the new conditions, since the new I^2t (for $I_M=50\text{kA}$) was expected to be in the range $3.5\div 4\text{GA}^2\text{s}$.

Therefore, an upgrade of the system became necessary and the only way to reduce the I^2t on the breakers was to install, in parallel to the main branch, an auxiliary branch, so that they can share the current (and hence the energy) during the loading phase of the magnetising winding. Several solutions were considered for the auxiliary branch: at the end, it was decided to install a branch identical to the main one (see Fig. 8.1.2 with the new PTSB). Furthermore, it has to be taken into account that D10 tubes are no longer in production and thus only D12 tubes could be considered for the auxiliary branch (PTSB); as a consequence, the choice was made of employing D12 tubes also for the main branch, in order to have the same components in all parts of the system.

It should be added that the two breakers are not operated simultaneously: the first branch to be opened is the auxiliary one (PTSB), while the main one is still closed; after contact aperture, the current starts commutating from PTSB to PTSO. When the whole current has been transferred, the opening command can be sent to the PTSO (with a delay of few tens of milliseconds with respect to the PTSB).

Two new protections have been conceived for the upgraded ETS.

The first new protection was designed in order to protect the breakers from excessive I^2t : should one of the two breakers not be closed before the pulse, the other would carry the total current and this event has to be avoided in case of high-current operations.

The second protection is related to the opening command for the PTSO: this trigger is released only if the current commutation from PTSB to PTSO has been properly performed, otherwise a request for protection is sent to the main crow-bar of the poloidal circuit.

The upgrade of the system was split in two phases:

- replace the “old” D10 tubes with D12 ones (PTSO branch);

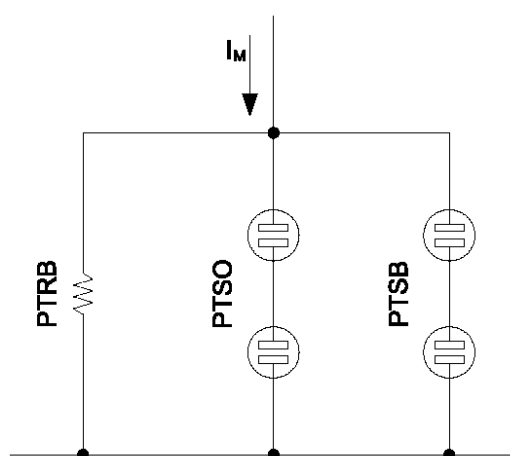


Fig. 8.1.2: scheme of the new interruption unit.

- install the auxiliary branches (PTSB).

The first step was carried out in autumn 2007; as for the second stage, a pilot test was carried out on one of the four units, before extending the modifications to the whole ETS, in order to verify the reliability of the scheme and overcome any possible inconvenience.

To carry out the pilot test, Unit number 4 of the ETS has been modified and one new breaker installed; the final installation is shown in Fig. 8.1.3: the auxiliary branch PTSB and the

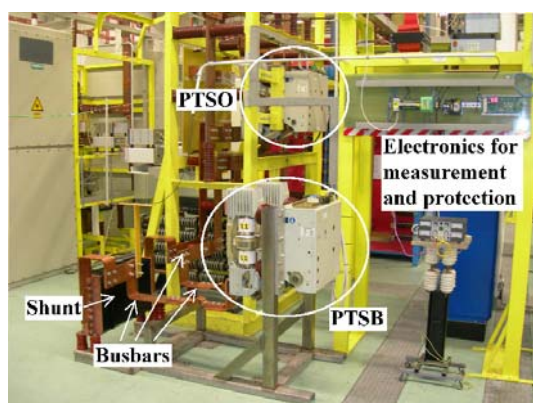


Fig.8.1.3: unit 4 of the ETS after the modifications: the auxiliary branch PTSB, the connecting busbars and the shunt in the foreground; the electronics for protection and measurement on the right-hand side; the main branch PTSO in the background

connecting busbars are in the foreground, whereas the main branch PTSO is visible in the background. A shunt ($R=30m\Omega$, on the left) was mounted for the measurement of the current in the PTSB branch (I_{PTSB}); some electronics was also installed, for protection and measurement (it can be seen on the right-hand side).

The first step of the commissioning was to assure equal current sharing among the two branches, as a preliminary test, carried out with a low-voltage power supply, showed that most of the current was still passing through the PTSO.

The resistances of the two paths were therefore equalised, by inserting in the PTSO branch an aluminium busbar; the following tests showed an even repartition of the current.

Fig. 8.1.4 gives, as an example, a plot of I_{PTSO} (top) and I_{PTSB} (bottom) in unit no. 4 for a pulse with $I_M=40kA$; it can be clearly seen that, at the beginning, the value of the current is very

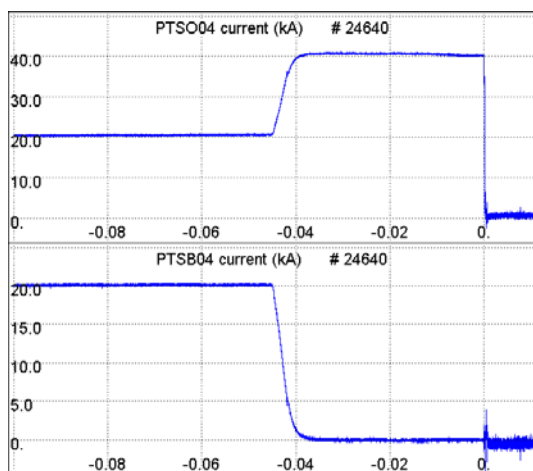


Fig.8.1.4: plots of current I_{PTSO} (top) and I_{PTSB} (bottom) of unit no. 4 for a typical RFX shot ($I_M=40kA$).

close to 20kA in both branches.

Unit no. 4, after the commissioning that took place between December 2007 and January 2008, performed almost 1,500 interruptions during the following months, without any major fault.

Therefore, in late summer 2008, the modifications were extended to the other three units. The final commissioning up to 50kA took place in October 2008 and the interruptions were performed regularly.

8.1.2 Installation of sensors for mechanical deformation measurements

Aimed at monitoring the behavior of the RFX-mod mechanical structure and coils under the

design maximum load (corresponding to 50 kA in the magnetizing winding), two systems have been implemented.

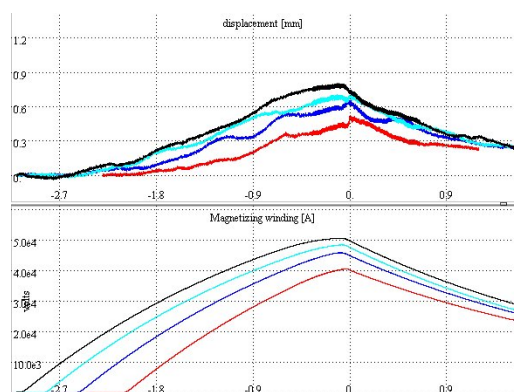


Fig. 8.1.5: displacements (top) of one coil terminal at different magnetizing current (bottom)

The first one is a system of sensors suitable to measure the displacement of the coil terminals and busbars in the central solenoid of the magnetizing winding, which is indeed the most severely stressed part of the coil system. Since the requirements (35 kV, 4 T compatibility) excluded the use of direct contact probes (such as linear transducers and strain gauges), sensors based on co-focal chromatic technology have

been chosen. A polychromatic white light is focused onto the target surface by a multi-lens optical system, which disperses the beam in such a way that each specific wavelength is focused at its own specific distance. Only the light which is focused on the target is used for the measurement. The distance, and so the displacement, between the lens and the target can be determined by measuring the wavelength of the light reflected by a target. The installed measuring system has been used for two purposes: as displacement measuring device (for a reliable determination of the stress level in the most critical components) and as protection device suitable to reveal abnormal displacements during normal operation which could be caused by a progressive delamination of the fibreglass insulation of coils and bus-bars. This last point is particularly important since, in vacuum-impregnated fibreglass insulation systems, electrical failures are often the consequence of the progressive degradation of a minor mechanical failure. Fig. 8.1.5 shows the measured displacements for I_M ranging from 40 to 50 kA.

The second system is devoted to evaluate the stresses induced in the struts of the mechanical structure (due to the electrodynamic forces induced by the magnetizing windings) measuring their deformations. To this purpose, during the RFX-mod assembly phase, a set of strain gauges have been installed both in the inner and outer side of the struts. Recently, the measuring system has been completed by cabling the connections inside the acquisition cubicle and developing a dedicated acquisition system based on Labview® architecture. This measuring system has been successfully used during the last high current commissioning and plasma campaigns to monitor the maximum compressive and flexural stresses in the support structure and the load distribution along the toroidal direction. The uniformity and the correspondence of the measured loads with the nominal calculated ones were good. Total load and stresses of each strut are visible at the central console in the control room after each pulse.

8.1.3 Implementation of controlled terminations

To improve machine protection during the RFX-mod high current campaigns, a careful analysis has been carried out on the fast protection actions in the case of pulse termination.

The interaction between the fast protection system of RFX-mod (SGPR), the real-time control and the fast timing systems has been analyzed to identify possible weak points and enhance the integration of the systems.

Existing run-time checks have been extended and new ones have been implemented during the pulse preparation sequence to detect possible situations that may lead to a pulse abort during the pulse execution phase (e.g. errors in the initialization of a real-time controller).

In the case of SGPR intervention, in order to avoid the abrupt interruption of the references to actuators not directly involved in the protection action, a new timing signal filtering card has been implemented and the real-time control system has been programmed to generate appropriate ramp down references. The card, based on FPGA technology, provides appropriate filters and delays for the timing signals, based on the protection signals received from SGPR.

Upon protection request from SGPR, the real-time control system of the MHD modes has been programmed to switch from the actual control algorithm to the virtual shell algorithm with pre-defined parameters that is the best algorithm to protect the first wall during plasma termination. The system has been also modified to generate a request for pulse termination if any value of radial field is detected larger than a pre-defined threshold.

8.2 Upgrade of offline computational resources

Already since 2007 there has been a growing demand of computational resources to run heavy numerical codes, a number of which suitable for parallel processing. Some of them have been introduced this year: Pixie3D and M3D for MHD modeling, GS2 for gyro kinetic calculations and the commercial applications COMSOL, which, together with the already installed ANSYS, are intensively used for design and simulation of the ITER neutral beam injector. This demand has driven the upgrade of the offline computer system, so far based on a small cluster of obsolete Linux servers. The architecture of the new system has been optimized for an efficient use of a set of new more powerful multi-core computers, with capabilities of parallel processing,

and designed to be expandable and flexible, tailored to fulfill the different requirements of old and new codes.

The upgrade has been carried out in two phases.

a) The first phase, completed in early 2008, comprises the following new hardware (fig. 8.2.1): a file server (8 CPU, 64 bit), a Storage Area Network based on Fiber Channel technology, a disk controller EMC CX3-20 and two servers (Intel, 16 CPU each, 64 bit) dedicated to parallel computing; this new system has been equipped with Message Passing Interface (MPI) architecture, based on Infiniband technology at 20 Gbit/s, and with Open MP; in addition all compilers and libraries have been installed, needed by parallel codes; finally all data in the old storage system (except RFX data) have been moved to the new one;

b) The second phase has been planned after evaluating the experience with the first two servers and updating the requests of computer resources by the users. The new upgrade includes three servers (24 CPU each), which will be delivered and installed by end 2008: the new cluster will then consist of 104 CPU at 2.4 GHz, also usable for parallel processing. New disks have been



Fig. 8.2.1: new offline Linux cluster (after first phase of upgrade)

ordered as well, to host also the RFX data in the new storage.

8.3 Upgrade of the video monitoring system of the experimental halls

The high current experimental campaigns planned for 2007 and 2008 to reach the 50kA nominal value in the magnetizing winding required to upgrade the video surveillance system in order to guarantee the safety of the equipment installed in the experimental halls. As a consequence the new system has been developed to improve, with respect to the previous one, the picture quality, the number of view points and to solve some electromagnetic compatibility interference causing video signal loss during the energy transfer.

Two types of color video camera have been selected: 9 standard cameras, based on the 1/4-CCD sensor and a horizontal resolution of 470 TV lines, to be used for the panoramic view across the halls and machine and two more sophisticated models, based on three 1/4.7 CCD sensors with a total of 1.070.000 pixels and a horizontal resolution of 600 TV lines, to be installed on the hall ceiling for a top view of the machine, in particular of the busbars and the coil terminals placed inside the central solenoid of the magnetizing winding where a flashover can occur. All the cameras are equipped with a pan/tilt/zoom mechanism remotely controllable from the control room, where all the camera signals are delivered in Super Video format both to be recorded and to be connected to the monitor; these were selected with a display resolution like the native one of the camera in order to obtain the best possible picture quality.

8.4 Installation of back-up machine electric current measurements

The winding electric current measurements represent one of the most important systems for RFX operation. In fact the current signals are used both for the feedback control of some plasma parameters and as protection system against the mechanical stresses of the field shaping winding due to electrodynamic loads.

As a consequence, a fault of one measurement could cause a long shutdown. At present the current measurements are performed by LEM type sensors built in 1990 and never upgraded up to now. The very long life of this diagnostic induced to install a new back-up system based on rogowski type sensors. The output signals, proportional to the derivative of the current, are integrated by means of the same conditioning electronic already adopted for the external magnetic measurements installed in RFX, which have shown a high degree of reliability and accuracy. The two systems of sensors are completely interchangeable.

The commissioning activity was focused to test the new system; the comparison between the signals of rogowski and LEM sensors showed a difference lower than 1% compatible with the measurement chain error.

8.5 JET EP2 - Plasma Control Upgrade

The Plasma Control Upgrade (PCU) is one of the most important enhancements included in JET EP2: it was launched in 2005 in order to double the survivable ELM size in JET operation and to validate the vertical stabilization systems for ITER. The project was divided into four tasks, with contributions from RFX to the second and third one.

The second task, named “Vertical Stabilization Hardware and Software”, was intended to study the implementation of the control system in both hardware and software.

In 2006 and 2007, RFX contributed to design and prototype innovative solutions for the realization of the control system based on hardware emerging technologies (AdvancedTCA) and distributed real-time and non-real-time processing (Linux with real-time extensions on multi-core architecture).

In 2008 RFX has continued to provide support especially for the development of the AdvancedTCA system and the real-time operating system. RFX has also contributed to the system commissioning and first operation.

The third task, named “Vertical Stabilization Power Amplifier”, was intended to study all the viable solutions for upgrading the Vertical Stability Power Supply.

The contribution of RFX, which started in 2006, was mainly in the design of the new amplifier and the preparation of the Technical Specifications. The contract was signed in June 2007. In 2008, during the construction and testing phase, RFX has collaborated with two professionals, one of them staying at JET, to:

- provide advice during the development of the detailed design, manufacturing and setting up of the Factory and Site tests.
- contribute to the activities supporting the development of the detailed design, such as analyses and numerical simulations to verify the performance of the amplifier and relevant electric circuit in different operating conditions and to check the effectiveness of certain design choices. Assistance was also provided to set up and carry out the experimental type tests on the prototype and the routine tests in factory.

8.6 Active in-vessel coils and conducting wall for MHD stabilization in Asdex UG

A system of Active in-vessel coils and conducting wall for MHD stabilization is being designed in the frame of the ASDEX Upgrade (AUG) enhancement, which got preferential support in 2007. This enhancement is a common proposal by four Associations and Consorzio RFX is one of the partners.

The enhancement consists of 24 saddle coils arranged in three toroidal rows of eight coils each (Fig. 8.6.1) and supplied by as many ac power supplies. The system will allow producing magnetic field perturbations for studies on the Edge Localized Modes (ELM) control and effect of Resonant Magnetic Perturbations (RMP) on the plasma.

The enhancement will be organized in five Stages: in Stage 1 and 2 the coils will be provided, the upper and lower ones (the B-coils) first and the central one in stage 2. In Stage 3, twelve fast ac power supplies will be added, in Stages 4 and 5, the conducting shell and the remaining 12 power supplies will be procured respectively.

In summer 2008, the preferential support for stage 1 was granted and the call for tender for the B-coils started.

Consorzio RFX during 2008 performed a critical revision of the specifications for the PS system in collaboration with the IPP colleagues. An approach to the design was agreed that allows assuring the highest modularity level while keeping the overall cost within the set limits; this implies identifying a basic module on which it is possible to outline a dedicated power supply scheme for A and B coils, where specifications in terms of magnetic field to be generated versus

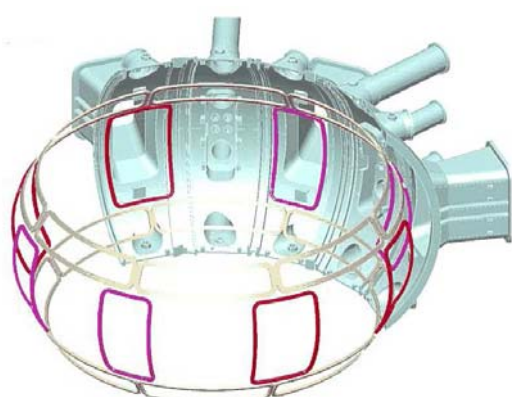


Fig 8.6.1 a) 3D view of the active in-vessel coils

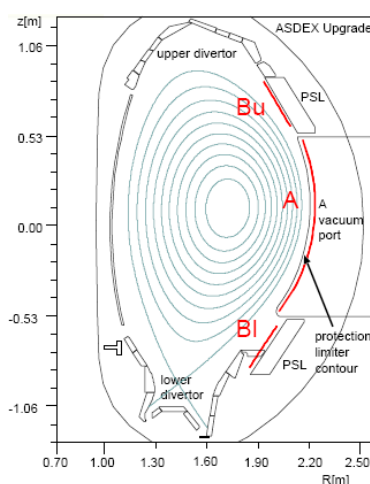


Fig. 8.6.1 b) Location of coils shown in a poloidal cross section.

frequency are quite different.

Then, we carried out preliminary studies on the PS topology, based both on Mosfet and IGBTs; the first results seems suggesting to prefer a solution based on IGBTs H-bridges connected in series and in parallel. The basic H-bridge should be the same for all the converters and should be the basic module; the rate of the basic module, the device size to be implemented and the

number of modules connected in series and in parallel is being optimized such as to maximize the bandwidth of the PS for the central A coils. The work is still in progress.

8.7 ITER engineering activities

8.7.1 Plasma Vertical Stabilisation

New solutions to increase the vertical plasma stability of ITER have been investigated via electromagnetic analysis of the new ITER blanket modules [Testoni08a]. The new blanket module is made of a First Wall (FW) panel and a Shielding Block (SB). The former, finely sliced in the poloidal direction, is made of three materials: Be, CuCrZr and 316 LN SS, subject to different temperatures and therefore different resistivities. The SB is made of SS. ANSYS simulations of a downward VDE disruption with a plasma exponential current quench of 16 ms time constant have been performed for both cases of blanket modules electrically insulated and of all toroidal rows of blanket modules electrically connected (except at the upper and equatorial ports levels). The solution with a single strap placed in the middle equatorial plane of each blanket and the solution with two symmetric straps with respect to this plane have been analyzed. The influence of the radial position of the straps has also been evaluated. The presence of the electrical straps between modules reduces the torque and increases the net force applied to each blanket. As far as the radial torque is concerned, two straps are better than one. Moving the straps closer to the plasma reduces the first peak of the torque, but the torque increases in the final part of the disruption. The option with two straps has the advantage to strongly reduce the vertical torque. The toroidal torque values are almost independent of the different options. On the other hand, the two straps option has the disadvantage to produce a slightly larger net force applied to each blanket module.

8.7.2 Electromechanical stress analysis on the ICRH antenna

A novel approach for the electromechanical disruption analysis of the ITER Ion Cyclotron antenna has been proposed [Testoni08b]. It is based on the use of the sub-modeling technique and can also be used for the analysis of other tokamak's in-vessel and out-vessel components. The disruption phenomenon is simulated by using a Finite Element model of one ITER sector and by imposing the plasma current density decay. A subsequent detailed electromagnetic analysis of the antenna and of the neighbouring components is performed by using the sub-modeling technique considering as boundary conditions the results of the previous analysis. Then, a transient mechanical analysis has been performed to compute stresses, displacements, forces and torques applied to the antenna structure. The results of the analysis have shown that all the stresses in the antenna are well below the maximum allowable stress.

8.7.2 Assessment of the key electromechanical features of EDIPO

The aim of EDIPO is to perform full size tests of superconducting conductors. The magnet will be initially devoted to the ITER conductor tests during the manufacturing phase and then it will be used for the needs of the European Fusion Program. The electromechanical analysis has addressed the magnetic field distribution in the superconducting and in the bore regions

showing that stresses are in the range of allowable limits [Testoni08c]. A coupled electromagnetic-circuit simulation has determined the voltage and current trend in the dump resistor during a quench. A coupled nonlinear harmonic electromagnetic and static heat transfer analysis of the AC coils has been performed in order to compute the AC field distribution, the current per turn, and to verify the cooling efficiency.

REFERENCES

- [Bonicelli05] T. Bonicelli et al., *Fusion Eng. Des.* **75-79**, 193-200 (2005).
- [Testoni08a] P. Testoni, A. Fanni, and A. Portone, "Electromagnetic analysis of the new ITER blanket modules for vertical passive stabilization," 2th Symposium on Fusion Technology (SOFT), 15-19 Settembre 2008, Rostock, Germany.
- [Testoni08b] P. Testoni, A. Fanni and P. Sonato, " A sub-modeling approach for the electromechanical disruption analysis of the ITER ICH antenna ," *Fusion Engineering and Design*, Volume **83**, Issues **5-6**, October 2008, Pages 695-701.
- [Testoni08c] P. Testoni, F. Cau, A. Fanni, A. Portone, P. Sonato, "Static and transient electromagnetic features of the EFDA dipole," *IEEE Trans. On Superconductivity*, vol. **18**, no. **2**, pp. 188-191, June 2008.

9 BROADER APPROACH

This chapter summarizes the activities carried out in 2008 concerning the Broader Approach, which consisted in a collaboration on the Integrated Design of the JT-60 SA machine and in particular on the design of the Quench Protection Circuits and of the in-vessel coil power supplies.

9.1 JT-60 SA

9.1.1 Contribution to the integrated design activities

JT60_SA, the Satellite Tokamak to be built in Naka, Japan, in the framework of the Broader Approach agreement, was redesigned during 2008 to achieve significant cost reductions while preserving the overall scientific capability of the device. The main machine modifications are shown in fig. 9.1.1.

The JT-60SA maximum plasma current will be 5.5 MA with a relatively low aspect ratio plasma ($R_p=2.95\text{m}$, $A=2.5$, $\kappa_x=1.93$, $\delta_{95}=0.46$); inductive operation with a flat top duration up to 100 s is possible within the available flux swing; heating and current drive will provide 34 MW NB injection and 7 MW ECRF. The present plans foresee the first plasma in 2016. The Integrated Design Report (IDR) of the machine is being submitted to the Steering Committee in December 2008.

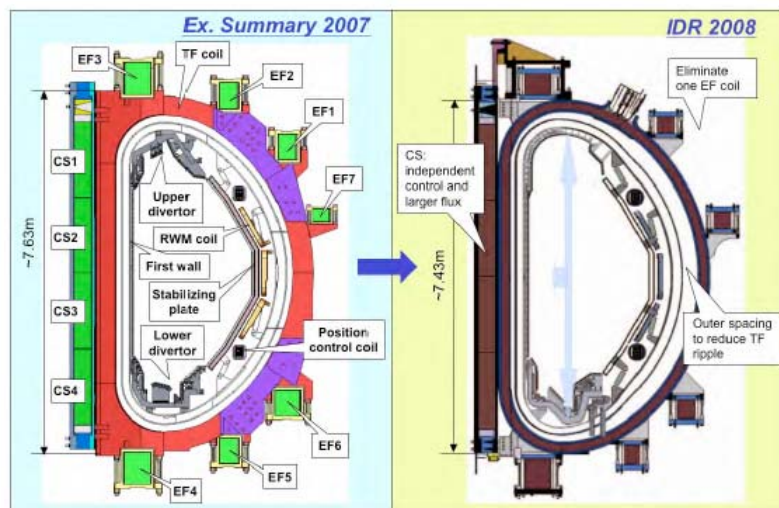


Fig. 9.1.1: Comparison of elevation view of the old and new magnets, vacuum vessel and in-vessel components. (From Re-baselining report V. 3.0 19 Sep 08)

procurement of the relevant assigned components.

During 2008 Consorzio RFX took part to the overall design activities by participating to the three Technical Coordination Meetings, by organizing an EU Technical Meeting on JT-60SA Power Supplies (PS) and by contributing to the preparation of the Plant Integration Document (PID) and of the IDR.

In addition, a contribution was given to the definition of the interfaces of the magnets and power supply system and to the main protection strategies in case of plasma disruption and fault conditions.

Consorzio RFX is part of the EU Home Team which in turn is part of the JT-60SA Integrated Team. In the frame of the EU organization, Consorzio RFX, like other Voluntary Contributor Designated Institutions, contributed to common integrated activities as well as to the design and

9.1.2 Quench Protection Circuits (QPC)

9.1.2.1 Completion of the QPC conceptual design and experimental tests to prove design feasibility

The studies for the Conceptual Design of the QPC were completed in the first months of 2008. These protection units must sustain steady-state currents up to 20 kA dc and to interrupt the current, diverting it into resistors with reapplied voltage on the order of 5 kV. A design solution based only on semiconductors was selected first; it would be highly desirable, being almost maintenance free, but it is affected by high losses in normal operation. Therefore, a new solution was devised and studied; it is based on a Hybrid Circuit Breaker (HCB) composed of a mechanical switch for conducting the continuous current, paralleled to a static circuit breaker for current interruption. This solution combines the advantages of each device: the low on-state power losses due to the low resistance of the former and the fast arc-less breaking of the latter. A simplified scheme of the proposed hybrid CB is shown in fig. 9.1.2.

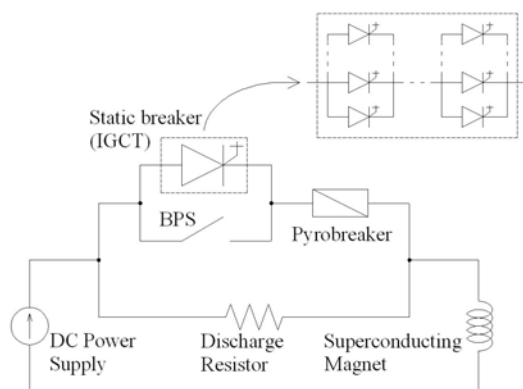


Fig.9.1.2: Scheme of the QPC based on a hybrid dc circuit breaker

Experimental tests were performed at RFX to assess the feasibility of this solution; they were in particular aimed at verifying the capability of the Integrated Gate Commutated Thyristors (IGCTs) selected as static CB to assure a safe turn-on with very low applied voltage. In fact this particular operating condition is not quite common in standard industrial applications, therefore required to be investigated. The tests were concluded with very satisfactory results,

the data were elaborated in the first months of 2008, and the results of the conceptual studies and of the experimental tests were documented in [Novello08].

Then, this conceptual design was developed and applied in detail to the JT-60SA case; the results of the work are described in [Gai08].

9.1.2.2 Analysis of circuit operation in the case of plasma disruption and QPC intervention

Consorzio RFX developed a complete model of the JT-60SA poloidal circuits including the superconducting coils (CS and EF coils), the HC in-vessel coils, the vacuum vessel, the stabilizing plates and the plasma. This model was utilized to analyze the effects of the plasma disruption and faults in terms of overcurrents in the coils and overvoltages applied across them. The fault conditions analyzed were the quench, the intervention of a Quench Protection Circuit (QPC) pyrobreaker, and the operation of the QPC of a single circuit in the case of protection requests different from quench. The development of the model and the first set of analyses were made in 2007, and then they were checked and upgraded during a period of joint work in Naka laboratory (autumn '07).

During 2008, the model was updated on the basis of the new geometric data of the machine, coming from the new baseline design. The vacuum vessel and stabilizing plates were

discretized with 154 and 36 conductors respectively and the plasma with 6 conductors placed in positions and with current values such to obtain a magnetic field similar to that produced by a 5.5 MA Double Null plasma current. Then the complete matrix describing the mutual coupling between all the coils, passive structures and plasma was worked out and used to evaluate the induced overcurrents in the coils in the cases of plasma disruption and faults.

The analyses to derive the current peak value reached in the poloidal coils in case of plasma disruption were made on the basis of 648 new sets of coil current initial values, called snapshots; the results do not show significant difference with respect to those already found during the last year and confirm that the maximum peak current never exceeds 5% of the nominal value (20kA).

During a second period of joint work in Naka, the analyses were further improved; a more accurate plasma model was introduced in the program; in this case, the plasma is simulated with 3436 conductors, with a current distribution deriving from the TOSCA code. These results were compared with the previous ones and even with the results of similar analyses performed by JAEA colleagues utilizing the DINA Code.

The three sets of results show significant differences, but in all cases the current in the poloidal coils, in case of plasma disruption, never exceeds the specified maximum value of 21kA. On the contrary, in the HC in-vessel coils the overcurrents reach more than 30 kA as shown in fig. 9.1.3.

The intervention of the QPC and even the case of failure of the dc circuit breaker with pyrobreaker intervention were also analyzed on the basis of the new set of 648 snapshots; the results always show that the total I^2t in the coils is well below the specified value of 2 GA²s, even using a dump resistance value reduced down to 0.15 Ω .

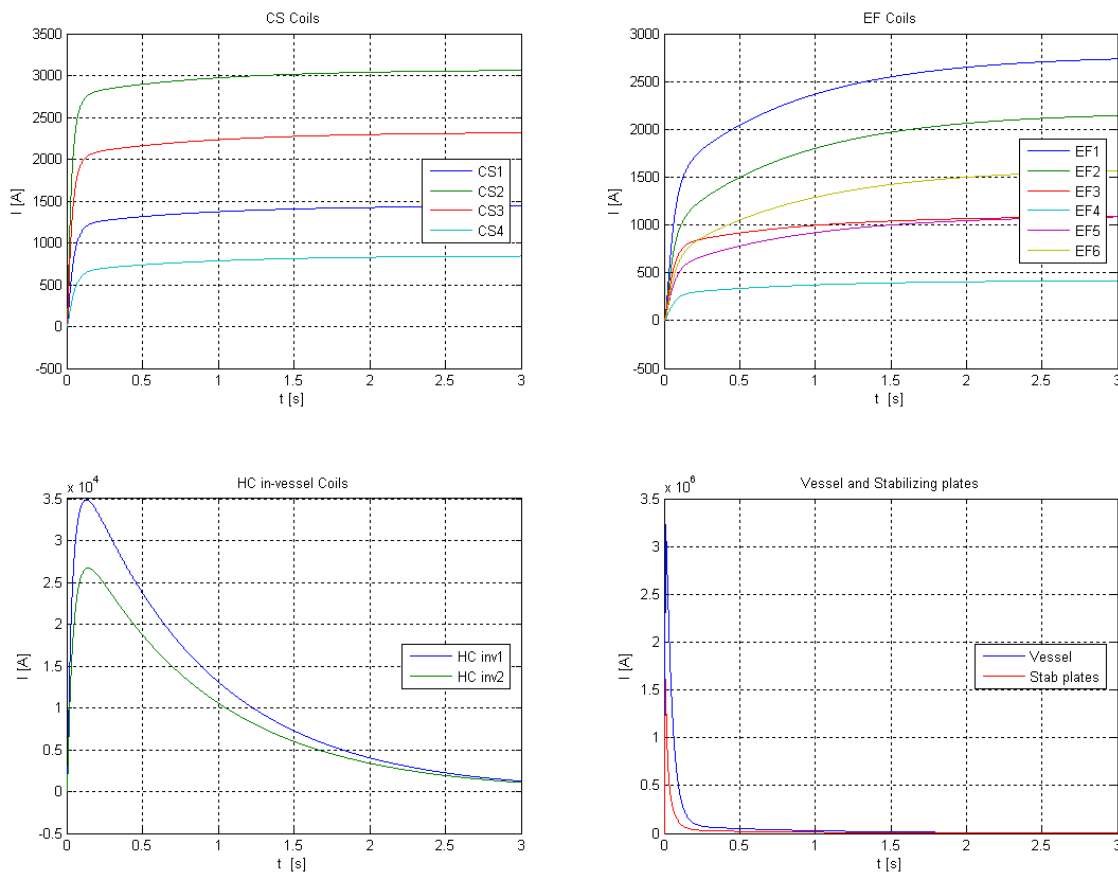


Fig. 9.1.3: Currents in coils and passive structures in case of plasma disruption

9.1.3 In vessel fast control coil power supply

A critical revision of the first conceptual design of the Power Supply (PS) for RWM control, included in the JA 2007 JT-60SA Conceptual Design Report (CDR), began in the second semester of 2008.

The conceptual design of the RWM control system is based on 18 sector coils, six in the toroidal direction and three in the poloidal one. They will be installed behind a stabilizing plate; a view of 1/6 of the system is shown in fig. 9.1.4.

Physics studies are still in progress to define the main specification of the system and in turn the current, voltage and frequency requirements for the power supplies.

During 2008 the possibility of a collaboration between RFX and JAEA in the field of the RWM physics was also explored (see section 6.5.1).

In parallel, FEM analyses were performed to check the effectiveness of the first design of the coils; to complete this work in close collaboration with the JA colleagues, a period of joint work in Naka was organized (Nov.2008). The first sector

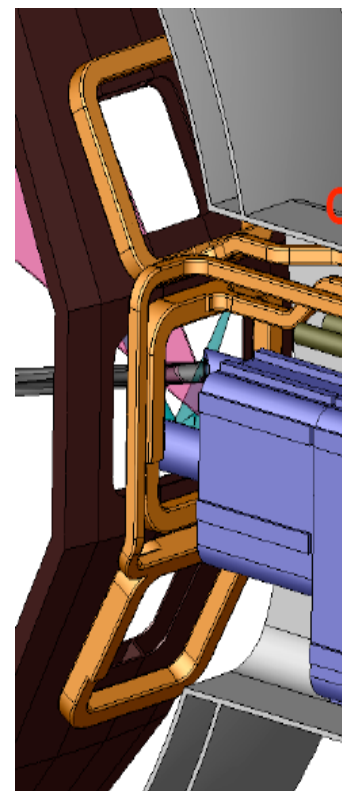


Fig. 9.1.4: 3D view of 1/6 of the sector coil system

coil conductor proposed in the CDR is shown in fig. 9.1.5. The FEM analyses highlighted that the shielding effect of the stabilizing plate is remarkable also at few Hz and that above some 100 Hz also the shielding effect of the coil plate becomes considerable. The analyses were repeated for another type of Mineral Insulated Conductor proposed by JA colleagues, assuming that it is provided both with a copper and a stainless steel sheath. The analyses showed that the efficiency is very poor, in particular with the copper shield, as expected. The results are shown in fig. 9.1.6.

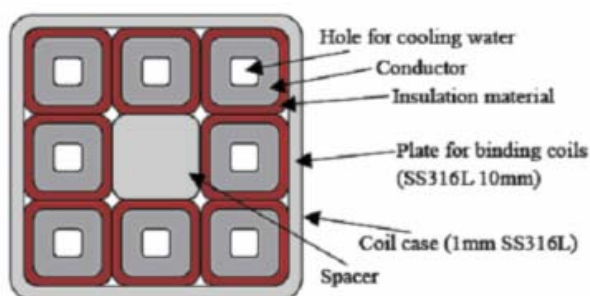


Fig. 9.1.5: section of the first sector coil conductor

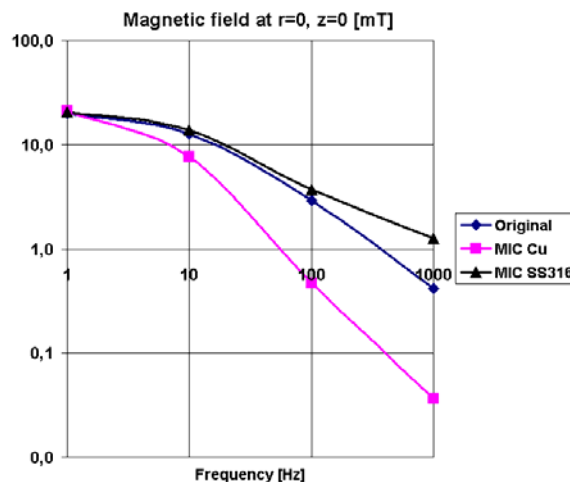


Fig. 9.1.6: section of the first sector coil conductor

Some additional analyses were performed to discriminate the shielding effect of the stabilizing plates and of the coils sheath, and even to compare the results in case of location of the coils at different distances from the stabilizing plate.

The analyses demonstrated that the present design of the sector coils needs to be further optimized and for this reason the work was particularly appreciated by the JA colleagues.

Finally, some preliminary considerations on the most suitable topology for the relevant power supply system were performed and discussed with JA colleagues, but further investigation on the assessment of the main specification data is necessary; therefore this work is still in progress and will continue during the next year.

REFERENCES

[Gai08] E. Gaio, L. Novello, R. Piovan, K. Shimada, T. Terakado, K. Kurihara, M. Matsukawa, Conceptual Design of the Quench Protection Circuits for the JT-60SA superconducting magnets, accepted for publication on Fusion Engineering and Design.

[Novello08] L. Novello, E. Gaio, R. Piovan, Feasibility studies of a hybrid Mechanical-static dc circuit breaker for Superconducting Magnet Protection; accepted for publication on IEEE Transactions of Applied Superconductivity.

10 NON FUSION APPLICATIONS

10.1 MHD control in Magneto-Plasma-Dynamic thrusters

The activity on the control of large scale MHD instabilities in Magneto-Plasma-Dynamic (MPD) thrusters for space applications has progressed during this year. The development of MHD instabilities when a critical current level is exceeded and the Kruskal-Shafranov criterion is violated has been demonstrated in the past to be responsible for the loss of efficiency and unstable behavior of this kind of devices [Zuin04]. A new experimental campaign has been carried out at Centrosazio, Pisa, where the MPD thruster previously used for instability studies has been installed in a new, larger vacuum chamber. In this chamber a cleaner environment is available, with lower vacuum levels (of the order of 5×10^{-8} mbar). As a consequence, the operational conditions are more similar to those present in real space missions.

The experimental results have shown that in this new environment the $m=1/n=1$ mode

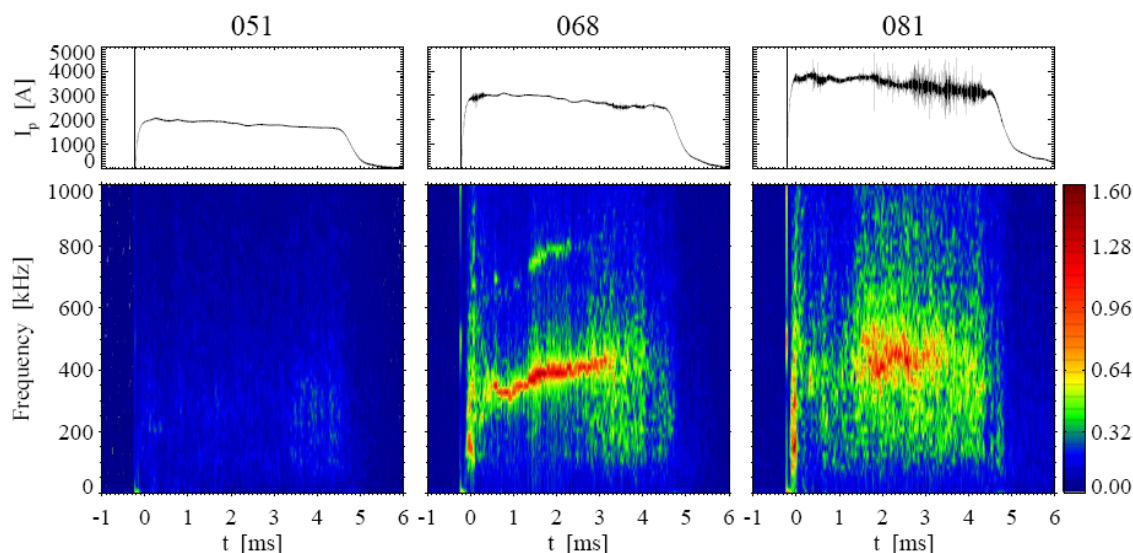


Fig. 10.1: Three MPD discharges with different plasma current levels. The plasma current waveform is shown in the top graph, while in the bottom graph is a time-frequency spectrogram of the magnetic field fluctuations. The onset of the 400 kHz mode is visible in the second and third cases.

previously observed displays somehow different features. In particular, a typical frequency of 400 kHz is measured, as opposed to frequencies around 100 kHz observed in the past (fig. 10.0). This could be attributed to the lower collisionality with the background gas, or to the lower impurity concentration. The axial wavelength of the mode appears also to be reduced with respect to previous measurements. The effectiveness of the control scheme developed in the past [Zuin06], which consists in a dielectric septum dividing the thruster chamber into two halves, thus suppressing the helical currents associated to the mode, has been tested in the new condition. The method has been shown to be effective when the axially applied magnetic field is 100 mT (the maximum level achievable in this device). However, at lower axial fields the effect is not so clear. It has been speculated that this result could be due to the deposition on the septum of a film of copper, which is the cathode material. Such film, which has been indeed found on the septum at the end of the experimental campaign, could help the helical

currents to close, thus enabling the mode to develop. The conclusion of this activity is that future tests will require a cathode made of a more robust material, less subject to sputtering.

10.2 Low-power plasma source for biomedical applications

The study on the effects on living matter of the low-power plasma source for biomedical applications, jointly developed with the Faculty of Medicine of the University of Padova [Leonardi07], have been continued.

The sterilizing effect of the plasma has been tested by treating different types of bacteria cultures, namely, in order of resistance, *Escherichia Coli*, *Staphylococcus Aureus* and *Pseudomonas Aeuroginosa*. Bacteria have been grown in the proper medium at 37°C, and then on the day of the experiment a fixed volume of culture was transferred to fresh medium and incubated with shaking. Bacteria were then serially diluted to obtain suspension concentrations of 10⁶ colony formation units (CFU) per ml, and 30 ml of the solutions were placed in micro wells of tissue culture. The treatment was performed positioning the plasma source external grid 1-2 mm above the bacteria cultures for the chosen treatment time interval (from 30 s to 5 min). After treatment, each sample was collected and vital microbial count was performed by seeding the sample on the proper agar-medium and incubating at 37°C for 16 hours. The number of CFU appearing on each culture dish was counted to assess the number of surviving organisms. As figure 10.2a shows, different bacteria have different fractions of surviving CFU, but, in all cases, an exponential decay is found [Aragona08].

The effect of the source on living cells has also been tested, to prove that the non-damaging

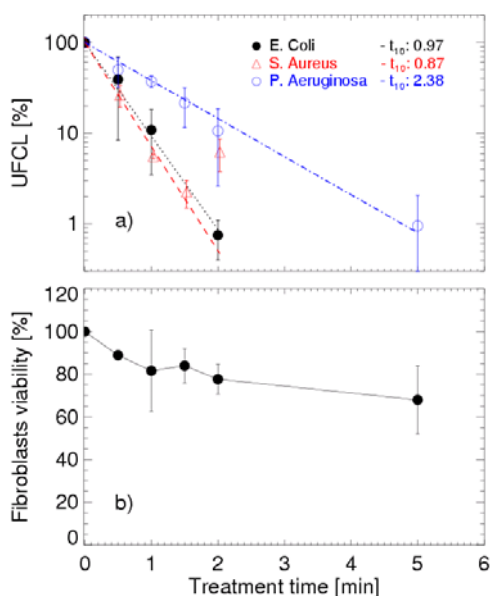


Fig 10.2: Counts of bacteria colonies after plasma treatment, as a function of treatment time (a) and conjunctival fibroblasts viability, expressed as percentage with respect to the control untreated cases, as a function of treatment time (b).

disinfection selectively kills the pathogens but not the tissue cells. This aim has been pursued using conjunctival fibroblasts isolated from human biopsies and cultured in the appropriate medium. Effects on cell viability were assessed by methyltetrazolium (MTT) test, after treatment of two-dimensional cell cultures for the same time interval (from 30 s to 5 min) used with bacteria, at room temperature. As figure 10.2b shows, for the tested time intervals cell cultures maintain viability comparable to that of untreated cells (control cultures).

The effects of plasma treatment on ex-vivo cultivated human corneas have been also studied by means of histological analysis and electronic spectroscopy. No damage, neither from the morphological nor from the structural point of

view, was induced by 5 minutes plasma treatment on human corneas.

The UV emission from the plasma could in principle cause DNA damage, responsible for cytotoxicity and mutagenicity in living cells, by forming thymine dimers (TD). To investigate the effect of plasma UV emission on conjunctival fibroblasts, the presence of TD was detected by immunofluorescence microscopy using a monoclonal antibody against thymine dimers, after plasma treatment. No TD detection was obtained.

In conclusion, the capability of the source to kill several different kinds of bacteria with decimal reduction times of 1-2 min, while preserving the living cells of the substrate, has been demonstrated. The likely origin of this selective effect, which is very promising for the potential applications of this technology in clinical practice, is likely to reside in the self-repairing mechanisms of the cells against the action of free radicals. Possible applications of the source are presently under study. In particular, the possibility of treating corneal infections, which constitute a cause of total loss of sight in the most serious cases, will be the object of future investigations.

An international patent request for the plasma source has been filed under the Patent Cooperation Treaty [Leonardi08].

REFERENCES

- [Aragona08] M. Aragona, Tesi di laurea del corso di laurea specialistica in Biotecnologie Mediche, Facoltà di Medicina e Chirurgia, Università di Padova, a.a. 2008-2009.
- [Leonardi07] A. Leonardi, V. Deligianni, E. Martines, et al., Domanda di brevetto per invenzione industriale n. RM 2007 A000521.
- [Leonardi08] A. Leonardi, V. Deligianni, E. Martines, et al., Patent application n. PCT/EP2008/063275.
- [Zuin04] M. Zuin, R. Cavazzana, E. Martines et al., Phys. Rev. Lett. **92**, 225003 (2004).
- [Zuin06] M. Zuin, R. Cavazzana, E. Martines et al., Appl. Phys. Lett. **89**, 041504 (2006).

11 EDUCATION AND INFORMATION TO THE PUBLIC

In January 2008, both the new “Joint Research Doctorate in Fusion Science and Engineering”, between the University of Padova and the Universidade Tecnica de Lisboa (Instituto Superior Tecnico), and the new “European Interuniversity Doctoral Network in Fusion Science and Engineering”, among the same two universities and the Ludwig Maximilian University of Munich (Garching), started. The number of students participating to the first cycle (three years duration) of the doctorate was: 5 students from Padua, 5 students from Lisbon and 3 students from Munich.

In this context, in the period from May 5th to May 16th, a 50 hours Basic Course on Engineering was given by teachers of Consorzio RFX. The lessons dealt with the following arguments: Fusion Power Plants; First Wall, Divertor, Vacuum Vessel and Remote Handling; Axisymmetric Equilibrium and Stability of Toroidal Plasmas; Magnets and Feedback Control Theory with application to Tokamak Control.

11 students followed this basic course and passed the final examination.

Moreover, in October 2008, three RFX teachers contributed to the first Advanced Course on Physics held in Garching.

Apart from these specific courses, significant effort was dedicated in 2008 to the management and to the research and teaching organization of this new important initiative, which is coordinated by Padova.

The other educational activity of Consorzio RFX on fusion related disciplines continued with a significant effort also in 2008

In particular RFX professionals were in charge of 17 postgraduate students of the PhD courses in Physics, Energy Research, Electrical Engineering and Fusion Science and Engineering and of 21 students preparing their graduation thesis on fusion related subjects.

Nine regular courses of the Padova University were given by teachers belonging to Consorzio RFX. Four of them have been given at the Faculty of Engineering, in particular “Plasma Physics”, “Plasma and Controlled Thermonuclear Fusion”, “Industrial Applications of Plasmas”, “Energy Technology and Economics”, and five at the Faculty of Sciences, in particular “Introduction to Plasma Physics”, “Experimental and Numerical Methods for Fluid Dynamics and Plasma Physics”, “Thermonuclear Fusion and Plasma Physics Applications”, “Fluid and Plasma Physics” and “Electrodynamics”.

As far as public information is concerned, apart from the permanent organization of visits to the RFX site (that has reached about 2.500 visitors in 2008), Consorzio RFX completed the activity for the Fusion Expo exhibition at the end of the relevant EFDA contract. The 5 year activity closed with an exceptional sequence of exhibitions and participation in major international events, characterized by a large number of visitors and media resonance. We believe it helped in laying the basis for a public wider knowledge to favour a conscious attitude towards fusion.

12 LIST OF PUBLICATIONS 2008

INTERNATIONAL AND NATIONAL JOURNALS

- R.1 F. Villone, Y.Q. Liu, R. Paccagnella, et.al., “Effects of three-dimensional electromagnetic structures on resistive-wall-mode stability of reversed field pinches”, *Phys. Rev. Lett.*, **100**, 255005 (2008)
- R.2 M. García-Muñoz, H.-U. Fahrbach, S. Günter, V. Igochine, M. J. Mantsinen, M. Maraschek, P. Martin, P. Piovesan, K. Sassenberg, and H. Zohm: “Fast-Ion Losses due to High-Frequency MHD Perturbations in the ASDEX Upgrade Tokamak”, *Phys. Rev. Lett.* **100**, 055005 (2008)
- R.3 R. Lorenzini, D. Terranova, A. Alfier, P. Innocente, E. Martines, R. Pasqualotto, P. Zanca: “Single helical axis states in reversed field pinch plasmas”, *Phys. Rev. Lett.*, **101**, 025005 (2008)
- R.4 P. Piovesan, V. Igochine, P. Lauber, K. Sassenberg, A. Flaws, M. García-Muñoz, S. Günter, M. Maraschek, L. Marrelli, P. Martin, P.J. Mc Carthy and the AUG team: “TAE internal structure through high-resolution soft x-ray measurements in ASDEX-Upgrade”, *Nucl. Fusion* **48**, 065001 (2008)
- R.5 A. Murari, G. Vagliasindi, P. Arena, L. Fortuna, O. Barana, M. Johnson and EFDA-JET Contributors: "Prototype of an adaptive disruption predictor for JET based on fuzzy logic and regression trees", *Nucl. Fusion*, **48** (2008) pp. 1-10
- R.6 L. Frassinetti, A. Alfier, R. Pasqualotto, F. Bonomo, P. Innocente: “Heat diffusivity model and temperature simulations in RFX-mod”, *Nucl. Fusion*, **48** (2008) 045007
- R.7 M.N.A. Beurskens, G. Arnoux, A.S. Brezinsek, C.D. Challis, P.C. de Vries, C. Giroud, A. Huber, S. Jachmich, K. McCormick, R.A. Pitts, F.G. Rimini, A. Alfier, E. de la Luna, W. Fundamenski, S. Gerasimov, E. Giovannozzi, E. Joffrin, M. Kempenaars, X. Litaudon, T. Loarer, P. Lomas, J. Mailloux, R. Pasqualotto, V. Pericoli-Ridolfini, R. Pugno, E. Rachlew, S. Saarelma, E. Solano, M. Walsh, L. Zabeo, K.-D. Zastrow and JET-EFDA Contributors: “Pedestal and ELM response to impurity seeding in JET advanced scenario plasmas”, *Nucl. Fusion* **48** (2008) 095004
- R.8 A Alfier, M Beurskens, E Giovannozzi, M Kempenaars, H R Koslowski, Y Liang, C McKenna, R Pasqualotto, S Saarelma, M Walsh, E De La Luna and JET-EFDA contributors: “Edge Te and ne profiles during Type-I ELM mitigation experiments with perturbation fields on JET”, *Nucl. Fusion*, **48** (2008) 115006
- R.9 D. Bonfiglio, S. Cappello, R. Piovan, L. Zanotto and M. Zuin: "3D nonlinear MHD simulations of ultra-low q plasmas", *Nucl. Fusion* **48** (2008) 115010
- R.10 M.Gobbin, R.B.White, L.Marrelli and P.Martin: “Resonance between passing fast ions and MHD instabilities both in the tokamak and the RFP configurations”, *Nucl. Fusion* **48** 075002 (2008)
- R.11 P. Piovesan, A. Almagri, B.E. Chapman, D. Craig, L. Marrelli, P. Martin, S.C. Prager and J.S. Sarff: “Filamentary current structures in the Madison Symmetric Torus”, *Nucl. Fusion* **48**, 095003 (2008)
- R.12 A. Alfier, R. Pasqualotto, G. Spizzo, A. Canton, A. Fassina and L. Frassinetti: “Electron temperature profiles in RFX-mod”, *Plasma Phys. Control. Fusion*, **50** (2008) 035013

- R.13 R Lorenzini, F Auriemma, P Innocente, E Martines, S Martini and D Terranova: "Confinement loss during dynamo relaxation event in RFX-mod", Plasma Phys. Control. Fusion, **50** (2008) 035004
- R.14 A. Pizzimenti, R. Paccagnella: "Mode coupling studies in the RFX-mod reversed field pinch", Plasma Phys. Control. Fusion, **50** (2008) 065006
- R.15 F. Turco, G. Giruzzi, J. F. Artaud, O. Barana, V. Basiuk, G. Huysmans, F. Imbeaux, P. Maget, D. Mazon and J-L. Ségui: "Investigation of MHD phenomena on Tore Supra by localised ecd perturbation experiments", Plasma Phys. Control. Fusion, **50** (2008) pp. 1-22
- R.16 J. Adamek, M. Kocan, R. Panek, J. P. Gunn, E. Martines, J. Stöckel, C. Ionita, G. Popa, C. Costin, J. Brotankova, R. Schrittwieser, G. Van Oost : "Simultaneous measurements of ion temperature by segmented tunnel and katsumata probe", Contributions to Plasma Physics, **48**, 395 (2008)
- R.17 J. Brotánková, E. Martines, J. Adámek, J. Stöckel, G. Popa, C. Costin, C. Ionita, R. Schrittwieser, G. Van Oost : "Novel technique for direct measurement of the plasma diffusion coefficient in magnetized plasma", Contributions to Plasma Physics, **48**, 418 (2008)
- R.18 F. Sartori, F. Crisanti, R. Albanese, G. Ambrosino, V. Toigo, J. Hay, P. Lomas, F. Rimini, S.R. Shaw, A. Luchetta, J. Sousa, A. Portone, T. Bonicelli, M. Ariola, G. Artaserse, M. Bigi, P. Card, M. Cavinato, G. De Tommasi, E. Gaio, M. Jennison, M. Mattei, F. Maviglia, F. Piccolo, A. Pironti, A. Soppelsa, F. Villone, L. Zanotto et al : "The JET PCU project: An international plasma control project", Fus. Eng. Des., **83**, Issues 2-3, April 2008, Pages 202-206
- R.19 M. Cavinato, R. Cavazzana, A. Luchetta, G. Manduchi, G. Marchiori, A. Soppelsa, M. Spolaore, C. Taliercio : "Control of plasma parameters by the externally applied toroidal field in RFX-mod", Fus. Eng. Des., **83**, Issues 2-3, April 2008, Pages 220-223
- R.20 G. Manduchi, A. Luchetta, C. Taliercio, T. Fredian, J. Stillerman : "Real-time data access layer for MDSplus", Fus. Eng. Des., **83**, Issues 2-3, April 2008, Pages 312-316
- R.21 T. Fredian, J. Stillerman, G. Manduchi : "MDSplus extensions for long pulse experiments", Fus. Eng. Des., **83**, Issues 2-3, April 2008, Pages 317-320
- R.22 A. Luchetta, A. Barbalace, G. Manduchi, A. Soppelsa, C. Taliercio : "Real-time communication for distributed plasma control systems ", Fus. Eng. Des., **83**, Issues 2-3, April 2008, Pages 520-524
- R.23 A. Soppelsa, G. Marchiori, L. Marrelli, P. Zanca: "Design of a new controller of MHD modes in RFX-mod", Fus. Eng. Des., **83**, Issues 2-3, April 2008, Pages 224-227
- R.24 B. Guillerminet, M. Airaj, P. Huynh, G. Huysmans, F. Iannone, F. Imbeaux, J.B. Lister, G. Manduchi, P. Strand and the Contributors to the European Task Force on Integrated Modelling Activity : "Integrated tokamak modeling: Infrastructure and Software Integration Project ", Fus. Eng. Des., **83**, Issues 2-3, April 2008, Pages 442-447
- R.25 H. J. Gardner, R. Karia, G. Manduchi: "A web-based, dynamic metadata interface to MDSplus", Fus. Eng. Des., **83**, Issues 2-3, April 2008, Pages 448-452
- R.26 E. Gaio, V. Toigo, A. De Lorenzi, R. Piovan., L. Zanotto: "The alternative design concept for the ion source power supply of the ITER neutral beam injector", Fus. Eng. Des., **83**, Issue 1, Pages: 21-29

- R.27 G. Manduchi, F. Iannone, F. Imbeaux, G. Huysmans, J.B. Lister, B. Guillerminet, P. Strand, L.-G. Eriksson, M. Romanelli and contributors to the ITM-TF work programme: "A universal access layer for the Integrated Tokamak Modelling Task Force", *Fus. Eng. Des.*, **83**, Issues 2-3, April 2008, Pages 462-466
- R.28 G.A. Rattá, J. Vega, A. Pereira, A. Portas, E. de la Luna, S. Dormido-Canto, G. Farias, R. Dormido, J. Sánchez, N. Duro, H. Vargas, M. Santos, G. Pajares, A. Murari and JET-EFDA Contributors: "First applications of structural pattern recognition methods to the investigation of specific physical phenomena at JET", *Fus. Eng. Des.*, **83**, Issues 2-3, April 2008, Pages 467-470
- R.29 P. Testoni, A. Fanni, P. Sonato: "A sub-modelling approach for the electromechanical disruption analysis of the ITER ICH antenna", *Fus. Eng. Des.*, **83**, Issues 5-6, Pages 695-701, (2008)
- R.30 A. Barbalace, A. Luchetta, G. Manduchi, M. Moro, A. Soppelsa, C. Taliercio: "Performance Comparison of VxWorks, Linux, RTAI, and Xenomai in a Hard Real-Time Application, Nuclear Science, IEEE Transactions, **55**, Issue 1, Part 1, Feb. 2008, 435 – 439
- R.31 O. Barana, A. Luchetta, G. Manduchi, C. Taliercio: "New Architecture for the RFX-mod Machine Control System", *Nuclear Science, IEEE Transactions*, **55**, Issue 1, Part 1, Feb. 2008 Page(s):311 – 315
- R.32 M. Cavenago, P. Veltri, F. Sattin, et al.: "Negative ion extraction with finite element solvers and ray maps", *IEEE Transactions on Plasma Science*, **36** Issue: 4 Pages: 1581-1588 (2008)
- R.33 F. Sattin: "Fick's law and Fokker-Planck equation in inhomogeneous environments", *Physics Letters A*, **372** Issue: 22 Pages: 3941-3945 (2008)
- R.34 M. Agostini, R. Cavazzana, P. Scarin, G. Serianni, Y. Yagi, H. Koguchi, S. Kiyama, H. Sakakita and Y. Hirano: "Electrostatic turbulence in the edge of TPE-RX and driving mechanisms". *Plasma Phys. Control. Fusion* **50** (2008) 095004
- R.35 M. Valisa, T. Bolzonella, P. Buratti, L. Carraro, R. Cavazzana, S. Dal Bello, P. Martin, R. Pasqualotto, J. Sarff, M. Spolaore, P. Zanca, L. Zanotto, M. Agostini, A. Alfier, V. Antoni, L. Apolloni, F. Auriemma, O. Barana, M. Baruzzo, P. Bettini, D. Bonfiglio, F. Bonomo, M. Brombin, A. Buffa, Alessandra Canton, Susanna Cappello, M. Cavinato, G. Chitarin, A. De Lorenzi, G. De Masi, D. F. Escande, A. Fassina, P. Franz, E. Gaio, E. Gazza, L. Giudicotti, F. Gnesotto, M. Gobbin, L. Grandi, L. Guazzotto, S.C. Guo, V. Igochine, P. Innocente, R. Lorenzini, A. Luchetta, G. Manduchi, G. Marchiori, D. Marcuzzi, L. Marrelli, S. Martini, E. Martines, K.J. McCollam, F. Milani, M. Moresco, L. Novello, S. Ortolani, R. Paccagnella, S. Peruzzo, R. Piovan, L. Piron, A. Pizzimenti, P. Piovesan, N. Pomaro, I. Predebon, M.E. Puiatti, G. Rostagni, Fabio Sattin, P. Scarin, Gianluigi Serianni, P. Sonato, E. Spada, A. Soppelsa, S. Spagnolo, G. Spizzo, C. Taliercio, D. Terranova, V. Toigo, N. Vianello, D. Yadikin, P. Zaccaria, B. Zaniol, E. Zilli and M. Zuin: "High current regimes in RFX-mod", *Plasma Phys. Control. Fusion* **50** (2008) 124031
- R.36 D. Escande, F. Sattin: "When can the Fokker-Planck equation describe anomalous or chaotic transport? Intuitive aspects", *Plasma Phys. Control. Fusion* **50** (2008) 124023
- R.37 A. Murari, T. Edlington, A. Alfier, A. Alonso, Y. Andrew, G. Arnoux, M. N. A. Beurskens, P. Coad, C. Crombe, E. Gauthier, C. Giroud, C. Hidalgo, S. Hong, M. Kempenaars, V. G. Kiptily, T. Loarer, A. Meigs, R. Pasqualotto, Tuomas J J Tala and EFDA Contributors JET: "Innovative diagnostics for ITER physics addressed in JET", *Plasma Phys. Control. Fusion* **50** 124043 (2008)

-
- R.38 A Alfier, S. Barison, T. Danieli, L. Giudicotti, C. Pagura, R. Pasqualotto: "In situ window cleaning by laser blowoff through optical fiber", *Rev. Sci. Instrum.* **79**, 10F338 (2008)
- R.39 E. Alessi, M. Cavinato, G. Chitarin: "Development of a reconstruction procedure for the halo current distribution," *Rev. Sci.Instrum.* **79**, Issue 10F332 (2008)
- R.40 G. Serianni, N. Pomaro, R. Pasqualotto, M. Spolaore, M. Valisa: "The diagnostic system of the Neutral Beam Injectors for ITER heating and current drive", *Rev. Sci. Instrum.* **79**, 10F307 (2008)
- R.41 R. Cavazzana and M. Moresco: "Robust measurement of group delay in the presence of density fluctuations by means of ultrafast swept reflectometry", *Rev. Sci. Instrum.* **79**, 10F105 (2008)
- R.42 K. Oki , R. Ikezoe, T. Onchi , A. Sanpei , H. Himura , S. Masamune, R. Paccagnella: "Observation of large-scale profile change of magnetic field in a low-aspect ratio reversed field pinch", *Jou. Phys. Soc. Japan*, **77** (2008) 075005
- R.43 B. Zaniol, M. Schiorlin, E. Gazza, E. Marotta, X. Ren, M. Puiatti, M. Rea, P. Sonato, and C. Paradisi: "An emission spectroscopy study of atmospheric plasmas formed by DC and pulsed corona discharges in hydrocarbon contaminated air" *I.J.PEST* **2** (2008)
- R.44 M. Matsukawa, M. Kikuchi, T. Fujii, T. Fujita, T. Hayas, S. Higashijima, N. Hosogane, Y. Ikeda, S. Ide, S. Ishida, Y. Kamada, H. Kimura, K. Kizu, K. Kurihara, G. Kurita, K. Masaki, G. Matsunaga, N. Miya, S. Moriyama, A. Sakasai, S. Sakurai, Y.K. Shibama, K. Shimada, A. Sukegawa, T. Suzuki, Y. Suzuki, Y. Takase, M. Takechi, H. Tamai, K. Tsuchiya, H. Urano, T. Yamamoto, K. Yoshida, R. Andreani, J. Alonso, P. Barabaschi, J. Botija, P. Cara, A. Coletti, R. Coletti, P. Costa, A. Cucchiaro, P. Decool, A. Della Corte, N. Dolgetta, J.L. Duchateau, W.H. Fietz, E. Gaio, A. Grosman, O. Gruber, R. Heller, D. Henry, P. Hertout, J. Hourtoule, B. Lacroix, R. Magne, M.Medrano, F. Michel, L. Muzzi, S. Nicollet, L. Novello, L. Petrizzi, R. Piovan, A. Pizzuto, C. Portafaix, E. Rincon, S. Roccella, L. Semeraro, S. Turtù, J. M. Verder S. Villari, L. Zani and A. Di Zenobio: "Status of JT-60SA tokamak under the EU-JA Broader Approach Agreement" *Fusion Engineering and Design*, In Press, Corrected Proof, Available online 13 August 2008
- R.45 P. Zanca: "Avoidance of tearing modes wall-locking in a reversed field pinch with active feedback coils", *Plasma Phys. Control. Fusion* **51** (2009) 015006

CONFERENCE PROCEEDINGS

- P.1 T. Bolzonella, P. Innocente, A. Alfier, F. Bonomo, L. Carraro, L. Marrelli, R. Pasqualotto, D. Terranova: "Insights on ohmic input power evaluation in the RFX-mod Reversed Field Pinch", 35th EPS Conference on Plasma Phys. Hersonissos, 9 - 13 June 2008, proceedings ECA Vol.32F, P-5.097 (2008)
- P.2 N. Vianello, M. Agostini, A. Alfier, A.Canton, R. Cavazzana, A. Fassina, R. Lorenzini, E. Martines, P. Scarin, G. Serianni, G. Spizzo, M. Spolaore and M. Zuin: "Turbulence, transport and their relation with magnetic boundary in the RFX-mod device", 35th EPS Conference on Plasma Phys. Hersonissos, 9 - 13 June 2008, proceedings ECA Vol.32F, O-4.049 (2008)
- P.3 F. Bonomo, D. Terranova, A. Alfier, M. Gobbin, R. Lorenzini, L. Marrelli, R. Pasqualotto: "QSH in high current RFX-mod plasmas: thermal and topological

- features”, 35th EPS Conference on Plasma Phys. Hersonissos, 9 - 13 June 2008, proceedings ECA Vol.32F, P-2.054 (2008)
- P.4 M. Gobbin, F. Sattin, S.C. Guo, S. Cappello, F. Sattin, L. Marrelli and L. Garzotti: “Numerical studies of particle transport in RFX-mod low chaos regimes”, 35th EPS Conference on Plasma Phys. Hersonissos, 9 - 13 June 2008, proceedings ECA Vol.32F, P-5.035 (2008)
- P.5 L. Carraro, D. Terranova, F. Auriemma, F. Bonomo, A. Canton, A. Fassina, P. Franz, P. Innocente, R. Lorenzini, R. Pasqualotto, M.E. Puiatti: “Particle transport in different magnetic field topological configurations in the RFX-mod experiment”, 35th EPS Conference on Plasma Phys. Hersonissos, 9 - 13 June 2008, proceedings ECA Vol.32F, P-4.019 (2008)
- P.6 A. Canton, S. Dal Bello, R. Cavazzana, P. Innocente, P. Sonato, C. Taliercio, M. Breda: “Density control in RFX-mod Reversed Field Pinch device”, 35th EPS Conference on Plasma Phys. Hersonissos, 9 - 13 June 2008, proceedings ECA Vol.32F, D-1.002 (2008)
- P.7 M.E. Puiatti, A. Agostini, A. Alfier, A. Canton, S. Cappello, L. Carraro, P. Innocente, R. Lorenzini, R. Paccagnella, I. Predebon, P. Scarin, G. Spizzo, D. Terranova, M. Valisa: “High density limit in a Reversed Field Pinch”, 35th EPS Conference on Plasma Phys. Hersonissos, 9 - 13 June 2008, proceedings ECA Vol.32F, P-4.074 (2008)
- P.8 V. Igochine, T. Bolzonella, M. Baruzzo, S.C. Guo G. Marchiori, A. Soppelsa, D. Yadikin, H. Zohm: “Externally induced rotation of the resistive wall modes in RFX-mod”, 35th EPS Conference on Plasma Phys. Hersonissos, 9 - 13 June 2008, proceedings ECA Vol.32F, P-2.066 (2008)
- P.9 C. Mazzotta, M. Romanelli, O. Tudisco, L. Carraro, S. Cirant, E. Giovannozzi, L. Gabellieri, G. Granucci, M. Marinucci, S. Nowak, V. Pericoli, M.E. Puiatti, A. Romano, L. Lauro, Taroni and the FTU team: “Particle density behavior in FTU electron heated plasmas”, 35th EPS Conference on Plasma Phys. Hersonissos, 9 - 13 June 2008, proceedings ECA Vol.32F, P-2.026 (2008)
- P.10 W. Suttrop, M. Rott, T. Vierle, B. Streibl, A. Herrmann, V. Rohde, U. Seidel, D. Yadikin, Neubauer, B. Unterberg, E. Gaio, V. Toigo, P. Brunzell, ASDEX Upgrade Team: “Design of in-vessel saddle coils for MHD control in ASDEX Upgrade”, 35th EPS Conference on Plasma Phys. Hersonissos, 9 - 13 June 2008, proceedings ECA Vol.32F, P-4.075 (2008)
- P.11 G. Serianni, N. Pomaro, R. Pasqualotto, M. Spolaore, M. Valisa: “The diagnostic system for the characterisation of ITER Neutral Beam Injectors”, 35th EPS Conference on Plasma Phys. Hersonissos, 9 - 13 June 2008, proceedings ECA Vol.32F, P-5.073 (2008)
- P.12 D.F. Escande, F. Sattin: “When can the Fokker-Planck equation describe anomalous or chaotic particle transport?” 35th EPS Conference on Plasma Phys. Hersonissos, 9 - 13 June 2008, Invited
- P.13 R. Bilato, E. Poli, F. Volpe, R. Paccagnella, M. Brambilla: “Eccd Feasibility study for RFX”, 35th EPS Conference on Plasma Phys. Hersonissos, 9 - 13 June 2008, proceedings ECA Vol.32F, P5.095 (2008)
- P.14 M. Valisa: “Physics issues in the new high current regimes on RFX-mod”, 35th EPS Conference on Plasma Phys. Hersonissos, 9 - 13 June 2008, Invited
- P.15 P. Piovesan, M. Zuin, A. Alfier, D. Bonfiglio, F. Bonomo, A. Canton, S. Cappello, L. Carraro, R. Cavazzana, M. Gobbin, L. Marrelli, P. Martin, E. Martines, R. Lorenzini, R. Pasqualotto, M. Spolaore, M. Valisa, N. Vianello, P. Zanca, and the RFX-mod team:

- “Magnetic order improvement through high current and MHD feedback control in RFX-mod”, 35th EPS Conference on Plasma Phys. Hersonissos, 9 - 13 June 2008, proceedings ECA Vol.32F, O-4.029 (2008)
- P.16 F. Villone, T. Bolzonella, Y. Q. Liu, G. Marchiori, R. Paccagnella, G. Rubinacci, A. Soppelsa, “RWM modelling in RFX-mod including 3D conducting structures”, 35th EPS Conference on Plasma Phys. Hersonissos, 9 - 13 June 2008, proceedings ECA Vol.32F, P-2.067 (2008)
- P.17 M. García-Muñoz, H.-U. Fahrbach, S. Günter, V. Igochine, M.-J. Mantsinen, M. Maraschek, P. Martin, S.-D. Pinches, P. Piovesan, K. Sassenberg, H. Zohm: “Observation and modelling of fast ion losses due to high frequency MHD perturbations in the ASDEX Upgrade tokamak”, 35th EPS Conference on Plasma Phys. Hersonissos, 9 - 13 June 2008, proceedings ECA Vol.32F, P1.055 (2008)
- P.18 G. Marchiori, L. Marrelli, P. Piovesan, A. Soppelsa, F. Villone “Comparison between an experimentally estimated and a finite element model of RFX-mod MHD active control system”, 35th EPS Conference on Plasma Phys. Hersonissos, 9 - 13 June 2008, proceedings ECA Vol.32F, P5.047 (2008)
- P.19 L. Marrelli, P. Zanca, R. Paccagnella, P. Piovesan, G. Marchiori, L. Novello, A. Soppelsa: “Advances in MHD mode control in RFX-mod”, 35th EPS Conference on Plasma Phys. Hersonissos, 9 - 13 June 2008, proceedings ECA Vol.32F, P-5.065 (2008)
- P.20 G. Bonheure, J. Mlynar, L. Bertalot, S. Popovichev, C. Giroud, P. Belo A. Murari and JET-EFDA Contributors: “A novel method for tritium transport studies and its validation at JET”, 35th EPS Conference on Plasma Phys. Hersonissos, 9 - 13 June 2008, proceedings ECA Vol.32F, P-4.084 (2008)
- P.21 M.K. Zedda, M. Camplani, B. Cannas, A. Fanni, P. Sonato, E. Solano, JET-EFDA contributors: “Dynamic behaviour of type I Edge Localized Modes in the JET”, 35th EPS Conference on Plasma Phys. Hersonissos, 9 - 13 June 2008, proceedings ECA Vol.32F, P-4.070 (2008)
- P.22 G P Maddison, A E Hubbard, J W Hughes, J A Snipes, B LaBombard, I M Nunes, M N A Beurskens, S K Erents, M A H Kempenaars, B Alper, S D Pinches, M Valovi, R Pasqualotto, A Alfier, E Giovannozzi and JET EFDA contributors: “Dimensionless pedestal identity plasmas on Alcator C-Mod and JET”, 35th EPS Conference on Plasma Phys. Hersonissos, 9 - 13 June 2008, proceedings ECA Vol.32F, O-4.034 (2008)
- P.23 G. Marchiori, L. Marrelli, L. Novello, R. Paccagnella, P. Piovesan, L. Piron, A. Soppelsa, P. Zanca, “Advanced MHD mode control in RFX-mod”, 35th EPS Conference on Plasma Phys. Hersonissos, 9 - 13 June 2008, proceedings ECA Vol.32F, P-5.065 (2008)
- P.24 G. Chitarin, R.S. Delogu, A. Gallo, S. Peruzzo "Technology developments for ITER in-Vessel equilibrium magnetic sensors", SOFT 25th Symposium on Fusion Technology. September 15-19, 2008. Rostock, Germany, proceedings, to be published in Fus. Eng. Des.
- P.25 G. Anaclerio, O. Barana, F. Fantini, F. Fellin, R. Pengo: "Progress on the Design of the cryogenic plant for the ITER Neutral Beam Injector Test Facility in Padova", SOFT 25th Symposium on Fusion Technology. September 15-19, 2008. Rostock, Germany, proceedings, to be published in Fus. Eng. Des.
- P.26 M. Dalla Palma, S. Dal Bello, F. Fellin, P. Zaccaria: “Design of a cooling system for the ITER Ion Source and Neutral Beam Test Facilities”, SOFT 25th Symposium on Fusion

- Technology. September 15-19, 2008. Rostock, Germany, proceedings, to be published in Fus. Eng. Des.
- P.27 M. Boldrin, M. Dalla Palma, F. Milani. "Design issues of the High Voltage Platform and Feedthrough for the ITER NBI Ion Source", SOFT 25th Symposium on Fusion Technology. September 15-19, 2008. Rostock, Germany, proceedings, to be published in Fus. Eng. Des.
- P.28 A. Pesce, A. De Lorenzi, L. Grandò: "A new approach to passive protection against High Energy and High Current breakdowns in the ITER NBI accelerator", SOFT 25th Symposium on Fusion Technology. September 15-19, 2008. Rostock, Germany, proceedings, to be published in Fus. Eng. Des.
- P.29 D. Marcuzzi, M. Dalla Palma, M. Pavei, B. Heinemann, W. Kraus, R. Riedl: "Detail design of the RF Source for the 1 MV Neutral Beam Test Facility SOFT 25th Symposium on Fusion Technology. September 15-19, 2008. Rostock, Germany, proceedings, to be published in Fus. Eng. Des.
- P.30 P. Sonato, V. Antoni, R. Piovan, A. De Lorenzi, V. Toigo, P. Zaccaria, A. Luchetta, G. Serianni, N. Pomaro, L. Grandò, M. Boldrin, E. Gaio, S. Dal Bello, D. Marcuzzi, F. Fantini, W. Rigato, A. Rizzolo, M. Dalla Palma, P. Agostinetti, M. Pavei, N. Pilan, G. Anaclerio, S. Peruzzo, M. Bigi, A. Ferro, F. Milani, L. Novello, F. Fellin, A. Zamengo, L. Zanutto, M. Recchia, G. Manduchi, O. Barana, C. Taliercio, M. Spolaore, R. Pasqualotto, M. Valisa, M. Cavenago, P. Veltri, A. Fiorentin, E. Gazza, F. Sattin, S. Sandri, M. D'Arienzo, P. Spolaore, and R. Pengo: "The ITER full size plasma source device design", SOFT 25th Symposium on Fusion Technology. September 15-19, 2008. Rostock, Germany, proceedings, to be published in Fus. Eng. Des.
- P.31 R. Chavan, G. Chitarin, R. Delogu, A. Encheva, E. R. Hodgson, C. Ingesson, A. Le-Luyer, J. B. Lister, P. Moreau, J. Moret, S. Peruzzo, D. Testa, Y. Gribov, G. Vayakis, and R. Vila, "The magnetic diagnostics set for ITER SOFT 25th Symposium on Fusion Technology. September 15-19, 2008. Rostock, Germany, proceedings, to be published in Fus. Eng. Des.
- P.32 S. Peruzzo, R. Albanese, V. Coccoresse, S. Gerasimov, N. Lam, F. Maviglia, I. Pearson, P. Prior, A. Quercia, and L. Zabeo: "Installation and commissioning of the JET-EP magnetic diagnostic system", SOFT 25th Symposium on Fusion Technology. September 15-19, 2008. Rostock, Germany, proceedings, to be published in Fus. Eng. Des.
- P.33 N. Pomaro, M. Boldrin, A. de Lorenzi, A. Fiorentin, L. Grandò, D. Marcuzzi, S. Peruzzo, W. Rigato and Gianluigi Serianni, "Potential failure mode and effects analysis for the ITER NB injector", SOFT 25th Symposium on Fusion Technology. September 15-19, 2008. Rostock, Germany, proceedings, to be published in Fus. Eng. Des.
- P.34 A. Zamengo, M. Recchia, W. Kraus, M. Bigi, C. Martens, V. Toigo: "Electrical and thermal analyses for the radio-frequency circuit of ITER NBI ion source", SOFT 25th Symposium on Fusion Technology. September 15-19, 2008. Rostock, Germany, proceedings, to be published in Fus. Eng. Des.
- P.35 M. Bigi, L. Grandò, A. De Lorenzi, K. Watanabe, M. Yamamoto: "A model for electrical fast transient analyses of the ITER NBI power supplies and the MAMuG accelerator", SOFT 25th Symposium on Fusion Technology. September 15-19, 2008. Rostock, Germany, proceedings, to be published in Fus. Eng. Des.
- P.36 W. Rigato, S. Dal Bello, D. Marcuzzi, A. Rizzolo: "Vessel Design and Interfaces Development For The 1 MV ITER Neutral Beam Injector and Test Facility", SOFT 25th Symposium on Fusion Technology. September 15-19, 2008. Rostock, Germany, proceedings, to be published in Fus. Eng. Des.

- P.37 B. Cannas, A. Fanni, G. Pautasso, G. Sias, P. Sonato and ASDEX-Upgrade Team: "Criteria and algorithms for constructing reliable data bases for statistical analysis of disruptions at ASDEX-Upgrade", SOFT 25th Symposium on Fusion Technology. September 15-19, 2008. Rostock, Germany, proceedings, to be published in Fus. Eng. Des.
- P.38 A. Luchetta, O. Barana, G. Manduchi, C. Taliercio: "Preliminary design of the control and data acquisition systems for the ITER Neutral Beam Test Facility", SOFT 25th Symposium on Fusion Technology. September 15-19, 2008. Rostock, Germany, proceedings, to be published in Fus. Eng. Des.
- P.39 G. Marchiori, A. Luchetta, G. Manduchi, L. Marrelli, A. Soppelsa, F. Villone, P. Zanca: "Advanced MHD mode active control at RFX-mod", SOFT 25th Symposium on Fusion Technology. September 15-19, 2008. Rostock, Germany, proceedings, to be published in Fus. Eng. Des.
- P.40 A. Soppelsa, G. Marchiori, L. Marrelli, P. Piovesan, F. Villone: "Integrated identification of RFX-mod active control system from experimental data and finite element model", SOFT 25th Symposium on Fusion Technology. September 15-19, 2008. Rostock, Germany, proceedings, to be published in Fus. Eng. Des.
- P.41 L. Zanotto, A. Ferro, V. Toigo: "Assessment of performances of the acceleration grid power supply of the ITER Neutral Beam Injector", SOFT 25th Symposium on Fusion Technology. September 15-19, 2008. Rostock, Germany, proceedings, to be published in Fus. Eng. Des.
- P.42 L. Grando, S. Dal Bello, A. De Lorenzi, N. Pilan, A. Rizzolo, P. Zaccaria: "Preliminary electrostatic and mechanical design of a Singap-mamug compatible Accelerator", SOFT 25th Symposium on Fusion Technology. September 15-19, 2008. Rostock, Germany, proceedings, to be published in Fus. Eng. Des.
- P.43 F. Bettini, F. Blanchini, R. Cavazzana, G. Marchiori, S. Miani, A. Soppelsa: "Real Time plasma current control strategies in RFX-mod", SOFT 25th Symposium on Fusion Technology. September 15-19, 2008. Rostock, Germany, proceedings, to be published in Fus. Eng. Des.
- P.44 F. Milani: "Upgrade of the RFX energy transfer system for a reliable 35kV, 50kA dc-current interruption", SOFT 25th Symposium on Fusion Technology. September 15-19, 2008. Rostock, Germany, proceedings, to be published in Fus. Eng. Des.
- P.45 P. Agostinetti: "Analytical and numerical models for estimates of power loads from calorimetric measurements", SOFT 25th Symposium on Fusion Technology. September 15-19, 2008. Rostock, Germany, proceedings, to be published in Fus. Eng. Des.
- P.46 E. Gaio, L. Novello, R. Piovan: "Conceptual design of the Quench Protection Circuits for the JT-60SA Superconducting Magnets", SOFT 25th Symposium on Fusion Technology. September 15-19, 2008. Rostock, Germany, proceedings, to be published in Fus. Eng. Des.
- P.47 A. Murari, J. Vega, A. Alonso, J. Farthing, C. Hidalgo, G. A. Ratta, J. Svensson, and G. Vagliasindi: "New methods of data mining and soft computing for JET with a view on ITER", SOFT 25th Symposium on Fusion Technology. September 15-19, 2008. Rostock, Germany, proceedings, to be published in Fus. Eng. Des.
- P.48 D. Lattanzi, M. Angelone, M. Pillon, S. Almaviva, M. Marinelli, E. Milani, G. Prestopino, A. Tucciarone, C. Verona, G. Verona-Rinati, S. Popovichev, R. M.

- Montereali, M. A. Vincenti, A. Murari, and JET-EFDA Contributors: "Single crystal CVD diamonds as neutron detectors at JET", SOFT 25th Symposium on Fusion Technology. September 15-19, 2008. Rostock, Germany, proceedings, to be published in Fus. Eng. Des.
- P.49 N. Duro, R. Dormido, J. Vega, S. Dormido-Canto, G. Farias, J. Sanchez, H. Vargas, A. Murari, and JET-EFDA Contributors: "Automated recognition system for ELM classification in JET", SOFT 25th Symposium on Fusion Technology. September 15-19, 2008. Rostock, Germany, proceedings, to be published in Fus. Eng. Des.
- P.50 J. Vega, A. Murari, A. Pereira, A. Portas, G. A. Ratta, R. Castro, and JET-EFDA Contributors: "Overview of intelligent data retrieval methods for waveforms and images in massive fusion databases, SOFT 25th Symposium on Fusion Technology. September 15-19, 2008. Rostock, Germany, proceedings, to be published in Fus. Eng. Des.
- P.51 B. Heinemann, H.-D. Falter, U. Fantz, P. Franzen, M. Froeschle, W. Kraus, R. Nocentini, R. Riedl, E. Speth, P. Agostinetti, and T. Jiang: "Design of the half-size"ITER neutral beam source test facility ELISE", SOFT 25th Symposium on Fusion Technology. September 15-19, 2008. Rostock, Germany, proceedings, to be published in Fus. Eng. Des.
- P.52 W. Suttrop, A. Herrmann, M. Rott, T. Vierle, U. Seidel, B. Streibl, D. Yadikin, O. Neubauer, B. Unterberg, E. Gaio, V. Toigo, P. Brunzell, and ASDEX Upgrade Team: "In-vessel saddle coils for MHD control in ASDEX Upgrade", SOFT 25th Symposium on Fusion Technology. September 15-19, 2008. Rostock, Germany, proceedings, to be published in Fus. Eng. Des.
- P.53 T. Bonicelli, A. Masiello, V. Antoni, A. De Lorenzi, M. Dremel, P. Franzen, R. S. Hemsworth, M. Liniers, D. Marcuzzi, D. Martin, R. Piovan, P. Sonato, L. Svensson, A. Tanga, V. Toigo, and P. Zaccaria: "Programme towards the 1 MeV ITER NB injector", SOFT 25th Symposium on Fusion Technology. September 15-19, 2008. Rostock, Germany, proceedings, to be published in Fus. Eng. Des.
- P.54 A. Neto, F. Sartori, F. Piccolo, A. Barbalace, R. Vitelli, and H. Fernandes: "Linux real time framework for fusion devices", SOFT 25th Symposium on Fusion Technology. September 15-19, 2008. Rostock, Germany, proceedings, to be published in Fus. Eng. Des.
- P.55 D. Ganuza, D. Rendell, S. Shaw, A. Arenal, B. Arenal, M. Zulaika, J. M. De La Fuente, V. Toigo: Design and Manufacture of the Enhanced Radial Field Amplifier (ERFA) for the JET Project, SOFT 25th Symposium on Fusion Technology. September 15-19, 2008. Rostock, Germany, proceedings, to be published in Fus. Eng. Des.
- P.56 O. Barana, A. Luchetta and C. Taliercio: "Renewal of the architecture of the RFX-mod control system", Proceedings of the 18th Topical Meeting on the Technology of Fusion Energy, September 28 - October 2, 2008, San Francisco (USA)
- P.57 S. Cappello, D. Bonfiglio, D.F. Escande, S.C. Guo, A. Alfier, R. Lorenzini and RFX Team: "The Reversed Field Pinch toward magnetic order: a genuine self-organization", Theory of Fusion Plasmas Joint Varenna-Lausanne International Workshop, Villa Monastero, Varenna, Italy 25-29 Aug 2008, Proceedings to be published in the book series "Theory of Fusion Plasmas"
- P.58 S. C. Guo: "Ion temperature gradient driven mode in RFP plasmas", Theory of Fusion Plasmas Joint Varenna-Lausanne International Workshop, Villa Monastero, Varenna, Italy 25-29 Aug 2008, Proceedings to be published in the book series "Theory of Fusion Plasmas"

- P.59 P. Martin, L. Apolloni, M. E. Puiatti, J. Adamek, M. Agostini, A. Alfier, S.V. Annibaldi, V. Antoni, F. Auriemma, O. Barana, M. Baruzzo, P. Bettini, T. Bolzonella, D. Bonfiglio, F. Bonomo, M. Brombin, J. Brotankova, A. Buffa, P. Buratti, A. Canton, S. Cappello, L. Carraro, R. Cavazzana, M. Cavinato, B.E. Chapman, G. Chitarin, S. Dal Bello, A. De Lorenzi, G. De Masi, D. F. Escande, A. Fassina, A. Ferro, P. Franz, E. Gaio, E. Gazza, L. Giudicotti, F. Gnesotto, M. Gobbin, L. Grando, L. Guazzotto, S. C. Guo, V. Igochine, P. Innocente, Y.Q.Liu, R. Lorenzini, A. Luchetta, G. Manduchi, G. Marchiori, D. Marcuzzi, L. Marrelli, S. Martini, E. Martines, K. McCollam, F. Milani, M. Moresco, L. Novello, S. Ortolani, R. Paccagnella, R. Pasqualotto, S. Peruzzo, R. Piovan, P. Piovesan, L. Piron, A. Pizzimenti, N. Pomaro, I. Predebon, J.A. Reusch, G. Rostagni, G. Rubinacci, J. S. Sarff, F. Sattin, P. Scarin, G. Serianni, P. Sonato, E. Spada, A. Soppelsa, S. Spagnolo, M. Spolaore, G. Spizzo, C. Taliercio, D. Terranova, V. Toigo, M. Valisa, N. Vianello, F. Villone, D. Yadikin, P. Zaccaria, A. Zamengo, P. Zanca, B. Zaniol, L. Zanutto, E. Zilli, H. Zohm, M. Zuin: "Overview of RFX-mod results", 22nd IAEA FEC, Geneva, 2008, proceedings to be published (OV/5-2Ra)
- P.60 A. Luchetta, G. Marchiori, G. Manduchi, L. Marrelli, L. Novello, A. Soppelsa, C. Taliercio, P. Zanca: "Technology Progress in Real-time Control of MHD Modes at RFX-mod", 22nd IAEA FEC, Geneva, 2008, proceedings to be published (FT-P2-20)
- P.61 L. Carraro, A. Alfier, F. Bonomo, A. Canton, A. Fassina, P. Franz, M. Gobbin, S.C. Guo, R. Lorenzini, P. Piovesan, M.E. Puiatti, G. Spizzo, D. Terranova, M. Valisa, M. Zuin, F. Auriemma, L. Marrelli, E. Martines, R. Pasqualotto, M. Spolaore, L. Zanutto: "Improved Confinement with Internal Electron Temperature Barriers in RFX-mod", 22nd IAEA FEC, Geneva, 2008, proceedings to be published (EX-P3-9)
- P.62 M.E. Puiatti, P. Scarin, G. Spizzo, M. Valisa, M. Agostini, A. Alfier, A. Canton, L. Carraro, R. Paccagnella, I. Predebon, R. Lorenzini, D. Terranova, D. Bonfiglio, S. Cappello, R. Cavazzana, S. Dal Bello, E. Gazza, P. Innocente, L. Marrelli, R. Piovan, F. Sattin, P. Zanca: "High density physics in Reversed Field Pinches: comparisons with tokamaks and stellarators", 22nd IAEA FEC, Geneva, Switzerland, 2008, proceedings to be published (P5-22)
- P.63 L. Grando, G. Manduchi, L. Marrelli, G. Marchiori, R. Paccagnella, P. Piovesan, L. Piron, A. Soppelsa, G. Spizzo, P. Zanca: "Active control of resonant MHD modes in RFX-mod", 22nd IAEA FEC, Geneva, Switzerland, 2008, proceedings to be published (P9-8)
- P.64 E. Martines, A. Alfier, M. Agostini, A. Canton, R. Cavazzana, G. De Masi, A. Fassina, P. Innocente, R. Lorenzini, P. Scarin, G. Serianni, M. Spolaore, D. Terranova, N. Vianello, M. Zuin: "Transport Mechanisms in the Outer Region of RFX-mod", 22nd IAEA FEC, Geneva, Switzerland, 2008, proceedings to be published (P5-26)
- P.65 J.R. Drake, T. Bolzonella, K.E.J. Olofsson, T.M. Baruzzo, P.R. Brunzell, L. Frassinetti, S.C. Guo, V. Igochine, Y.Q. Liu, G. Marchiori, R. Paccagnella, G. Rubinacci, A. Soppelsa, F. Villone, D. Yadikin, P. Martin, H. Zohm: "Reversed Field Pinch contributions to RWM physics and control", 22nd IAEA FEC, Geneva, Switzerland, 2008, proceedings to be published (EX-P9-7)
- P.66 M. Garcia-Munoz, H.-U. Fahrbach, V. Bobkov, M. Brüdger, M. Gobbin, S. Günter, V. Igochine, Ph. Lauber, M.J. Mantsinen, M. Maraschek, L. Marrelli, P. Martin, S.D. Pinches, P. Piovesan, E. Poli, K. Sassenberg, H. Zohm, and the ASDEX Upgrade Team: "MHD induced Fast-Ion Losses on ASDEX Upgrade", 22nd IAEA Fusion Energy Conference", 13-18 October 2008, Geneva, Switzerland, proceedings to be published paper IAEA-CN-165/EX/6-1
- P.67 M.J. Walsh, K. Beausang, M.N.A. Beurskens, L. Giudicotti, T. Hatae, D. Johnson, S. Kajita, E.E. Mukhin, R. Pasqualotto, S.L. Prunty, R.D. Scannell, G. Vayakis for the

- ITPA Thomson Scattering Working Group Performance Evaluation of ITER Thomson Scattering Systems”, paper IAEA-CN- IT/P6-25 , 22nd IAEA Fusion Energy Conference”, 13-18 October 2008, Geneva, Switzerland, proceedings to be published
- P.68 M.N.A. Beurskens, A. Alfier, B. Alper, I. Balboa, J. Flanagan, W. Fundamenski, E. Giovannozzi, M. Kempenaars, A. Loarte, E. de La Luna I. Nunes, R. Pasqualotto, R. A. Pitts, G. Saibene, M. Walsh, and JET-EFDA contributors: “Pedestal dynamics in ELMY H-mode plasmas in JET”, 22nd IAEA Fusion Energy Conference”, 13-18 October 2008, Geneva, Switzerland, proceedings to be published paper IAEA-CN- EX/P3-4
- P.69 V Riccardo, G Arnoux, P Beaumont, S Hacquina, J Hobirkb, D Howell, A Huberc, E Joffrin, R Koslowskic, N Lam, H Leggate, E Rachlewd, G Sergienko, A Stephen, T Todd, M Zerbini, R Delogu, L Grando, D Marcuzzi, S Peruzzo, N Pomaro, P Sonato, and JET EFDA Contributors, "Progress in understanding halo current at JET", proceedings of the 22nd IAEA Fusion Energy Conference 13th-18th October 2008, Geneva, Switzerland
- P.70 L. Giudicotti, R. Pasqualotto, A. Alfier, M. Beurskens, M. Kempenaars, and M. J. Walsh, "Study of Fast, Near-Infrared Photodetectors for the ITER Core LIDAR Thomson Scattering", International Conference on Burning Plasma Diagnostics, Varenna (Italy), 24-28 September 2007, AIP Conf. Proc. 988, 144 (2008)
- P.71 P. Agostinetti, V. Antoni, M. Cavenago, H.P.L. de Esch, G. Fubiani, D. Marcuzzi, S. Petrenko, N. Pilan, W. Rigato, G. Serianni, M. Singh, P. Sonato, P. Veltri and P. Zaccaria. "Design of a low voltage, high current extraction system for the ITER Ion Source", 1st International Conference on Negative Ions, Beams and Sources, 10-12 September 2008, Aix en Provence, France, to be published in AIP Conf. Proc.
- P.72 Piero Agostinetti, Vanni Antoni, Marco Cavenago, Giuseppe Chitarin, Nicolò Marconato, Mauro Pavei, Nicola Pilan, Gianluigi Serianni, Piergiorgio Sonato: “Optimisation of the magnetic field configuration for the negative ion source of ITER neutral beam injectors” , ITC 18 Conference, December 9-12, 2008 Ceratopia Toki, Toki Gifu Japan, proc. to be published
- P.73 Marco Cavenago, Gianluigi Serianni, Vanni Antoni, Nicola Pilan, Pierluigi Zaccaria: “Active steering system for the Neutral Beam Injector for ITER”, ITC 18 Conference, December 9-12, 2008 Ceratopia Toki, Toki Gifu Japan, proc. to be published

CONTRIBUTIONS TO INTERNATIONAL AND NATIONAL CONFERENCES

- C.1 M. Zuin, N. Vianello, M. Spolaore, V. Antoni, T. Bolzonella, R. Cavazzana, E. Martines, G. Serianni, D. Terranova : “Experimental characterization of current sheets associated to spontaneous magnetic reconnection in a reversed field pinch plasma”, EFTSOMP2008 11th Workshop on Electric Fields Turbulence and Self-Organisation in Magnetized Plasmas, 16-17 June 2008, Hersonissos, Crete Greece, to be published in Plasma Physics Report
- C.2 M. Agostini, R. Cavazzana, F. Sattin, P. Scarin, G. Serianni, M. Spolaore, N. Vianello, R.J. Maqueda, S.J. Zweben, Y. Yagi, H. Sakakita, H. Koguchi, S. Kiyama, Y. Hirano, J. Terry: “Universal properties of edge intermittent turbulence in different fusion devices”, EFTSOMP2008 11th Workshop on Electric Fields Turbulence and Self-Organisation in Magnetized Plasmas, 16-17 June 2008, Hersonissos, Crete Greece, to be published in Plasma Physics Report
- C.3 N. Vianello, M. Spolaore, R. Cavazzana, E. Martines, G. Serianni, E. Spada, M. Zuin, V. Antoni: “Magnetic and electrostatic structures measured in the edge region of the RFX-

- mod experiment”, EFTSOMP2008 11th Workshop on Electric Fields Turbulence and Self-Organisation in Magnetized Plasmas, 16-17 June 2008, Hersonissos, Crete Greece, to be published in Plasma Physics Report
- C.4 P. Scarin, M. Agostini, R. Cavazzana, F. Sattin, G. Serianni: “Edge turbulence scaling in RFX-mod with GPI diagnostic”, 18th International Conf. on Plasma Surface Interactions, Toledo, Spain 26-30 May 2008, Book of Abstracts P3-32
- C.5 M. Spolaore, N. Vianello, M. Agostini, R. Cavazzana, E. Martines, G. Serianni, P. Scarin, E. Spada, M. Zuin, V. Antoni: “Magnetic and electrostatic structures measured in the edge region of the RFXmod experiment” 18th International Conf. on Plasma Surface Interactions, Toledo, Spain 26-30 May 2008, Book of Abstracts P3-33
- C.6 P. Bettini, R. Specogna, F. Trevisan, “Electroquasistatic analysis of the Gas Insulated Line for the ITER Neutral Beam Injector”, CEFC 2008 Conference, May 11 - 15, 2008, Athens, Greece
- C.7 L. Giudicotti, R. Pasqualotto, A. Alfier, M. Beurskens, M. Kempenaars, and M. J. Walsh: “Near-infrared detectors for ITER LIDAR Thomson scattering, 17th Topical Conference on High-Temperature Plasma Diagnostics”, Albuquerque, New Mexico, May 11-15, 2008, to be published in Rev. Scien. Instrum.
- C.8 M. Brombin, A. Boboc, L. Zabeo, A. Murari, E. Zilli, L. Giudicotti and JET-EFDA contributors: “Real-time electron density measurements from Cotton Mouton effect in JET machine”, 17th Topical Conference on High-Temperature Plasma Diagnostics”, Albuquerque, New Mexico, May 11-15, 2008, to be published in Rev. Scien. Instrum.
- C.9 E. Alessi, M. Cavinato, G. Chitarin: “Development of a Reconstruction Procedure for the Halo Current Distribution”, 17th Topical Conference on High-Temperature Plasma Diagnostics”, Albuquerque, New Mexico, May 11-15, 2008, to be published in Rev. Scien. Instrum.
- C.10 A Alfier, S. Barison, T. Danieli, L. Giudicotti, C. Pagura, R. Pasqualotto: “In-situ window cleaning by laser blow-off through optical fiber”, 17th Topical Conference on High-Temperature Plasma Diagnostics”, Albuquerque, New Mexico, May 11-15, 2008, to be published in Rev. Scien. Instrum.
- C.11 G. Serianni, N. Pomaro, R. Pasqualotto, M. Spolaore, M. Valisa: “The diagnostic system of the Neutral Beam Injector for ITER heating and current drive”, 17th Topical Conference on High-Temperature Plasma Diagnostics”, Albuquerque, New Mexico, May 11-15, 2008, to be published in Rev. Scien. Instrum.
- C.12 R. Cavazzana, M. Agostini, P. Scarin and G. Serianni: “Measurements of Local Magnetic Fluctuations and Gas Puff Emissivity in Edge Plasmas”, 17th Topical Conference on High-Temperature Plasma Diagnostics”, Albuquerque, New Mexico, May 11-15, 2008, to be published in Rev. Scien. Instrum.
- C.13 M. Moresco, R. Cavazzana: “Robust Measurement of Group Delay in Presence of Density Fluctuations by means of Ultra Fast Swept Reflectometry”, 17th Topical Conference on High-Temperature Plasma Diagnostics”, Albuquerque, New Mexico, May 11-15, 2008, to be published in Rev. Scien. Instrum.
- C.14 L. Guazzotto, R. Paccagnella: “New capabilities of the equilibrium code FLOW”, Sherwood Fusion Theory Conference, Boulder, USA, 30 March - 2 April 2008
- C.15 L. Guazzotto, M. Gobbin, S.C.Guo, I. Predebon, F. Sattin, G. Spizzo, P. Zanica, S. Cappello: “Trapped particles in Reversed Field Pinches”, ICPP Int. Conf. on Plasma

- Physics, 8-12 Sept 2008 Fukuoka, JP, to be published in Journal of Plasma and Fusion Research Series
- C.16 P. Zanica: "Beyond the intelligent-shell concept: the clean-mode-control for tearing perturbations", ICPP Int. Conf. on Plasma Physics, 8-12 Sept 2008 Fukuoka, JP, to be published in Journal of Plasma and Fusion Research Series
- C.17 D.F. Escande, F. Sattin: "When can the Fokker-Planck Equation Describe Anomalous or Chaotic Particle Transport?", ICPP Int. Conf. on Plasma Physics, 8-12 Sept 2008 Fukuoka, JP, to be published in Journal of Plasma and Fusion Research Series
- C.18 C. Ionita, N. Vianello, H. W. Muller, F. Mehlmann, M. Zuin, V. Naulin, J. J. Rasmussen, V. Rohde, R. Cavazzana, C. Lupu, M. Maraschek, R. W. Schrittwieser, P. C. Balan, ASDEX Upgrade Team: "Simultaneous Measurements of Electrostatic and Magnetic Fluctuations in ASDEX Upgrade Edge Plasma", ICPP Int. Conf. on Plasma Physics, 8-12 Sept 2008 Fukuoka, JP, to be published in Journal of Plasma and Fusion Research Series
- C.19 M. Valisa and the RFX-mod Team: "High Density Limit in RFP's", 13th IEA/RFP Workshop, October 9-11, 2008, Stockholm; Sweden
- C.20 M. E. Puiatti: "Overview of RFX-mod results", 13th IEA/RFP Workshop, October 9-11, 2008, Stockholm, Sweden
- C.21 A. Alfier: "2D characterization of thermal core topology changes in controlled RFX-mod QSH states", 13th IEA/RFP Workshop, October 9-11, 2008, Stockholm, Sweden
- C.22 T. Bolzonella, P. Franz, D. Terranova, L. Zanotto, J.A. Reusch, J.S. Sarff: "Results on new PPCD experiments on RFX-mod", 13th IEA/RFP Workshop, October 9-11, 2008, Stockholm, Sweden
- C.23 P. Scarin, M. Agostini, N. Vianello, R. Cavazzana, F. Sattin, G. Serianni, M. Spolaore: "Analysis of edge turbulence in RFX-mod from GPI data and comparison with other toroidal devices", 13th IEA/RFP Workshop, October 9-11, 2008, Stockholm, Sweden
- C.24 P. Scarin, M. Agostini, R. Cavazzana, F. Sattin, G. Serianni, M. Spolaore, N. Vianello: "Measurements of characteristic pressure profile lengths and comparison to turbulence scale lengths in RFX-mod edge", 13th IEA/RFP Workshop, October 9-11, 2008, Stockholm, Sweden
- C.25 N. Vianello, M. Spolaore, M. Agostini, R. Cavazzana, E. Martines, P. Scarin, G. Serianni, E. Spada, M. Zuin, V. Antoni: "Current filaments and electrostatic structures measured in the edge region of the RFX-mod experiment", 13th IEA/RFP Workshop, October 9-11, 2008, Stockholm, Sweden
- C.26 R. Bilato, F. Volpe, A. Koehn, R. Paccagnella, D. Farina, E. Poli, M. Brambilla: "Feasibility study of electron Bernstein wave coupling via O-X-B mode conversion in RFX-mod", 13th IEA/RFP Workshop, October 9-11, 2008, Stockholm, Sweden
- C.27 M. Zuin: "Self-organized helical equilibria emerging at high current in RFX-mod", 13th IEA/RFP Workshop, October 9-11, 2008, Stockholm, Sweden
- C.28 A. Canton, S. Dal Bello: "Density control in RFX-mod", 13th IEA/RFP Workshop, October 9-11, 2008, Stockholm, Sweden
- C.29 D. Terranova: "Experimental studies of particle transport with pellet injection in the helical structure", 13th IEA/RFP Workshop, October 9-11, 2008, Stockholm, Sweden

- C.30 A. Alfier, T. Bolzonella, A. Fassina, P. Franz, P. Innocente, R. Pasqualotto and L. Zanotto, A. Almagri, W. Bergerson, D.J. Den Hartog, W.X. Ding, G. Fiksel and J.S. Sarff: "Similarity Experiments on RFX-mod and MST Standard Discharges: Kinetics", 13th IEA/RFP Workshop, October 9-11, 2008, Stockholm, Sweden
- C.31 S.C. Guo, M. Baruzzo, T. Bolzonella, V. Igochine, G. Marchiori, A. Soppelsa, D. Yadikin, H. Zohm: "Experiments and modeling on active RWM rotation in RFP plasmas", 13th IEA/RFP Workshop, October 9-11, 2008, Stockholm, Sweden
- C.32 P. Innocente, A. Alfier, A. Canton, R. Pasqualotto: "Scaling studies in RFX-Mod", 13th IEA/RFP Workshop, October 9-11, 2008, Stockholm, Sweden
- C.33 S.C. Guo, F. Sattin: "Drift instabilities in RFP plasmas", 13th IEA/RFP Workshop, October 9-11, 2008, Stockholm, Sweden
- C.34 M. Gobbin, L. Carraro, L. Marrelli, G. Spizzo: "Numerical studies of particle transport mechanisms in RFX-mod low chaos regimes", 13th IEA/RFP Workshop, October 9-11, 2008, Stockholm, Sweden
- C.35 M. Valisa, M. Gobbin, L. Grando, L. Marrelli, S. Martini, R. Piovan, A. Rizzolo, P. Zaccaria: "Power Neutral Beam on RFX-mod: Design and Mission", 13th IEA/RFP Workshop, October 9-11, 2008, Stockholm
- C.36 R. Paccagnella, F. Villone, Y.Q. Liu, G. Rubinacci, T. Bolzonella: "Effect of a tri-dimensional boundary on RWM stability", 13th IEA/RFP Workshop, October 9-11, 2008, Stockholm, Sweden
- C.37 A.Fassina, A. Alfier, F.Bonomo, L.Carraro, G. Spizzo, M.E.Puiatti, R. Pasqualotto, M.Valisa: "First experiments of impurity LBO injection in RFX-mod", 50th Annual Meeting of the Division of Plasma Physics, November 17-21, 2008; Dallas, Texas, Bulletin of the American Physical Society, Volume 53, Number 14. Copyright (c) 2008 American Physical Society
- C.38 M. Spolaore, N. Vianello, M. Agostini, V. Antoni, R. Cavazzana, E. Martines, G. Serianni, P. Scarin, E. Spada, M. Zuin: "Current density filaments measured by electrostatic, magnetic and optical diagnostics in RFX-mod", 50th Annual Meeting of the Division of Plasma Physics, November 17-21, 2008; Dallas, Texas, Bulletin of the American Physical Society, Volume 53, Number 14. Copyright (c) 2008 American Physical Society NP6-00073
- C.39 M. Agostini, P. Scarin, N. Vianello, R. Cavazzana, F. Sattin, G. Serianni, M. Spolaore, R.J. Maqueda, S.J. Zweben, J.L. Terry, Y. Yagi, H. Sakakita, H. Koguchi, S. Kiyama, Y. Hirano: "Universal properties of the edge turbulence in different fusion experiments and its driving mechanisms", 50th Annual Meeting of the Division of Plasma Physics, November 17-21, 2008; Dallas, Texas, Bulletin of the American Physical Society, Volume 53, Number 14. Copyright (c) 2008 American Physical Society GP6-00109
- C.40 D. Bonfiglio, S. Cappello, M. Gobbin, G. Spizzo: "Helical states with ordered magnetic topology in the Reversed Field Pinch", 50th Annual Meeting of the Division of Plasma Physics, November 17-21, 2008; Dallas, Texas, Bulletin of the American Physical Society, Volume 53, Number 14. Copyright (c) 2008 American Physical Society NP6-00074
- C.41 L. Guazzotto, R. Paccagnella: "Applications of the equilibrium code FLOW and its integration within the Integrated Tokamak Modelling initiative", 50th Annual Meeting of the Division of Plasma Physics, November 17-21, 2008; Dallas, Texas, Bulletin of the American Physical Society, Volume 53, Number 14. Copyright (c) 2008 American Physical Society

- C.42 P. Scarin, M. Agostini, R. Cavazzana, F. Sattin, G. Serianni, M. Spolaore, N. Vianello: "Measurements of characteristic pressure profile lengths and comparison to turbulence scale lengths in RFX-mod edge", 50th Annual Meeting of the Division of Plasma Physics, November 17–21, 2008; Dallas, Texas, Bulletin of the American Physical Society, Volume 53, Number 14. Copyright (c) 2008 American Physical Society NP6-00076
- C.43 R. Paccagnella, H.R. Strauss and J. Breslau: "3D MHD disruptions simulations of tokamaks plasmas", 50th Annual Meeting of the Division of Plasma Physics, November 17–21, 2008; Dallas, Texas, Bulletin of the American Physical Society, Volume 53, Number 14. Copyright (c) 2008 American Physical Society
- C.44 I. Predebon, R. Paccagnella, M. E. Puiatti, M. Valisa: "An MHD-integrated model for impurity and core transport studies in RFP plasmas", 50th Annual Meeting of the Division of Plasma Physics, November 17–21, 2008; Dallas, Texas, Bulletin of the American Physical Society, Volume 53, Number 14. Copyright (c) 2008 American Physical Society
- C.45 D. Bonfiglio, S. Cappello, L. Chacon: "Nonlinear 3D visco-resistive MHD modeling of fusion plasmas: a comparison between numerical codes", 50th Annual Meeting of the Division of Plasma Physics, November 17–21, 2008; Dallas, Texas, Bulletin of the American Physical Society, Volume 53, Number 14. Copyright (c) 2008 American Physical Society YP6-00059
- C.46 G Spizzo, R B White, S Cappello, L Marrelli: "Nonlocal Levy flight transport in the RFX", 50th Annual Meeting of the Division of Plasma Physics, November 17–21, 2008; Dallas, Texas, Bulletin of the American Physical Society, Volume 53, Number 14. Copyright (c) 2008 American Physical Society NP6-00079
- C.47 M Agostini, S Cappello, P Innocente, R Lorenzini, R Paccagnella, I Predebon, M E Puiatti, P Scarin, G Spizzo, D Terranova, M Valisa: "Density limit in the Reversed Field Pinch", 50th Annual Meeting of the Division of Plasma Physics, November 17–21, 2008; Dallas, Texas, Bulletin of the American Physical Society, Volume 53, Number 14. Copyright (c) 2008 American Physical Society NP6-00075
- C.48 R. Lorenzini and RFX-mod team (invited): "Improvement of the magnetic configuration in the RFP through successive bifurcations", 50th Annual Meeting of the Division of Plasma Physics, November 17–21, 2008; Dallas, Texas, Bulletin of the American Physical Society, Volume 53, Number 14. Copyright (c) 2008 American Physical Society NP6-00072
- C.49 M. Spolaore RFX-mod team: "Overview of the recent results of RFX-mod", 50th Annual Meeting of the Division of Plasma Physics, November 17–21, 2008; Dallas, Texas, Bulletin of the American Physical Society, Volume 53, Number 14. Copyright (c) 2008 American Physical Society NP6-00072
- C.50 A Buffa, R Cavazzana, M T Orlando, G Spizzo: "Public Information Activities at Consorzio RFX, Padova", 50th Annual Meeting of the Division of Plasma Physics, November 17–21, 2008; Dallas, Texas, Bulletin of the American Physical Society, Volume 53, Number 14. Copyright (c) 2008 American Physical Society
- C.51 K.J. Caspary, M.D. Wyman, B.E. Chapman, A.F. Almagri, J.K. Anderson, D.J. Den Hartog, F. Ebrahimi, D.A. Ennis, G. Fiksel, S. Gangadhara, J.A. Goetz, S.T. Limbach, R. O'connell, S.P. Oliva, S.C. Prager, J.A. Reusch, J.S. Sarff, H.D. Stephens, F. Bonomo, P. Franz, D.L. Brower, B.H. Deng, W.X. Ding, T. Yates, S.K. Combs, C.R. Foust, D. Craig: "Pellet-Fueled, High- β , Improved Confinement RFP Plasmas", 50th Annual Meeting of the Division of Plasma Physics, November 17–21, 2008; Dallas, Texas,

- Bulletin of the American Physical Society, Volume 53, Number 14. Copyright (c) 2008 American Physical Society NP6-00072
- C.52 M.B. McGarry, J.A. Goetz, D.J. Den Hartog, B.E. Chapman, P. Franz, F. Bonomo, L. Marrelli: “Multicolor SXR Tomography on MST”, 50th Annual Meeting of the Division of Plasma Physics, November 17–21, 2008; Dallas, Texas, Bulletin of the American Physical Society, Volume 53, Number 14. Copyright (c) 2008 American Physical Society
- C.53 Y. In, J.S. Kim, I.N. Bogatu, G.L. Jackson, R.J. La Haye, M.J. Schaffer, E.J. Strait, A.M. Garofalo, M.J. Lanctot, H. Reimerdes, M. Okabayashi, L. Marrelli, P. Martin: “Feedback stabilization of current-driven resistive-wall-modes (RWMs) near $q_{95} \gg 4$ in DIII-D”, 50th Annual Meeting of the Division of Plasma Physics, November 17–21, 2008; Dallas, Texas, Bulletin of the American Physical Society, Volume 53, Number 14. Copyright (c) 2008 American Physical Society
- C.54 N. Vianello, M. Spolaore, R. Cavazzana, E. Martines, G. Serianni, E. Spada, M. Zuin: “Filamentary structures detected in the edge region of RFX-Mod”, 13th EU-US TTF workshop 2008 and 1st EFDA Transport Topical Group Meeting, 1-4 September 2008 in Copenhagen, Denmark
- C.55 C. Giroud, C. Angioni, P. Belo, G. Bonheure, L. Carraro, I.H. Coffey, V. Naulin, M. Valisa, A.D. Whiteford, K-D. Zastrow and the JET-EFDA Contributors: “Characterisation of impurity transport at JET”, 13th EU-US TTF workshop 2008 and 1st EFDA Transport Topical Group Meeting, 1-4 September 2008 in Copenhagen, Denmark
- C.56 I. Predebon, L. Carraro, R. Paccagnella, M. E. Puiatti, M. Valisa: “Impurity and Core transport studies in RFP plasmas: a new numerical tool”, 13th EU-US TTF workshop 2008 and 1st EFDA Transport Topical Group Meeting, 1-4 September 2008 in Copenhagen, Denmark
- C.57 R. Lorenzini, P. Innocente, E. Martines, D. Terranova, F. Sattin: “Confinement improvement due to magnetic topology change in RFX-mod”, 13th EU-US TTF workshop 2008 and 1st EFDA Transport Topical Group Meeting, 1-4 September 2008 in Copenhagen, Denmark